UNIVERSITÀ DEGLI STUDI DI PADOVA

Facoltà di Scienze MM.NN.FF.
Facoltà di Ingegneria

ISTITUTO NAZIONALE DI FISICA NUCLEARE

Laboratori Nazionali di Legnaro

in collaboration with Confindustria Veneto

MASTER THESIS
in
"Surface Treatments for Industrial Applications"

Electropolishing of Niobium 6 GHz rf cavities in fluorine-free electrolyte

Supervisor: *Prof. V. Palmieri*
Assistant supervisor : Dr. V. Rampazzo

Student: *Dott. Rupp Vitalii*
            Volodymyrovych

Matr. №:   *934605*

Academic Year 2008-09

Contents

Acronym

EP –   Electropolishing

BCP –   Buffered Chemical Polishing

IL –   ionic liquid

ChCl –   Choline Chloride

SA –   Sulfamic acid

PS -   Ammonium persulfate

SRF –   Superconducting Radio Frequency

BSC –   microscopic theory of superconductivity, proposed by Bardeen, Cooper, and Schrieffer in 1957

WE –   working electrode

CE –   counter electrode

RE –   reference electrode

Abstract

Electropolishing is one of the oldest electrochemical techniques which is widely adapted in industry. Since many years electropolishing has been growing and from day to day it fills more and more niches in different fields of science and technology. Among possible Surface Treatments, electropolishing occupies a key role, because it is the cleanest way for removing hundreds of microns of material.

Most galvanic processes start their life from water solutions. Electropolishing is not an exception, even now Nb electropolishing based on water solution with sulfuric and hydrofluoric acids is the most used. Literature results with this standard mixture are excellent, however the EP of thousands of cavities could become an industrial nightmare from the point of view of security at work. HF is not like other highly corrosive acids: if, by accident, it gets in contact with skin, pain is not felt, but F^- ions begin to pass through, searching for the bone calcium.

Since many years world's science has been interested in ionic liquids and it is not for nothing. A green chemistry based on ionic liquids has come to the fore, and at INFN-LNL laboratories was done the first Niobium electropolishing by a harmless mixture of Choline Chloride and urea heated around 150°C.

In my work I will try to study influence of adding to the mixture some regulators. While it has already been showed the possibility of Nb dissolving with electropolishing effect, I will try to find recipe for technological Nb electropolishing. My second goal is to put ready recipe to application on 6 GHz cavities.

Introduction

0.1   Superconducting cavities

A superconducting cavity is the device used to provide energy to the particles that are crucial to an accelerator. Most commonly used are radio frequency (rf) cavities, an example of which is shown in Figure 0.1.
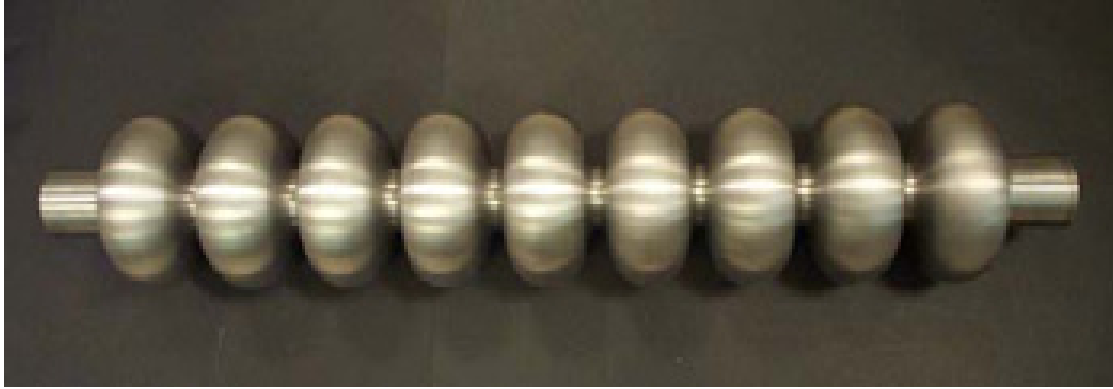
Figure 0.1: *The first Niobium seamless 9-cell cavity ever fabricated* [1]

In the past, copper cavities were used for acceleration (e.g., at SLAC). However, superconducting niobium technology has proven itself over the last 20 years as a promising alternative, being used in machines such as HERA (Hamburg, Germany) and TJNAF (Newport News, VA). Continuous wave (cw) accelerating gradients of 10 MV/m have been achieved, exceeding levels that are possible with copper cavities. Many of the present and future projects (among them TESLA, LEP-II, the KEK B-factory, and the LHC) are relying on superconducting cavities to achieve their design goals. Thus, superconductors will play a pioneering role at both the energy frontier and the high current frontier.

Extensive research has therefore been performed to understand the performance limitations of superconducting cavities and to improve upon the achieved accelerating gradients.

0.1.1   Advantages of superconducting cavities

Although not completely loss free above T = 0 K, as in the dc case, superconducting cavities dissipate orders of magnitude less power than normal conducting cavities. Niobium cavities, like those installed at TJNAF, routinely achieve quality (Q_0) factors 10^5 to 10^6 times that of copper cavities. The dramatically reduced resistivity translates into a number of very important advantages.

0.1.2 Radio-frequency fields in cavities

The rf field in cavities is derived from the eigenvalue equation

$$\left(\nabla^2 - \frac{1}{c^2}\frac{\partial^2}{\partial t^2}\right)\binom{E}{H} = 0 \tag{0.1}$$

which is obtained by combining Maxwell's equations [2; 3]. It is subject to the boundary conditions

$$\hat{n} \times \mathbf{E} = 0 \tag{0.2}$$

and

$$\hat{n} \times \mathbf{H} = 0 \tag{0.3}$$

at the cavity walls. Here $\hat{n}$ is the unit normal to the rf surface, c is the speed of light and $\mathbf{E}$ and $\mathbf{H}$ are the electric and magnetic field respectively. In cylindrically symmetric cavities, such as the pillbox shape, the discrete mode spectrum given by equation (0.1) splits into two groups, transverse magnetic (TM) modes and transverse electric (TE) modes. For TM modes the magnetic field is transverse to the cavity symmetry axis where as for TE modes it is the electric one to be transverse. For accelerating cavities, therefore, only TM modes are useful.

The typical shape of speed of light cavities [3] is shown in Figure 0.2.
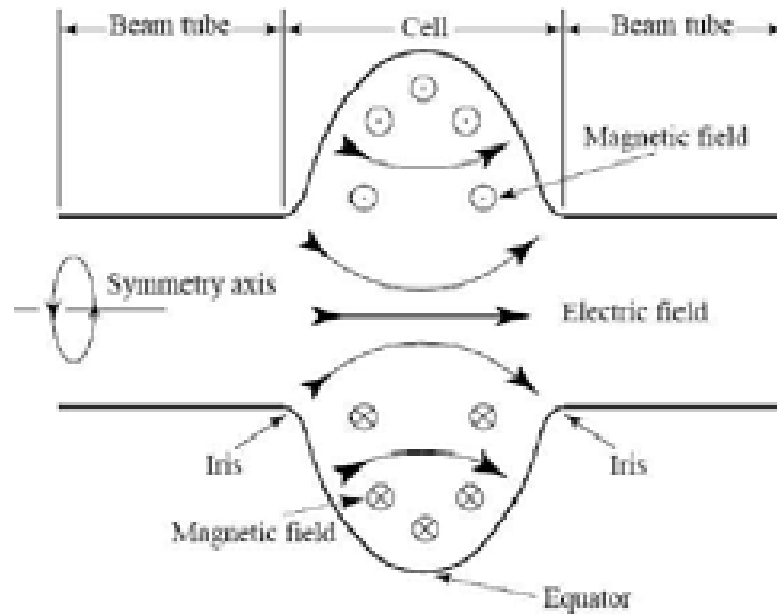
Figure 0.2: *Schematic of a generic speed-of-light cavity. The electric field is strongest near the symmetric axis, while the magnetic field is concentrated in the equator region.*

0.1.3   The accelerating field

The accelerating voltage (V_{acc}) of a cavity is determined by considering the motion of a charged particle along the beam axis. For a charge q, by definition,

$$V_{acc} = \frac{1}{q} \cdot \left(\text{maximum energy gain possible during transit} \right) \tag{0.4}$$

We used speed-of-light structures in our tests, and the accelerating voltage is therefore given by

$$V_{acc} = \left| \int_{z=0}^{d} E_z(\rho=0,z) e^{f w_0 z / c} \, dz \right| \tag{0.5}$$

where d is the length of the cavity and ω_0 is the eigenfrequency of the cavity mode under consideration. Frequently, one quotes the accelerating field E_{acc} rather than V_{acc}. The two are related by

$$E_{acc} = \frac{V_{acc}}{d} \tag{0.6}$$

0.1.4   Peak surface fields

When considering the practical limitations of superconducting cavities, two fields are of particular importance: the peak electric surface field (E_{pk}) and the peak magnetic surface field (H_{pk}). These fields determine the maximum achievable accelerating gradient in cavities. The surface electric field peaks near the irises, and the surface magnetic field is at its maximum near the equator.

To maximize the potential cavity performance, it is important that the ratios of $E_{pk} = E_{acc}$ and $H_{pk} = E_{acc}$ be minimized.

0.1.5 RF power dissipation and cavity quality

To support the electromagnetic fields in the cavity, currents flow in the cavity walls at the surface. If the walls are resistive, the currents dissipate power. The resistivity of the walls is characterized by the material dependent surface resistance R_s which is defined via the power Pd dissipated per unit area:

$$\frac{dP_d}{da} = \frac{1}{2} R_s |H|^2 \tag{0.7}$$

In this case, *H* is the local surface magnetic field.

Directly related to the power dissipation is an important figure of merit called the cavity quality (Q_0). It is defined as

$$Q_0 = \frac{w_0 U}{P_d}$$ (0.8)

U being the energy stored in the cavity. The Q_0 is just 2π times the number of rf cycles it takes to dissipate an energy equal to that stored in the cavity.

For all cavity modes, the time averaged energy in the electric field equals that in the magnetic field, so the total energy in the cavity is given by

$$U = \frac{1}{2}\mu_0 \int_V |H|^2 dv = \frac{1}{2}\varepsilon_0 \int_V |E|^2 dv$$ (0.9)

where the integral is taken over the volume of the cavity. The dissipated power becomes

$$P_d = \frac{1}{2}\int_s R_s |H|^2 ds$$ (0.10)

where the integration is taken over the interior cavity surface. (By keeping Rs in the integral we have allowed for a variation of the surface resistance with position.) Thus one finds for Q$_0$:

$$Q_0 = \frac{w_0\mu_0 \int_V |H|^2 dv}{\int_s R_s |H|^2 ds}$$ (0.11)

The Q_0 is frequently written as

$$Q_0 = \frac{G}{R_s}$$ (0.12)

where

$$G = \frac{w_0\mu_0 \int_V R_s |H|^2 dv}{\int_s |H|^2 ds}$$ (0.13)

is known as the geometry constant, and

$$\overline{R_s} = \frac{\int\limits_{s} R_s \left|H\right|^2 ds}{\int\limits_{s} \left|H\right|^2 ds} \tag{0.14}$$

is the mean surface resistance (weighted by $|H|^2$).

Although superconductors do not exhibit any dc resistivity, there are small losses for rf currents.

0.2   Cavities configurations

Superconducting cavities are (or were) in operation in many storage rings (HERA [4], LEP [5], Tristan [6], KEK [7], CESR [8]) or linacs (Jefferson Lab [9], TFF-FEL [10]). At present the superconducting proton linac for the SNS spallation source is under construction [11]. In total more than 1000 meter of superconducting cavities have been operated and delivered about 5 GeV of accelerating voltage [12]. TESLA [13] is a proposal for a superconducting linear collider using more than 20000 Niobium cavities. Many other projects using superconducting cavities are under discussion (light sources, muon colliders,…). Most existing cavities are made from Niobium sheet metal.

The fabrication of Niobium cavities has become a mature technology. Several companies are qualified as competent producers. The fabrication process of resonators for electron acceleration (relative velocity beta = v/c =1) is described with special reference to the TESLA design (Figure 0.3), especially considering mass production aspects. The design for medium beta application as for protons looks very similar. The shape of resonators for low beta application (like heavy ions) is different but the fabrication principles are the same.

Two classes of considerations govern the structure design. The particular accelerator application forms one class, and superconducting surface properties the other. Designing a superconducting cavity is a strong interplay between these two classes. Typical accelerator driving aspects are the desired voltage, the duty factor of accelerator operation, beam current or beam power. Other properties of the beam, such as the bunch length, also play a role in cavity design. Typical superconducting properties are the microwave surface resistance and the tolerable surface electric and magnetic fields. These properties, set the operating field levels and the power requirements, both RF power as well as AC operating power, together with the warning temperature.

Figure 0.3: *Modified TESLA 9-cell resonator (with LHe tank at lower picture) as example for a β = 1 structure for acceleration of electrons (courtesy of Accel Instruments GmbH).*

Figure 0.4 shows a variety of superconducting accelerating cavities, ranging in frequency from 200 MHz to 3000 MHz and ranging in number of cells from one to nine. Most are cavities fabricated from pure sheet niobium. All the cavities of Figure 0.4 are intended for accelerating particles moving at nearly the velocity of light, i.e. $v/c = \beta \approx 1$. Accordingly, the period of a long structure (or the accelerating gap) is $\lambda/2$, where λ is the RF wavelength. Particles moving at $v \approx c$ will cross the gap in exactly a half RF period to receive the maximum acceleration.
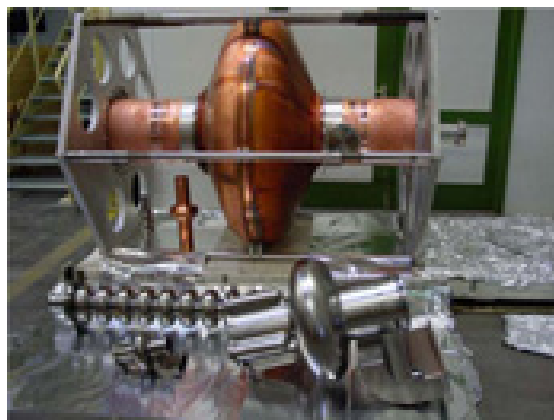
Figure 0.4: *A spectrum of superconducting cavities.*

0.3   Accelerator requirements and example systems

Superconducting cavities have found successful application in a variety of accelerators spanning a wide range of accelerator requirements. High current storage rings for synchrotron light sources or for high luminosity, high energy physics with energies of a few GeV call for acceleration voltages of less than 10 MV, and carry high CW beam currents up to one amp. Figure 0.5 [14] shows the accelerating structure based on a 500 MHz, single cell cavity that evolved for the Cornell storage ring CESR/CHESS. The cavity was fabricated from pure sheet niobium. Four such systems provide the needed voltage of 7 MV and beam power of more than

one MW. Similar systems are under construction to upgrade the beam current of the existing Taiwan Light Source (SRRC), and for the new Canadian Light Source (CLS). The accelerating gradient choice for all these cases is 7 MV/m or less.
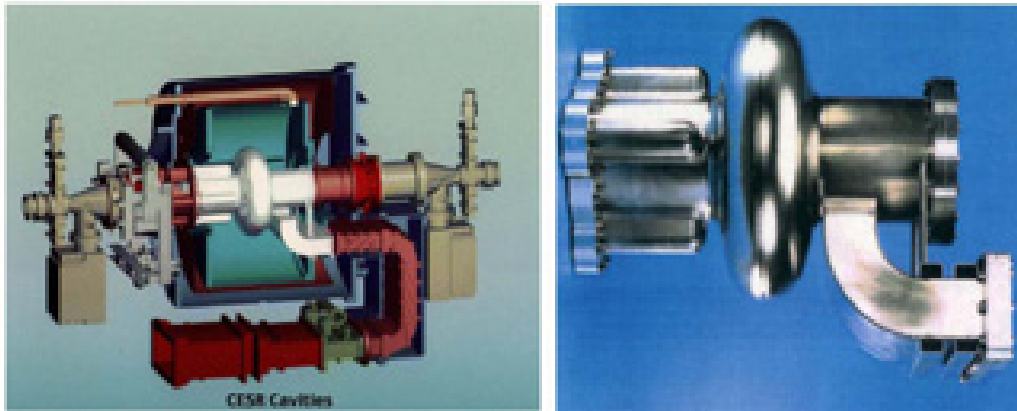
Figure 0.5 *(Left) 3D-CAD drawing of the CESR superconducting cavity cryomodule . (Right) 500 MHz Nb cavity.*

Near the energy frontier, LEP-II at CERN called for an accelerating voltage for nearly 3 GV to upgrade the beam energy from 50 to 100 GeV per beam, with a beam current of a few mA. With a frequency choice of 350 MHz, dominated by higher order mode (HOM) power loss and beam stability considerations, a 4-cell structure emerged [15]. To build 300 such units there was considerable savings in material cost by fabricating the cavity out of copper and coating it with niobium by sputtering. The LEP-II cavities (Figure 0.6) operated successfully at an average gradient of 6 MV/m.

Figure 0.6: *A 4-cell, 350 MHz Nb-Cu cavity for LEP-II*

A one GeV CW linac forms the basis for CEBAF, a 5-pass recirculating accelerator providing 5-6 GeV CW beam for nuclear physics [16]. The total circulating beam current is a few mA. Developed at Cornell, the 5-cell, 1500 MHz cavities (Figure 0.7) are also fabricated from solid sheet niobium. CEBAF cavities operate at an average accelerating field of 6 MV/m.

Figure 0.7: *A pair of 5-cell Nb cavities developed at Cornell for CEBAF*

All the above accelerators run CW at 100% duty factor. The first pulsed superconducting linac will be for the Spallation Neutron Source (SNS) at Oak Ridge. 6-cell niobium cavities at 804 MHz will accelerate a high intensity (≈10 mA) proton beam from 200 MeV to 1000 MeV. Figure 0.8 shows the medium β =0.64 cavity that resembles a β = 1 cavity that is squashed [17]. The duty factor for SNS is 6% and the RF pulse length is one ms. With recent improvement in cavity gradients the anticipated gradient is near 15 MV/m. Besides spallation neutron sources SNS technology could become suitable for high intensity proton linacs for various applications, such as transmutation of nuclear waste or generation of intense muon beams.

Figure 0.8: *b = 0.6, 6-cell cavity for SNS, frequency 804 MHz*

The dream machine for the future will be a 500 GeV energy frontier linac colliding electrons and positrons, upgradable to one TeV. As we will see, refrigerator power considerations drive the duty factor of operation to one percent. The average beam current is about 10 µA. A 9-cell niobium cavity design (Figure 0.9) has emerged from the TESLA collaboration [18]. With gradients improving steadily over the last decade, the choice of 25 MV/m will lead to 20 km of cavities for the 500 GeV machine. TESLA technology is likely to become the basis for the free electron lasers providing high brightness beams with wavelengths from the infra-red to ultraviolet and ultimately x-rays.

Figure 0.9: *1300 MHz 9-cell cavity for TESLA*

For the far future, acceleration of muons will also benefit from superconducting cavities [19]. A neutrino factory providing an intense neutrino beam from decaying muons may be the first step towards a muon collider that will penetrate the multi-TeV energy scale. At low energies (< a few GeV), where the muons have a large energy spread, the RF frequency has to be very low, e.g 200 MHz, leading to gigantic structures. Once again economics will favor thin film Nb-Cu cavities over sheet Nb cavities. For comparison, a single cell Nb-Cu cavity at 200 MHz (Figure 0.4) dominates the size of superconducting cavities for the variety of accelerator applications discussed.

0.4   6 GHz cavities

People study the effectiveness of innovative surface treatments, new thin film deposition techniques, new suprconducting materials for rf applications using samples. Their rf characterization is an useful diagnostic tool to accurately investigate local properties. However a common limitation of the systems used often consists in the difficulty of scaling the measured results to the real resonator [20; 21].

0.4.1   Application

The rf performance testing of a sample and its extrapolation to the frequency of a cavity is and will always remain an indirect way of measuring superconducting rf properties. Obviously the most direct way to test rf properties would be the use of cavities but 1.5 GHz resonant structures would be too onerous both for the material cost and the cryogenic expense. The idea was to build micro cavities completely equal in shape to the real scale model.

Using 6GHz cavities is possible to perform a high numbers of rf tests reducing research budget. RF measured samples will never be comparable to a real large cavity. It is always an indirect measurement. 6 GHz cavities are at the same time easy to handle like a sample but they are "real" cavities.

They are made from larger cavities fabrication remaining material using spinning technology, they don't need welding (even for flanges) and finally they can be directly measured

inside a liquid helium dewar. While 1,3 – 1,5 GHz cavities need no less than 1 week time preparation for the RF test. With 6 GHz cavities it is possible to perform more than one rf test per day.

With a tool like this it is possible to study traditional and innovative surface treatments and to perform rf tests on a large amount of cavities with a research budget much lower than the one necessary to treat and tests real cavities. It is also possible to study new thin film superconducting materials grown for example by sputtering or thermal diffusion.

0.4.2   Geometry
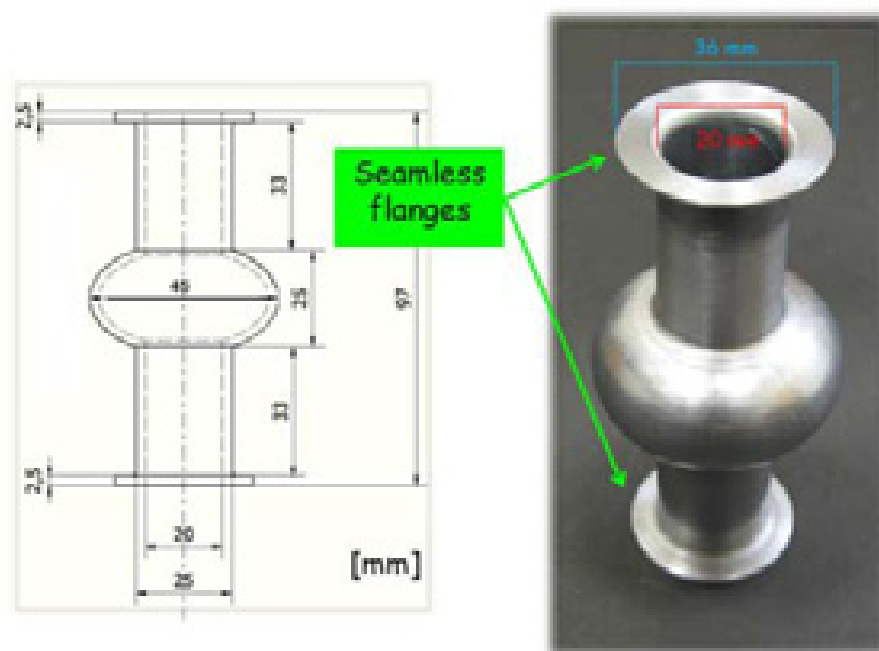
Figure 0.10: *The 6 GHz cavity geometry.*

6 GHz cavities are 97 mm long and have a 45 mm diameter cell, an electrical length of 25 mm and the same shape as a large resonator. They have two large flat flanges at the ends. For each of them the available surface to ensure the vacuum sealing is equal to 7 cm^2.

0.4.3   Fabrication technique

6 GHz cavities are made using the spinning technology (Figure 0.11). it can be used, also for real resonators.

High beta superconducting cavities are commonly manufactured by spinning two half-cells, which are then electron-beam welded together from the inside. Welding is a complicated

and costly operation that places severe limitations on the fabrication of high frequency cavities due to the narrow size of the bore.

At the National Institute of Nuclear Physics in Legnaro (LNL-INFN) [22] the well-known spinning technique has been adapted to form a fully seamless resonator without electron beam welding. In this way, starting from a disk or a seamless tube, it is possible to build seamless cavities with no intermediate annealing, more rapidly, simply, and with a uniform thickness. Both 1,5 GHz niobium and copper cavities can be easily manufactured with high reproducibility and significant savings in manufacture costs.
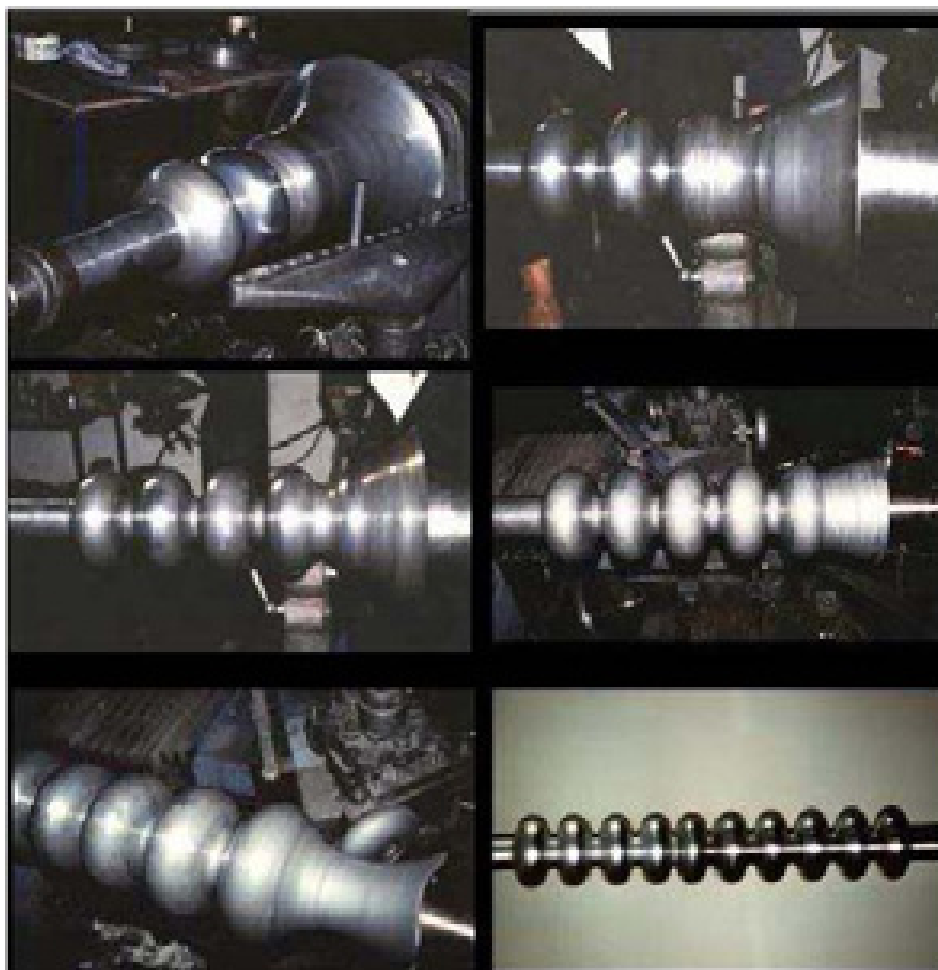
Figure 0.11: *Snapshots of a 9cell cavity during the spin moulding.*

The 6 GHz cavities produced by spinning are obtained using larger cavities fabrication remaining material (scraps) as shown in Figure 0.12.
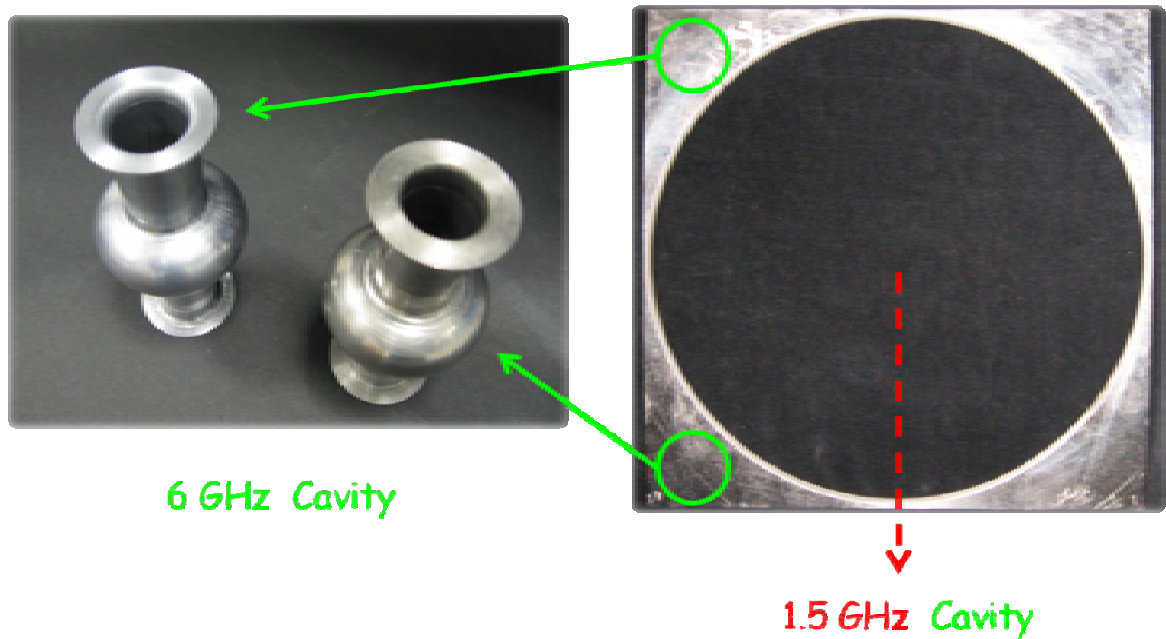
Figure 0.12: *On the right a scrap, of a large Nb cavity, from which are obtained 4 small 6 GHz resonators from the 4 corners.*

0.4.4 Summary

6 GHz cavities don't need any kind of electron beam welding (even for flanges) as shown in Figure 0.10, finally their production requires a short fabrication time, half a day per cavity. For these reasons it is possible to control the costs of production and to realize a large amount of cavities (Figure 0.13) with a low research budget.
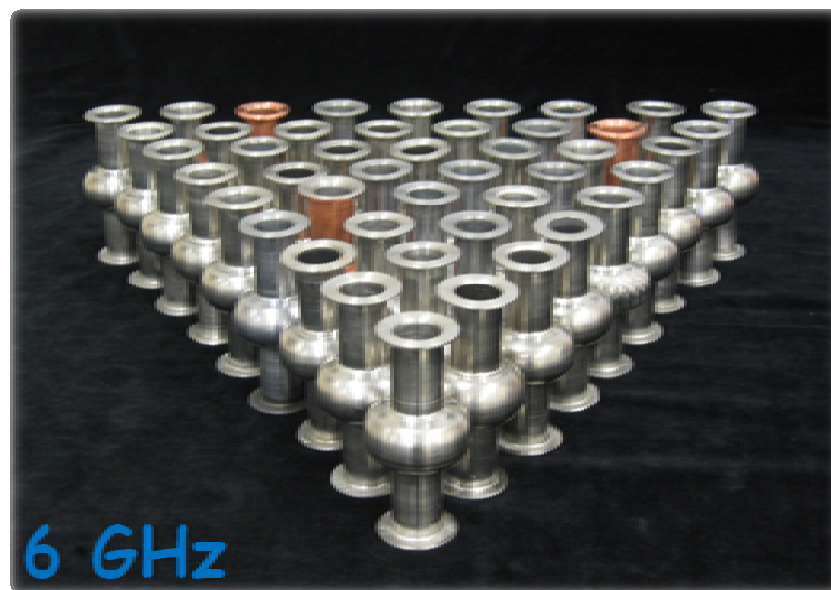
Figure 0.13: *"A great army of small soldiers"*

Using rf characterization of superconducting samples would be an useful diagnostic way to accurately investigate local properties of a bulk superconductor, of the grown superconducting films and given surface treatments on them.

However, common limitations of systems used for RF characterization of superconducting samples, often consist in the difficulty of samples preparation and scaling up the measured results to the real resonator.

Obviously the most direct way to test RF properties of a superconductor would be the use real size cavities, but 1.5 GHz resonant structures would be too onerous both for costs and time consuming.

✓ For chemical surface treatments it is necessary to use a huge quantity of acids: they are expensive and dangerous.

✓ Experimental infrastructures are big and pricy, in particular the cryogenic apparatus. It is complex and it has to be filled with more than 400 litres of liquid helium for a single RF test.

✓ Moreover the RF testing procedure takes a long time. It includes the cavity pumping, bake out, cooling at 4,2 K and cooling at 1,8 K. Generally to perform only one RF test one week is not enough!

Therefore the idea to build micro-cavities completely equal in shape to the real scale model brings a lot of opportunities. In Figure 0.14 is illustrated accordance of rf superconducting properties of samples and superconducting 6 GHz cavities to reality. Any sample extrapolation will be far from the accuracy obtainable with a real superconducting resonator like a 6 GHz cavity.

Figure 0.14: *A visual of accordance to reality of RF properties of superconducting samples and superconducting 6 GHz cavities. Any sample extrapolation will be far from the accuracy obtainable with a real superconducting resonator like a 6 GHz cavity.*

1   Electropolishing fundamentals

Electropolishing (EP) is a process in which a metallic surface is made smoothed by anodic dissolution [23]. The discovery of EP goes back to the beginning of the 20th century [24; 25]. Jacquet was the first to investigate EP systematically and received a patent in the 1930s [26]. Today, EP is a well-developed method divided into various research branches such as the practical applications including medical device fabrication and mechanical deformation-free preparation of metals for imaging in transmission electron microscopy (TEM), and the fundamental researches including the mechanism investigation and quantitative simulation.

1.1   Macrosmoothing and microsmoothing

In the literature, EP regimes are commonly referred to as anodic leveling and brightening, or macrosmoothing and microsmoothing [23; 27]. Meanings of macrosmoothing can be the elimination of roughness with heights over 1 μm, and microsmoothing to the elimination of roughness under 1 μm. However, the distinction of macrosmoothing and microsmoothing based on roughness is just a simplification. The value of 1 μm is not a criterion. There is no simple correlation between profile heights measured by mechanical means such as profilometry and that corresponding to optical brightness testing [28].

It is thought that different mechanisms are suitable for macrosmoothing and microsmoothing [23; 29; 30; 31; 32]. Macrosmoothing results from the higher current leading to the higher local dissolution rate on peaks. This is under an ohmic control (or voltage control). Theoretical prediction of local macrosmoothing rate based on the Nernst diffusion layer model is in good agreement with experimental results.

Microsmoothing on the other hand results from the suppression of the influence of surface defects and crystallographic orientation on the dissolution process [23]. Microsmoothing is the final finish of EP. The mechanism of microsmoothing is rather complex [26; 33; 34]. It is accepted that microsmoothing occurs under mass transport limiting current with the presence of an anodic film on the metal surface [35; 36; 37; 38; 39]. About the nature of anodic film, some researchers favor a thin compact salt film consisting of an oxide contaminated with significant amounts of anions from solution, and others favor a highly viscous and anhydrous film. Only the metal ion is mobile in the anodic salt film. One performing EP usually wants to achieve both macrosmoothing and microsmoothing, but in practice it is possible to only achieve macrosmoothing without microsmoothing and vice versa [40].

1.2   Nernst diffusion layer

Figure 1.1 is a schematic diagram of the Nernst diffusion layer model under ideal conditions [23]. The macrosmoothing rate is equal to the difference in dissolution rate between peaks and valleys of a rough surface. The difference in dissolution is determined by the local current distribution along the surface profile [23]. An arbitrary two-dimension surface profile is treated as a Fourier sine series [41]. The corresponding parameters are: the initial profile height ε_0, the wavelength λ, and the diffusion layer thickness δ. When $\delta \gg \varepsilon_0$, the interface between the diffusion layer and the bulk electrolyte will be flat. The difference in distance from the metal surface to the interface – for example in Figure 1.1, AB < CD – results in a difference in resistance, that is, $R_{AB} < R_{CD}$. The current density at point A (peak) is larger than that at point C (valley), resulting in the reduction of peak heights typically > 1 μm. If $\varepsilon_0 \gg \delta$, the diffusion layer will follow the surface profile in a perfect way as shown by the broken line in Figure 1.1. In this case, there is no difference in resistance along the surface, in Figure 1.1 for example, AB' = CD' => $R_{AB'} = R_{CD'}$. The current density is uniform, i.e. no profile flattening. The wavelength λ also contributes to the macrosmoothing rate. Wagner and McGeough conclude that the larger the ratio of λ/ε_0, the smaller the smoothing rate [41; 42].
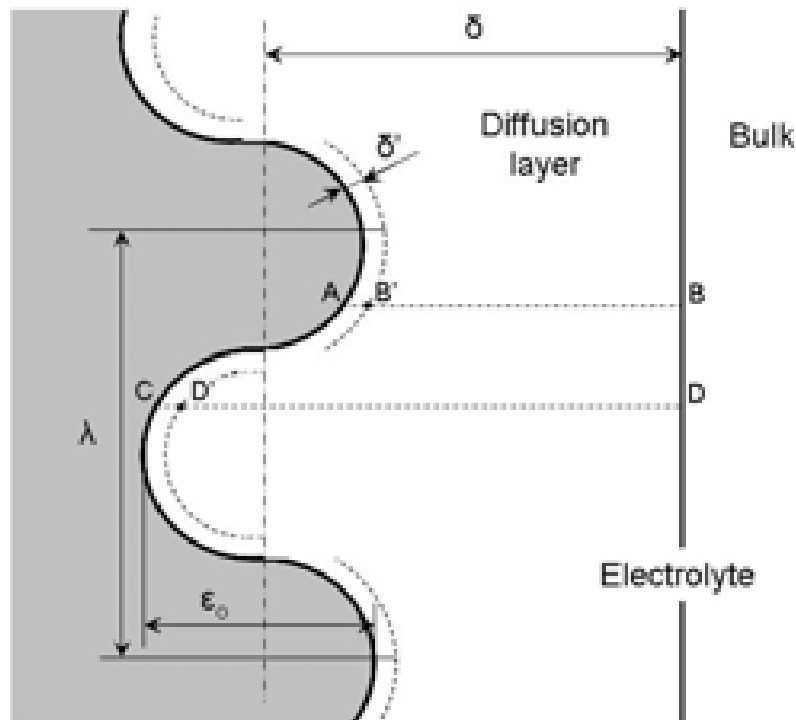
Figure 1.1: *Schematic diagram of the Nernst diffusion layer model* [23].

1.3   Mass transport mechanism

Mass transport is the only condition that leads to microsmoothing. Figure 1.2 summarizes the three possible mass transport mechanisms proposed in the literature [23]. Mechanism 1 – salt precipitation - considers rate limiting diffusion of cations (M^+) of the dissolving metal from the anode to the electrolyte. During EP within the limiting current region a salt film presents on the anodic surface where the concentration of M^+ in the salt film is equal to the saturation concentration. The anions (A^-) from the electrolyte also accumulate within the anodic film to maintain the electro-neutrality. Mechanism 2 – acceptor anion limited – is limited by the transport of acceptor anions (A^-) to the metal surface. Mechanism 3 – hydrogen limited – considers the diffusion of water from the electrolyte to the anode as the rate limiting process. Regardless of the mechanisms, mass transport of the dissolved metal ions is the limiting factor responsible for the shift from surface etching to microsmoothing. In all these EP cases, the estimation of the surface concentration of the dissolving metal ions at the limiting current yields values in reasonable agreement with the saturation concentration.
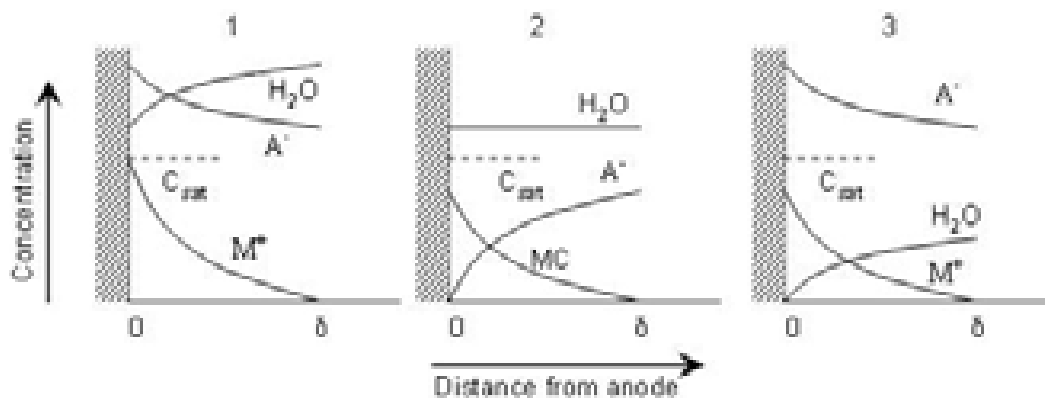
Figure 1.2: *Schematic diagram of three mass transport mechanisms involving (1) salt film, (2) acceptor, and (3) water as transport species. C_{sat} is the saturation concentration and δ is the thickness of Nernst diffusion layer* [35].

2   Niobium properties

2.1   Physical properties

Niobium is a transition metal of V group and fifth period. It is a chemical element that has the symbol Nb and atomic number 41. A soft, gray, ductile transition metal, Niobium is found in pyrochlore and columbite. It was first discovered in the latter mineral and so was initially named columbium; now that mineral is also called "niobite". Niobium is also used in special steel alloys as well as in welding, nuclear industries, electronics, optics and jewelry. In the family of superconducting element it has the highest critical temperature and its properties are collected in Table 2.1.

Atomic number	41
Atomic weight	92,9 g/mol
Atomic radius	2.08
Density	8570 kg m^{-3}
Crystalline lattice	b.c.c.
Space group	Im3m
a	3,3033
Electrical resistivity (300K)	14.9 $\mu\Omega$·cm
Thermal conductivity (300K)	53.7 W m^{-1}K^{-1}
Debye Temperature	275K
Melting Point	2741K
Critical temperature	9.26K
Density	8570 kg m^{-3}

Table 2.1: *List of the niobium properties*

2.2   Superconductive properties

Of the known practically usable superconductors, Nb has the highest bulk $\mu_0 H_{c1} = 170$ mT and, hence, is used for RF cavity applications. An overview of relevant material properties for Nb is presented in Table 2.2. The parameters are given at $T = 0$ K. Since Nb cavities will be mainly operated at about 2 K and derivatives for $T \rightarrow 0$ are zero, the zero temperature values can be expected to be sufficiently accurate. Nb cavities can exhibit a drop in Q_0 towards higher E_{acc}. This so-called *Q*-drop is not fully understood, but appears to be related to Nb-oxides at the cavity surface. For bulk cavities, the *Q*-drop can be significantly reduced by baking the cavity at about

500°C, which presumably redistributes the oxygen. For thin Nb film on Cu cavities the *Q*-drop cannot, for now, be prevented. The present state-of-the-art bulk Nb cavities exhibit, at *T* = 2 K, a Q_0 above 10^{10} until an E_{acc} of about 50 MV/m, at which point the cavities quench. Note that Nb cavities have to be operated in superfluid Helium (i.e. below 2.2 K) at frequencies above about 1 GHz, since at higher temperatures the BCS losses become too excessive.

An $E_{acc} \cong 50$ MV/m corresponds closely to the magnetic field limit for Nb. Differences between achieving H_{c1}, H_{sh} or H are virtually indistinguishable for Nb. Nevertheless, achieving the magnetic field limitation for Nb cavities means that Nb is exhausted for a further increase in the accelerating voltage.

Property	Nb
T_c [K]	9.2
$\mu_0 H_{c1}$ [T]	0.17
$\mu_0 H_c(0)$ [T]	0.2
$\mu_0 H_{c1}(0)$ [T]	0.4
$\xi_{GL}(0)$ [nm][1]	29
$\lambda_{eff}(0)$ [nm][2]	41
$k \cdot (0)$[3]	1.4
$\Delta(0)$ [meV][4]	1.4
ρ_n [$\mu\Omega$cm]	< 100(VERIFY!)

Table 2.2: *Characteristic superconductive parameters of Nb* [43]

2.3   Chemical properties

Niobium is in many ways similar to its predecessors in group 5. It reacts with most non-metals at high temperatures: niobium reacts with fluorine at room temperature, with chlorine and hydrogen at 200 °C, and with nitrogen at 400 °C, giving products that are frequently interstitial and nonstoichiometric [44]. The metal begins to oxidize in air at 200 °C [45], and is resistant to corrosion by fused alkalis and by acids, including aqua regia, hydrochloric, sulphuric, nitric and

[1] From $\sqrt{\phi_0 / (2\pi\mu_0 H_{C2}(0))}$

[2] From $\sqrt{\phi_0 \mu_0 H_{C2}(0) / (4\pi H_C^2)}$

[3] From $k(0) = \lambda_{eff}(0) / \xi_{GL}(0)$

[4] From $\Delta(0) = C k_B T_C$, assuming a week coupling limit for pure Nb

phosphoric acids [44]. Niobium is attacked by hot, concentrated mineral acids, such as hydrofluoric acid and hydrofluoric /nitric acid mixtures. Although niobium exhibits all the formal oxidation states from +5 down to -1, its most stable state is +5 [44].

Niobium is able to form oxides with the oxidation states +5 (Nb_2O_5), +4 (NbO_2) and +3 (Nb_2O_3), [45] as well as with the rarer oxidation state +2 (NbO) [46]. The most stable oxidation state is +5, the pentoxide which, along with the dark green non-stoichiometric dioxide, is the most common of the oxides [45]. Niobium pentoxide is used mainly in the production of capacitors, optical glass, and as starting material for several niobium compounds [47]. The compounds are created by dissolving the pentoxide in basic hydroxide solutions or by melting it in another metal oxide. Examples are lithium niobate ($LiNbO_3$) and lanthanum niobate ($LaNbO_4$). In the lithium niobate, the niobate ion NbO_3^- is not alone but part of a trigonally distorted perovskite-like structure, while the lanthanum niobate contains lone NbO_4^{3-} ions [45]. Lithium niobate, which is a ferroelectric, is used extensively in mobile telephones and optical modulators, and for the manufacture of surface acoustic wave devices. It belongs to the ABO_3 structure ferroelectrics like lithium tantalate and barium titanate [48].

Niobium forms halogen compounds in the oxidation states of +5, +4, and +3 of the type NbX_5, NbX_4, and NbX_3, although multi-core complexes and substoichiometric compounds are also formed [45; 49] Niobium pentafluoride (NbF_5) is a white solid with a melting point of 79.0 °C and niobium pentachloride ($NbCl_5$) is a yellowish-white solid (see image at left) with a melting point of 203.4°C. Both are hydrolyzed by water and react with additional niobium at elevated temperatures by forming the black and highly hygroscopic niobium tetrafluoride (NbF_4) and niobium tetrachloride ($NbCl_4$). While the trihalogen compounds can be obtained by reduction of the pentahalogens with hydrogen, the dihalogen compounds do not exist [45]. Spectroscopically, the monochloride (NbCl) has been observed at high temperatures [50].The fluorides of niobium can be used after its separation from tantalum [51]. The niobium pentachloride is used in organic chemistry as a Lewis acid in activating alkenes for the carbonylene reaction and the Diels-Alder reaction. The pentachloride is also used to generate the organometallic compound niobocene dichloride (($C5H5$)$_2NbCl_2$), which in turn is used as a starting material for other organoniobium compounds [52].

Figure 2.1: *Niobium pentachloride (NbCl$_5$)*

Other binary compounds of niobium include niobium nitride (NbN), which becomes a superconductor at low temperatures and is used in detectors for infrared light, and niobium carbide, an extremely hard, refractory, ceramic material, commercially used in tool bits for cutting tools. The compounds niobium-germanium (Nb$_3$Ge) and niobium-tin (Nb$_3$Sn), as well as the niobium-titanium alloy, are used as a type II superconductor wire for superconducting magnets [53; 54]. Niobium sulphide as well as a few interstitial compounds of niobium with silicon are also known [44].

2.4   Electrochemical properties

Nb is classical example of refractory metals. Thermodynamically Nb is very unstable so it is covered by strong film of oxides. Most stable is Nb$_2$O$_5$. On a Figure 2.2 is shown Pourbaix diagram which explains why there is no way to avoid oxide formation during Nb dissolving. Only one way how is possible to dissolve Nb is to break oxide film for example using fluoride anions. Table 2.3 shows reactions which can run according to Pourbaix diagram and gives their equations. Nb   situated   in   second   group   of   metals   overvoltage   [55] Electrodissolving/electroplating overvoltage is 10…100mV and exchange current density $10^{-3}…10^{-4}$A/cm^2.
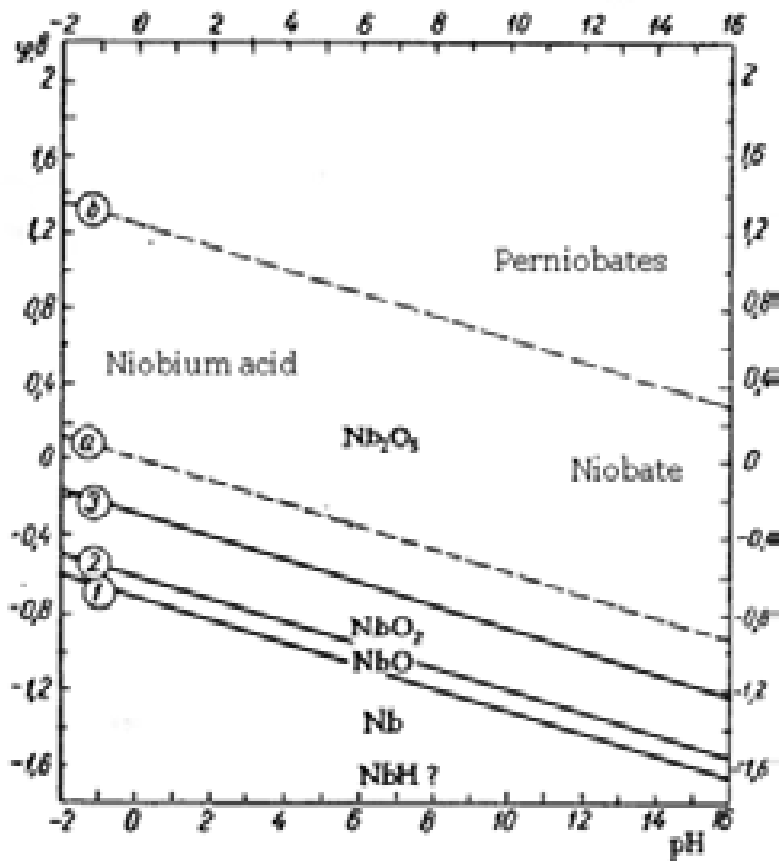
Figure 2.2: *Diagram E – pH for system Nb –H_2O; 1 – equilibrium Nb/NbO; 2 - equilibrium NbO/NbO_2; 3 - equilibrium NbO_2/Nb_2O_5; a – electrolytic hydrogen evolution; b – electrolytic oxygen evolution.*

№	Reaction	Line
1	$Nb+H_2O \rightarrow NbO+2H^++2e^-$	$E=-0,733-0,0591 \cdot pH$
2	$NbO_2+H_2O \rightarrow NbO_2+2H+2e^-$	$E=-0,625-0,0591 \cdot pH$
3	$2NbO_2+H_2O \rightarrow Nb_2O_5+2H+2e^-$	$E=-0,289-0,0591 \cdot pH$
a	$H^++2e^- \rightarrow H^{\bullet}$ $H_2O+e^- \rightarrow H^{\bullet}+OH^-$ $(2H^{\bullet} \rightarrow H_2)$	$E= -0,0591 \cdot pH$
b	$4OH^- \rightarrow 2H_2O+O_2+4e$ $4OH^- \rightarrow 2H_2O+O_2+4e$	$E= 1,23 - 0,0591 \cdot pH$

Table 2.3: *Reaction which are present on Figure 2.2.*

№	Reaction	$E^{0,}$ V
1	$4OH^- \rightarrow 2H_2O + O_2 + 4e$	+0,8
2	$2Cl^- \rightarrow Cl_2 + 2e$	+1,35
3	$ROH + e \rightarrow RO^{-\bullet} + H^\bullet$	0,0
4	$2H_2O + O_2 + 4e \rightarrow 4OH^-$	-0,4
5	$Nb_3^+ + 3e- \rightarrow Nb$	-1,1
6	$RNH_2 + e \rightarrow RNH^{-\bullet} + H^\bullet$	
7	$Nb \rightarrow Nb^{5+} + 5e^-$	-0,96
8	$Nb \rightarrow Nb^{3+} + 3e^-$	-1.1
9	$2Nb + 5Cl_2 \rightarrow 2NbCl_5$	-
10	$NbCl_5 + 4H_2O \rightarrow 5HCl + H_3NbO_4$	-

Table 2.4: *Reactions which can run on Nb electrode and their potentials.*

Niobium is totally passivated in urea melts. Its passivation in urea-chloride melt is also rather strong and the depassivating action of Cl⁻ ions is insufficient do dissolve this metals [56; 57]. The electrochemical behavior of Nb dissolution in urea-chloride melt has some features. There is no Nb dissolution during first polarization (Figure 2.3, curve 1). Earlier was shown that only after reaching transpassive potential region, where a reactive compound (presumably *NCl₃*) is formed which is the electrode surface depassivator, Nb dissolution wave appears at the backward sweep. Nb dissolution may be observed at the forward sweep in subsequent cycles (Figure 2.3, curves 2-4). The cathodic reduction of *Nb(V)* ions formed in the melt upon electrochemical dissolution takes place only in *Nb* electrode (in contrast to inert *Pt* and glassy carbon electrodes) after electrode prepolarization to the anodic region. The cathodic wave corresponds to the recharge of *Nb(V) – Nb(IV)* ions. We failed to detect the formation of ions in the lowest oxidation state(by electrochemical spectroscopic methods). *Nb(V) – Nb(IV)* ions are in the melt in the form of chloride complexes, such as *[NbCl₆]⁻* and *[NbCl₆]²⁻*.
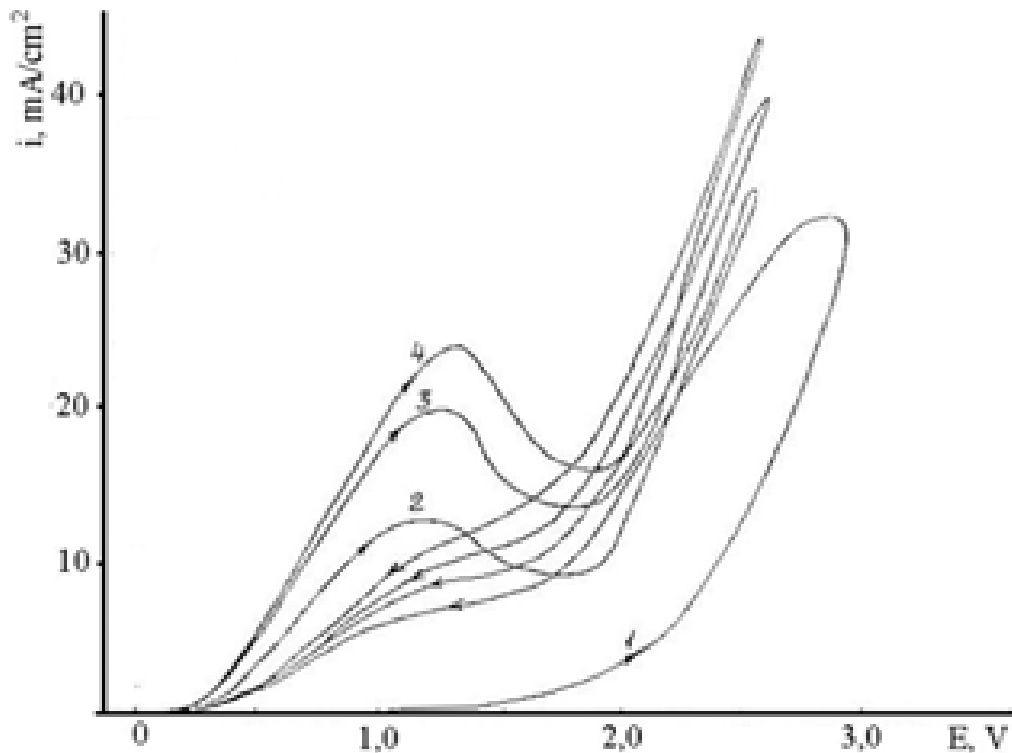
Figure 2.3: *The anodic part of the cyclic voltammogram taken at a Nb electrode in the urea-NH$_4$Cl melt, t-130 °C, scan rate 0,1 V/s*

2.5   Techniques of Nb surface finishing

To improve the cavity performance it is necessary to reduce the surface resistance as much as possible. To achieve this goal each Nb cavity undergoes to a series of successive treatments (mechanical polishing, buffered chemical polishing, electropolishing, annealing). They will be described in detail in chapter 3 .

Due to the pillbox-like shape of the cavity, chemical or electrochemical etching is the most efficient technique for Nb surface finish. Etching to a depth of 100 to 400 μm is believed to be enough to remove the mechanically damaged layer [58]. Two widely practiced etching techniques are buffered chemical polishing (BCP) and electropolishing (EP) [59]. A BCP process is usually performed in a typical solution of 1:1:1 or 1:1:2 (volume ratio) HNO$_3$ (69%), HF (49%), and H$_3$PO$_4$ (85%). The process is performed for a time sufficient to remove the layer containing mechanical damage and contaminations. BCP commonly results in Nb dissolution at a rate of 10 μm/min and a final surface roughness of 2 to 5 micron [60; 61].

The final surface finish is EP [62]. Cavity fabrication by EP is also known as "Siemens method" because it was Siemens Company that firstly employed EP to treat SRF cavity surface in the 1970s. Researchers in KEK further developed this technique and claimed that the

improved SRF cavity performance – such as the higher acceleration gradient – would be achieved by EP over BCP [63]. This discovery has been confirmed by other laboratories that were also investigating this process [16]. The currently accepted EP process for Nb surface treatment is performed in a solution of HF (49%) and sulfuric acid electrolyte (98%) at volume ratio of 1:8 to 1:10. During the EP, the Nb cavity is polarized anodically in an electrolytic cell at temperature of 30°C to 40°C. The cathode is an aluminum rod with high purity. The area ratio of anode and cathode is 10:1.The applied voltage is usually from 12 to 25 V and causes a current density of 30 to 100 mA/cm^2 [64]. EP results in a corrosion rate—around 0.5 μm/min—that is lower than BCP but with a much better surface finish, especially at a microscopic scale. It has been accepted widely that the best EP condition occurs under the voltage within the range of limiting current plateau and that parameters such as electrolyte concentration, electrolyte temperature, and viscosity strongly impact the surface finish [65; 66].

2.5.1   Hydrofluoric acid-based system

Nb performs a large negative free energy and is highly reactive toward oxygen [67; 68; 69]. In an aqueous electrolyte, it is easy for Nb to react with water molecules to form non soluble niobium pentoxide (Nb_2O_5) by the reaction:

$$2Nb+5H_2O \rightarrow Nb_2O_5+10H^++10e^- \tag{2.1}$$

The thickness of oxide layer with Nb_2O_5 is about 2 to 6 nm [70]. Suboxides such as NbO_2, NbO, and Nb_2O are observed to form between the Nb_2O_5 outer layer and the underlying Nb surface [71]. In additional to its negligible solubility in water, Nb_2O_5 is difficult to dissolve in majority of acids as well. The oxides form a stable protective film on metal surface, thus prevent further polishing of the metal surface during EP in aqueous electrolytes [72].

Hydrofluoric acid (HF) has good ability to destabilize Nb_2O_5 with the following reactions to form soluble niobium fluorides and niobium oxifluorides:

$$Nb_2O_5+14HF \rightarrow 2H_6NbO_2F_7+H_2O \tag{2.2}$$
$$Nb_2O_5 +12HF \rightarrow 2HNbF_6+5H_2O \tag{2.3}$$
$$Nb_2O_5+10HF \rightarrow 2NbF_5 + 5H_2O \tag{2.4}$$
$$Nb_2O_5+10HF \rightarrow 2H_6NbOF_5+3H_2O \tag{2.5}$$
$$HNbF_6 + HF \rightarrow H_2NbF_7 \tag{2.6}$$
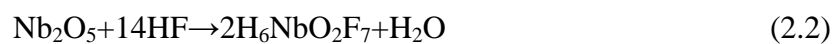
The presence of HF is necessary in practical electrolytes for EP processes of Nb. However, for a one single-cell cavity (e.g., the 1.5GHz single-cell cavity in Jefferson Lab) treatment at least needs 1 liter of HF is used. It must be carefully managed to prevent human

exposure and must be disposed in environmentally appropriate way. At present, about 300 five- to nine-cell cavities are processed per year in Jefferson Lab. This is a manageable concern. However, ILC will require the operations capable of processing over 20000 nine-cell cavities per year. The tremendous cost of managing large amounts of HF demands the development of HF-free electrolytes.

2.5.2 Sulfuric acid-methanol electrolytes

One of alternatives found for Nb electropolishing is sulfuric acid solution in methanol. Methanol is wildly used as a solvent instead of water [73; 74]. Piotrowski et al report the successful EP of tantalum (Ta) and Titanium (Ti) by sulfuric acid-methanol electrolytes [75; 76]. The nature of sulfuric acid-methanol electrolytes is still under investigation. The best surface finishing was obtained under mass transport limiting current. The value of limiting current decreased as the concentration increased and the temperature decreased [75; 76]. The observed current decrease with increasing concentration is suggested to be due to the corresponding decrease in solubility of metal ions. Compact film was characterized to explain the mass transport mechanism. One of the advantages of methanol-based electrolyte is the much-decreased water content; therefore, the formation of Nb_2O_5 is expected to be avoided. Piowtroski observed the current reduces by adding water into the methanol-based electrolyte – when the water content in a 3 M sulfuric acid-methanol electrolyte increased from 0.02wt% to 5wt%, the current during Ti EP decreased approximately 75 percent (about 0.8 A/cm^2 to 0.2 A/cm^2). When the water content reached 10wt%, the Ti anode became passive. It is important to use sulfuric acid with a weight ratio as high as possible and prevent it from water condensing from air. On the other hand, Nb has a very close chemical property to Ta, so it is promising to electropolish Nb in the methanol-based electrolyte.

3   Standard surface treatment of 6 GHz cavities

3.1   Tumbling

The spinning process implies material surface defects, stress and dislocations. The cavity cell is characterized by the presence of evident vertical scratches due to the used mandrel. Obviously the internal surface finishing of a resonant structure is directly correlated to its performance, especially at high fields. Moreover the lubricant, necessary for the metal mechanical processing can contaminate the used material. The idea is to make the surface smooth and free from contaminants.

In order to remove surface roughness and contaminations introduced during the spinning process, we use a compact and portable tumbler in spite of the bigger and complicated designed ad hoc for large cavities.
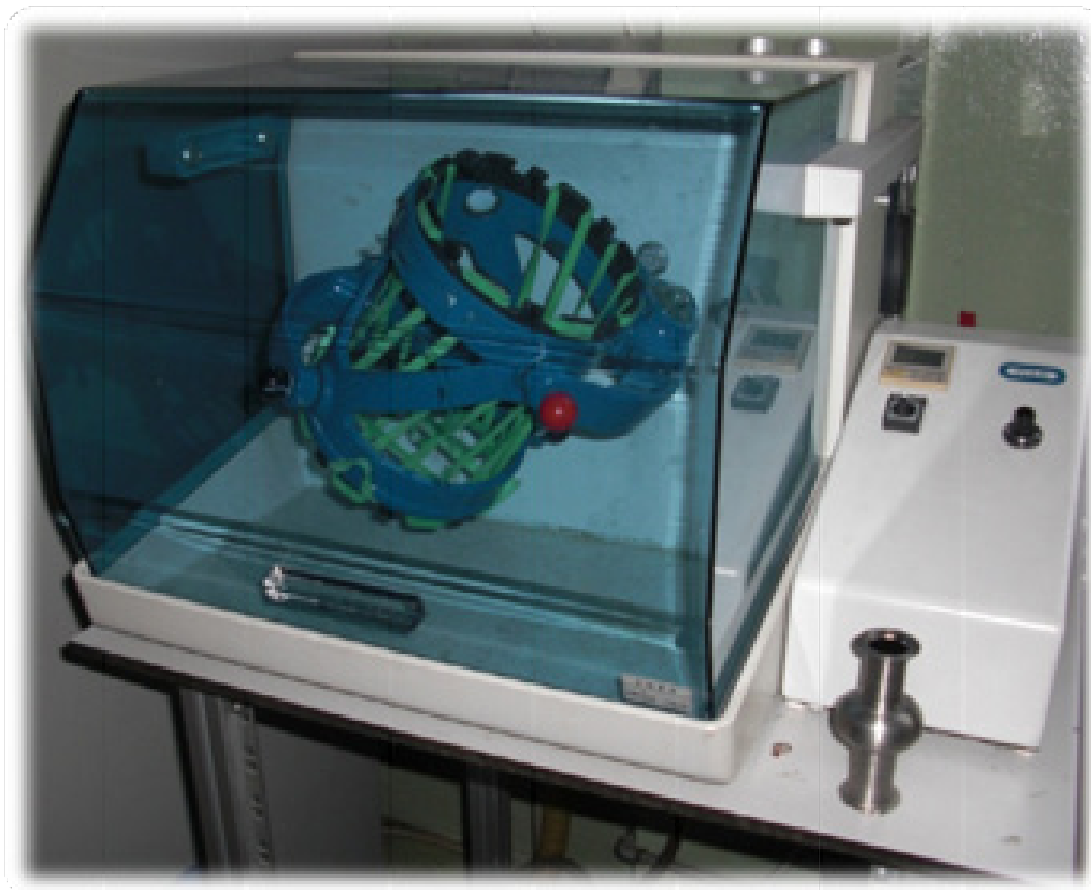
Figure 3.1: *Compact tumbling system for small resonators.*

The 6 GHz cavity is filled with a certain number of abrasive agent pieces (media) Figure 3.2, plugged up and fixed to the machine. The tumbler makes the cavity rotate so that the small media pieces can erode the metal surface in a uniform, controllable and reliable way.

Different materials could be used for this kind of mechanical polishing: for example small SiC triangular shaped blocks, 5 mm sphere of yttria stabilized zirconium dioxide and flakes of Al_2O_3 and SiO_2 powders embedded in a polyester matrix.
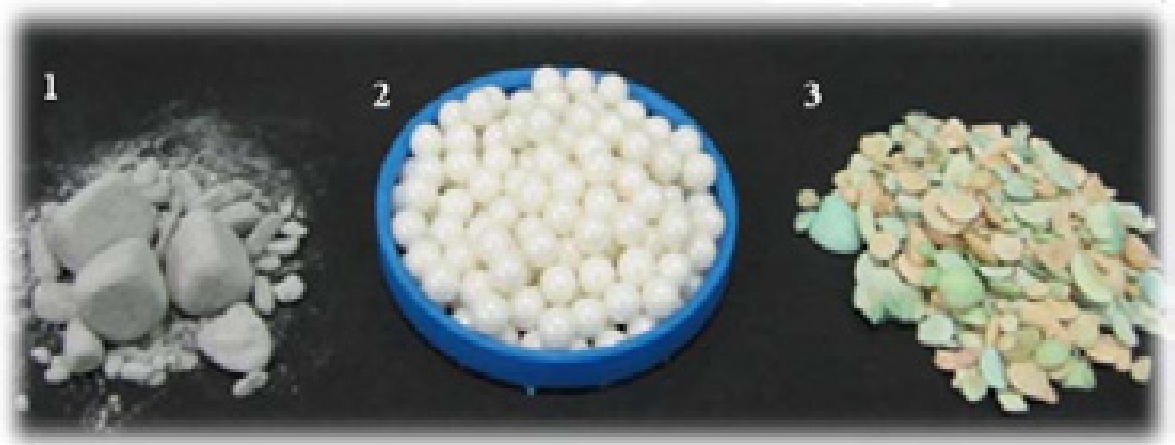
Figure 3.2 *Three types of different abrasive media.*

1 – SiC; 2 – ZrO_2; 3 – Al_2O_3 + SiO_2

Silicon carbide is a very hard material and it can be used for the first low level mechanical polishing. ZrO_2 is a high density material and can be used for the intermediate smoothing. Al_2O_3 plus SiO_2 (in PET) flakes are soft and can be used for the final surface finishing.

During a mechanical treatment, for each cavity, it is easy to stop the process and monitor the smaller resonator weight change with a balance and internal surface finishing with the help of a miniature camera (visible on Figure 3.3).
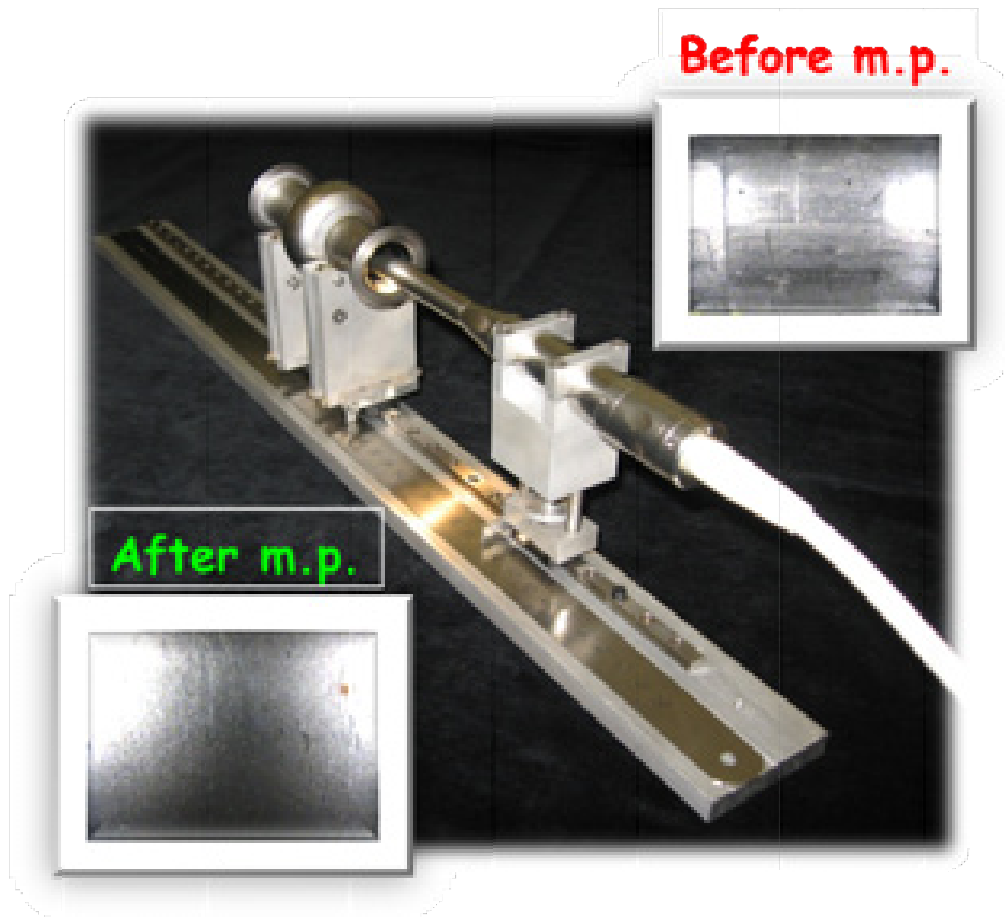
Figure 3.3: *The miniature camera tool used for the cavity inspection.*

The idea is to check an eventual defect evolution after each polishing treatment without any risk to touch the small cavity internal surface. It is composed by two different parts: a computer interfaced firm base and a mobile tool equipped with the optical and lighting devices. They are connected by an optical fibers cable. The acquired images magnification is around 60x. Positioning the mobile tool near the point of interest, focusing and eventually correcting the lightening are the only necessary operations to obtain the desired image. To make the tool positioning on defects reliable a support system has to be used. The latter is equipped with a fixed protractor, so the resonator rotation angle (relative to its axis) can be easily measured. The miniature camera tool can be moved forward, backward, up and down inside the cavity. The tool displacement along the cavity axis can be easily measured with the ruler fixed to the system basis.

Using this procedure it's easy to choose the right media and to establish the right treatment duration to perform the best internal surface finishing in a few steps.

On the top part on the right a picture of the cavity cell before the mechanical polishing. On the bottom part on the left a picture of the same place of the cell after the mechanical

polishing. The surface after the treatments appears smoother than before. The vertical scratches due to the used mandrel have disappeared.

3.2 Lapping

After all mechanical operations follows cavities flanges preparation. Flanges surface must be flat and polished to prevent leaks on cavities rf testing stand. For this aim is using polishing circle with different abrasive papers wetted with water. First is paper 400 for rough treatment which produces flat surface. Next will go 600, 800, 1000 which will decrease roughness. Final is 1200 with using alcohol instead of water. After lapping is necessary to make precise washing of cavity in ultrasound bath with soap in few steps and rinsing.

Figure 3.4: *Lapping plant.*

Figure 3.5: *Difference between flanges surface before(1) and after(2) lapping.*

3.3   BCP

Following the classical and well known surface treatments general protocol of large cavities, after the mechanical polishing the procedure counts a chemical polishing. Chemical treatments are performed to smooth further on the cavity surface, to remove the possible niobium sub-oxide and contaminants.

To perform the traditional surface chemical treatments, buffer chemical polishing (BCP) and electrochemical polishing (EP), on a 6 GHz cavity can be used a small system as the one reported in Figure 3.6.

In particular can be seen on the right a 6 GHz cavity installed in vertical position, equipped with special flanges for EP. The acid flux is directed from the bottom to the top of the cavity in order evacuate the hydrogen, produced during the process, quickly. The 3-way valves are useful to invert the flux direction.
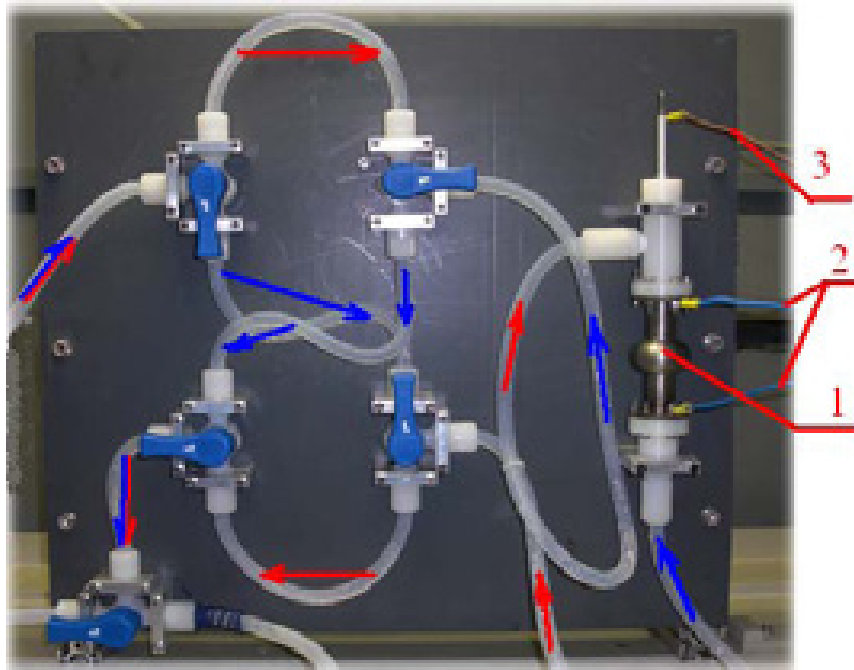
Figure 3.6: *Stand for BCP and EP.*

1 – cavity; 2 – anode contacts; 3 – cathode contact; Blue indicator – direct flow, red – indirect.

For buffer chemical polishing are used simple holed PVDF flanges as is shown in Figure 3.7.
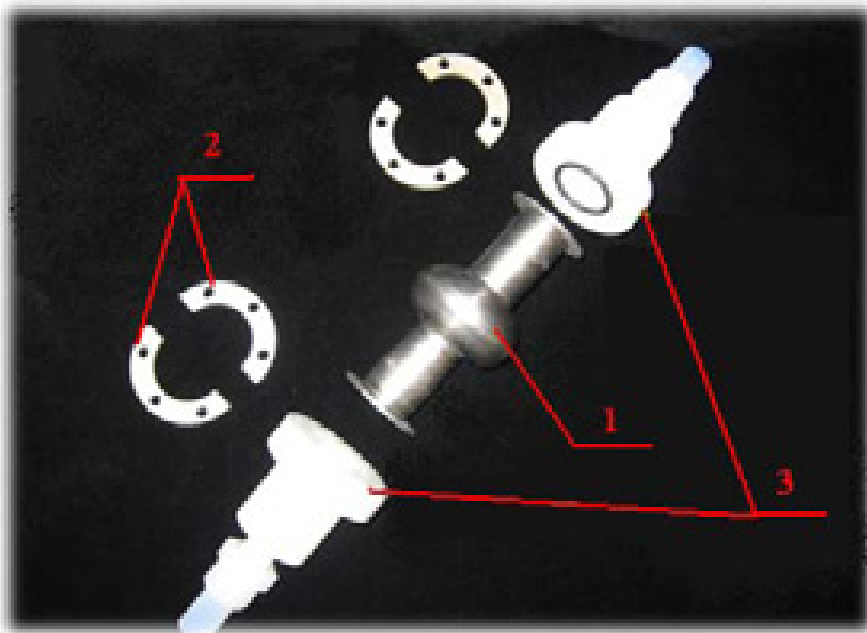
Figure 3.7: *Details of the cavity closing system for buffer chemical polishing.*
1- 6GHz cavity;2 – SS half round rings; 3 – BCP flanges.

In the case of electrochemical polishing are used particular PVDF flanges able to hold a aluminum cathode conveniently designed as reported in Figure 3.8.

The flanges are expressly designed to obtain the highest acid flow through the cavity to allow hydrogen bubbles, produced during the oxi-reduction reaction, to escape freely.

The evaluations of damaged layer thickness produced by the spinning process could be vary from 150 to 250 μm. For this reason it is convenient to remove with BCP/EP at least 300 μm: in average this thickness corresponds to about 30 g of removed material.

3.4   EP

6GHz cavities are polished on classical EP solution with acid ratio HF:H_2SO_4 . During the process solution is pumped throw the cavity from bottom part to top part for a easier removing hydrogen from the cavity which is forming on cathode. After the half of process time cavity is swapped the position on 180 for flux substitution. Controling parameter of EP process is electrical tension between cathode and cavity. Usually electrical tension is 10…20V.
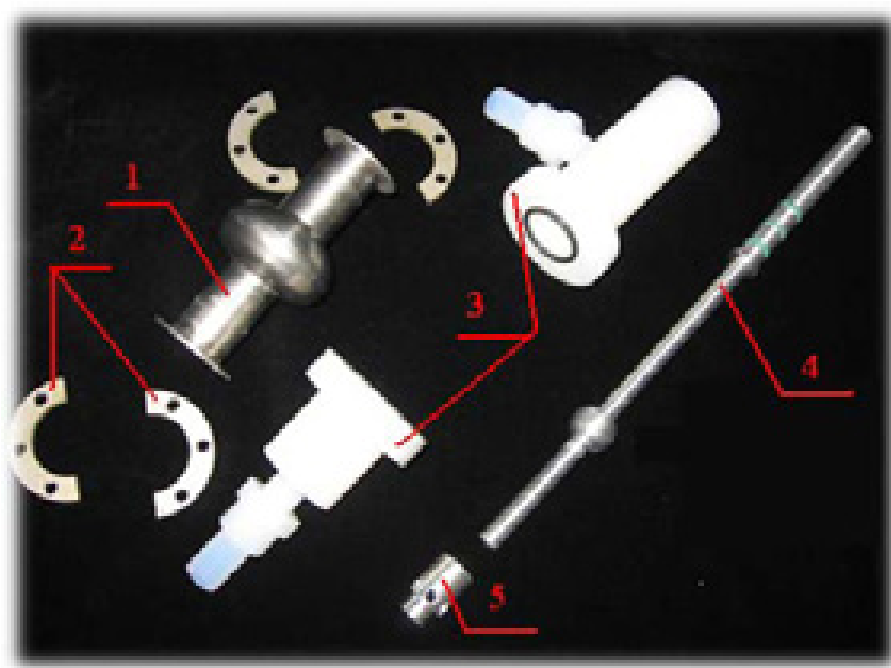
Figure 3.8: *Details of the cavity closing system for electropolishing.*
1 – 6GHz cavity;2 – SS half round rings; 3 – EP flanges; 4 - aluminum cathode; 5 –

holed guiding ring

Figure 3.9 shows an example of EP process result on 6GHz cavity which was produced and electropolished in SC laboratory in LNL INFN.

.
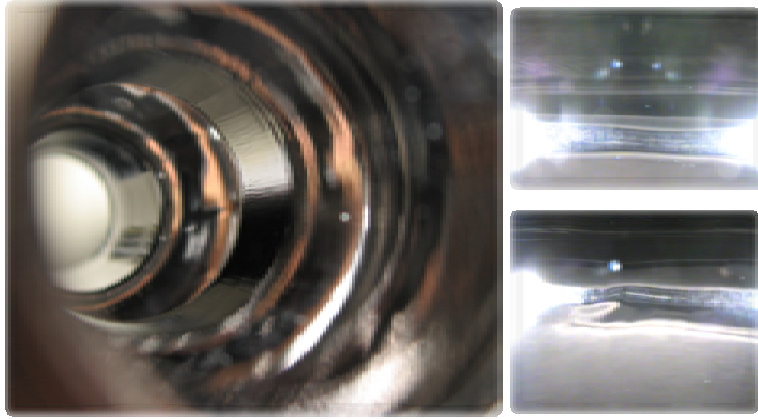
Figure 3.9: *EP result obtained in 6GHz cavity*.

4   Apparatus and procedures

4.1   Potentiostat instrumentation

A potentiostat is an instrument that provides the control of the potential difference between the working electrode and the reference electrode [77]. The potentiostat implements this control by applying current into the cell between the working electrode (WE) and the counter electrode (CE) until the desired potential between the working electrode and the reference electrode (RE) is reached. Figure 4.1 shows the schematic diagram of a potentiostat with computer control.

In an electrochemical cell for EP, the working electrode is the electrode to be polished. A well-working reference electrode should have a constant electrochemical potential. In this work Nb wire using like a RE. It is not the best reference but is simple and it is enough to understand kinetic especially when potential reaches to 20V. The counter electrode completes the cell circuit. In this work graphite rod was used like CE. Working electrode for this work was made from 3mm diameter Nb rod which was isolated on lateral surface with epoxyresin. Bottom part of electrode was polished in way which is using for 6GHz cavities flanges.
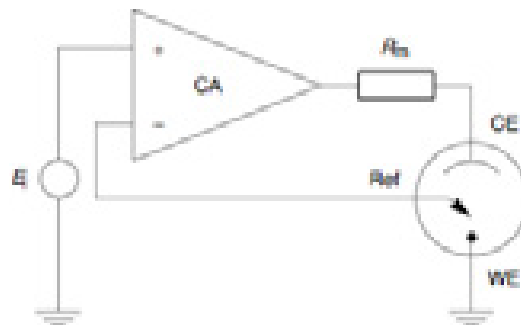
Figure 4.1: *Schematic diagram of a potentiostat.*

4.2   Anodic polarization scan

Polarization is measured as overpotential, i.e. as a change in potential from the equilibrium half-cell electrode potential or the corrosion potential. During an anodic polarization scan the potential on the working electrode is varied linearly with the time and the change in current is recorded. Figure 4.2 shows a typical anodic polarization curve. In region B, the active region, metal oxidation is the dominant reaction. When the potential increases above the passivation potential (point C), the current will decrease rapidly to region E, the passive region. When the potential reaches a sufficiently positive value (point F), the current will increase rapidly to region G, the transpassive region. Region G may be another process which has

equilibrium potential equal to potential in the point F. Classical example which can be found for this situation is Fe (in the sulfuric acid water electrolytes) Ni, Nb. Experimental polarization curve may show some - but not necessarily all of the features described in figure below. If curve will go through the way H than it is possible to see the electrode polishing. Usually this type of curve is a goal for research in field surface treatments. G can be obtained on metals which do not passivate. A classical example is Cu (in acid sulfate water electrolyte) or Fe (in water sulfuric acid electrolytes in presence of Cl⁻-ions).
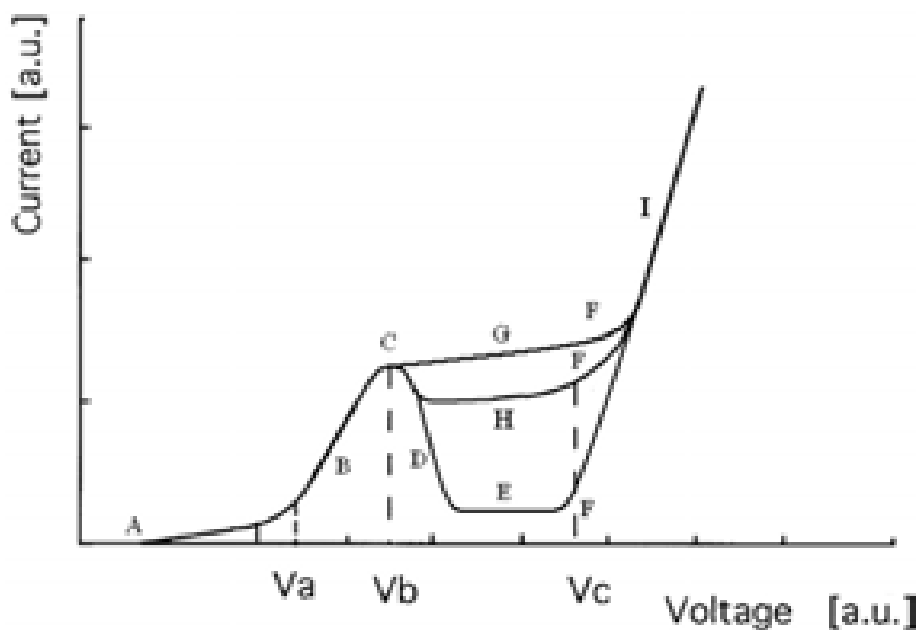
Figure 4.2: *Schematic diagram of an anodic polarization.*

4.3   Solutions and samples preparing

Choline chloride – urea melts are prepared fresh for all experiments. Normally was prepared 2 liters of solution. For this amount of solution is used a 5 liters baker. ChCl(calculated quantity of weight) was put on the bottom and after urea in mol proportion. This mixture was placed on heater and was heated slowly to temperature 120°C. Is necessary to keep melt at this temperature at least half an hour for the evaporation of residual water.

In this work it was determined that it is necessary to pass some quantity of electricity throw solution using Nb anode. At the beginning the anode potential should be more than 50V. If it is lower than it will be observed the Nb passivation instead of dissolution. This behavior is not understood now.

Samples were cut from residual material which was left from 6GHz production. Sample size 5cm lengs and 3cm width. Samples were pulled down in a half of length inside solution.

Cleaning of samples was in next order: washing with dichloromethane. Washing in ultrasound with soap, washing in ultrasound in, rinsing demonized water, drying with alcohol and acetone using nitrogen blowing.

4.4 Two electrodes system

Experiments were done in a backer with quantity of electrolyte ranging from 200 to 400 ml. the solution temperature was increased using heater with thermocouple covered with PTFE. The electrolyte is always stirred (Figure 4.3). Electric power was taken from power supply HP Alintel using automatic control software(Figure 4.4) designed at SC Lab LNL INFN written in Labview 7.1.
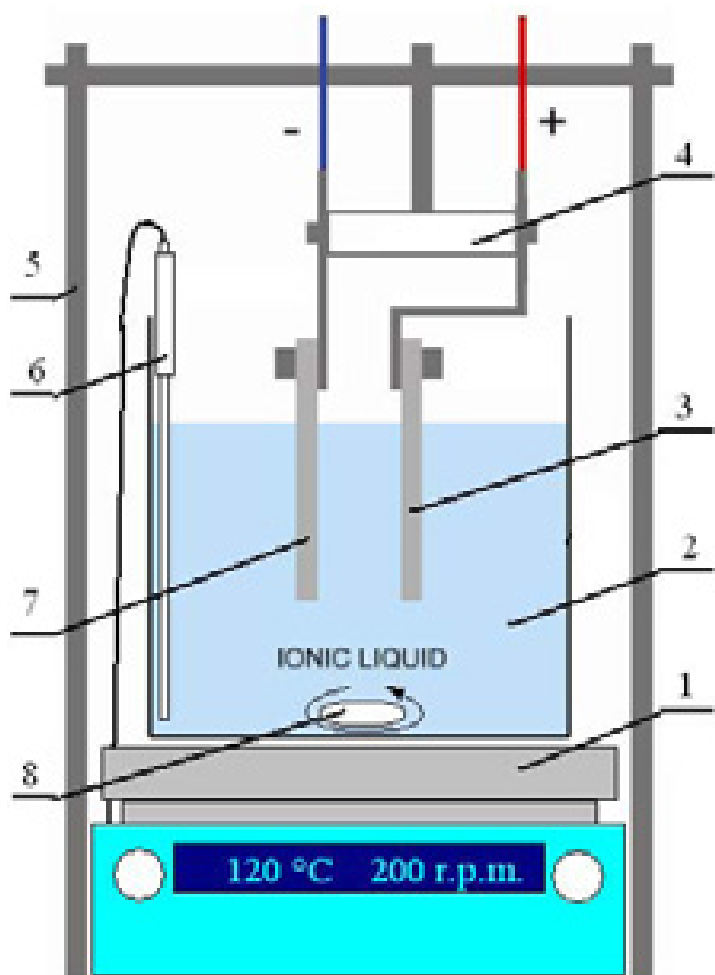
Figure 4.3: *Investigation samples system*

1 – heater; 2 – beaker;3 – anode(WE); 4 - sample holder; 5 – support; 6 –thermocouple covered by PTFE; 7 – cathode(CE); 8 -stirrer .
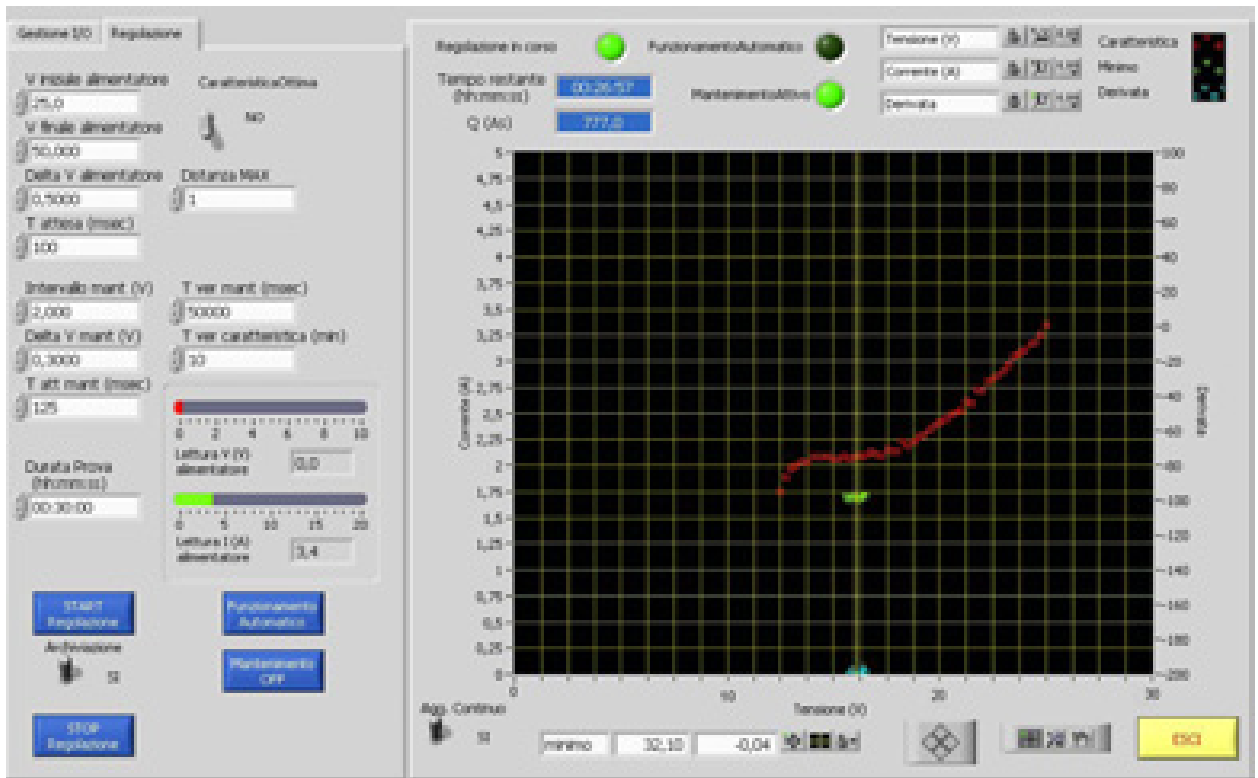
Figure 4.4: *Automatic software for controlling potential.*

4.5   6GHz cavity electropolishing system in ionic liquids

6GHz cavities electropolishing was done in vertical way with pumping solution through the cavity. Cavity is used like a chamber.

Cavity *1* (Figure 4.5) is mounted on support. Holed cathode is immersed inside the cavity connect to electrical contact *2*. Cavity is connected by flanges screws to a anodic contact *3*. Cathode is centered by flanges. Flanges have the same design like flanges for classical EP. Thermocouple *4* is immersed inside the backer *8*. with solution. Cavity is connected from bottom part to the output from the pump *9* and up side to the tube which brings solution back to the backer.

4.6   Stylus profilometry

Profilometry is a method used to measure the profile of a surface, in order to quantify its roughness. The surface roughness values discussed in this dissertation were measured by contact profilometry. A diamond stylus scans laterally across a sample surface under a specified force for a specified distance. The stylus detects small variations in vertical displacement as a function of lateral position. A typical profilometer is sensitive to vertical height variations ranging from 10 nm to 1 mm. Scan speed, contact force, and stylus radius all affect the lateral resolution. A

typical stylus radius ranges from 5 to 25 μm. The profilometer used in this work was Veeco Dektat 32.
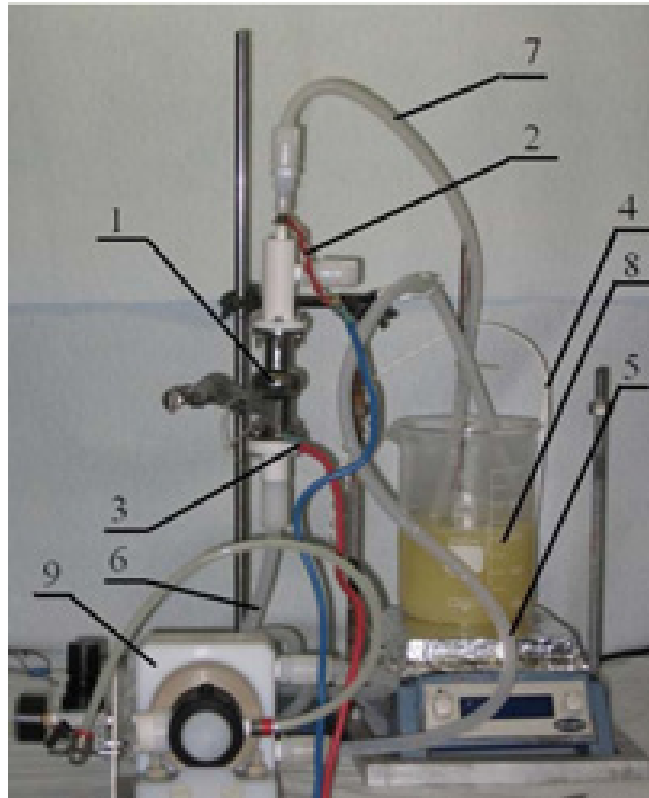
Figure 4.5: *6GHz cavities electropolishing system.*

1 – cavity; 2 – cathode contact; 3 – anode contact; 4 – thermocouple; 5 – input pump; 6 – input cavity(output pump); 7 – output cavity; 8 – baker with ionic liquids; 9 – pump.

The scan length was 1000 μm. Scan duration was 13,0 sec. The contact force was 10 mg. The stylus radius was about 5 μm. Measure range – middle was 65000nm. Analyses were done using average roughness (4.1):

$$R_a = \frac{1}{N} \sum_{i=1}^{N} z_i$$
(4.1)

where z_i illustrated on Figure 4.6
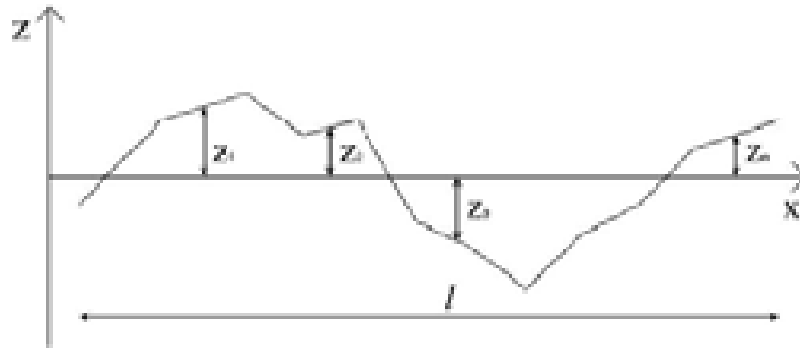
Figure 4.6: *Example of surface profile.*

z_i – is a difference between measured value and averaged measured values on length l.

All samples were measured 6 times as is shown on a Figure 4.7. After were calculated average value by equation (4.2) and error of measuring by equation (4.3).

Figure 4.7: *Scheme of profilometry analysis performance.*

$$Medium = \frac{\sum_{i=1}^{N} Scan_i}{N} \tag{4.2}$$

$$\sigma(Medium) = \sqrt{\frac{1}{N-1}\sum_{i=1}^{N}(Scan_i - Medium)^2} \tag{4.3}$$

where N is the number measures. In the Figure 4.8 some examples of roughness profiles are shown. Three samples have been treated in different ways. The electropolished one is most smooth.
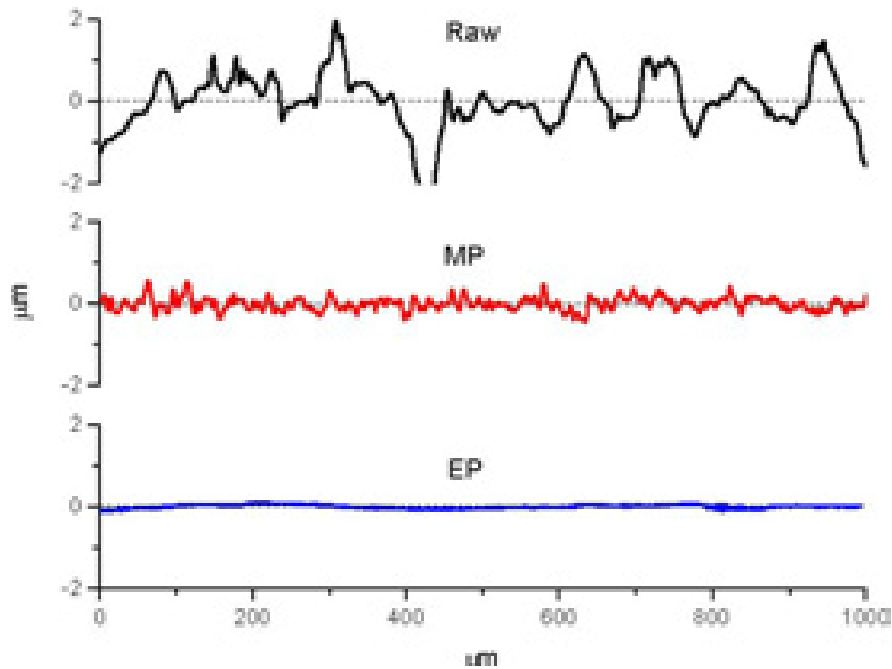
Figure 4.8: *Surface profiles of the raw surface (Raw), the mechanically polished (MP) surface, and the electropolished (EP).*

5   Experimental part

Is well known that Nb is covered with solid oxide film. Formation speed of this oxides isso fast that even at anodic polarization on aggressive concentrative environments like nitric, sulfuric and alkaline water contained solutions current doesn't pass. Instead of dissolution there is anodization (Figure 5.1 *a*) or small dissolving with pitting formation(Figure 5.1 *b*). Adding hydrofluoric acid destroys oxides and provides dissolution. As much water inside the solution as more difficult dissolves metal and more hydrofluoric acid needs.

a)   b)
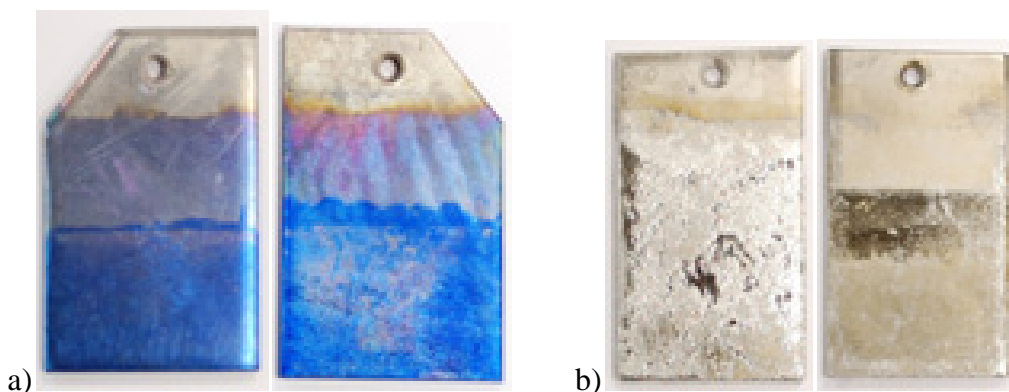
Figure 5.1: *Results obtained in water solutions.*

On previous work [78; 79; 80; 81] found that in Choline Chloride – urea melt is possible to dissolve Nb but dissolving is very sensitive to geometrical factor of the electrochemical cell. One of the trick points is that impurities of water are insignificant because of temperature which is using on the process higher than boiling temperature of water. So there is two things which must be solved:

1. Find approach to break oxides film.
2. Provide equal speed dissolution on all surface of anode with viscous film formation during the electrolyses.

Has been found that there is a possibility to dissolve Nb using high overpotential in 1-4 ChCl-urea melt. First have been put 30V into the 2 electrode system and have been obtained current and dissolving of Nb together with gas formation on back side of sample(Figure 5.2). There are pitting and oxidized spots on the places where gas was evaluating. When we have put 65V we observed less gas evaluating on both sides of the electrode and yellow film formation around the electrode – viscous film. Almost all surface became polished (Figure 5.3). There are some not deep pitting on the front side and not treated part in the back side. Overvoltage heats electrolyte in few seconds from 120°C till 190°C and higher. Which has very bad effect on stability of melt (Figure 5.5).

Figure 5.2: *Front(left) and back(right) of sample electropolished with overpotential 30 V.*
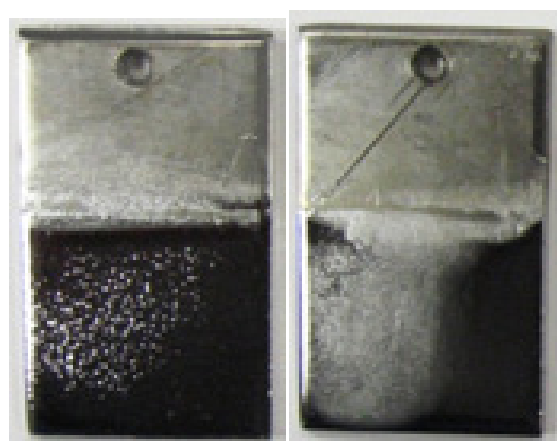
Figure 5.3: *Front(left) and back(right) of sample electropolished with overpotential 65V.*

Figure 5.4: *Degradation of solution.*

From thermodynamic point of view applying potential to electrode is to much big so that's why was performed series of experiments in order to find approaches to decrease electrical tension and may by current density. Later was observed influence of presence S-NH$_2$-containing compounds on EP. Mostly, practical interest has Sulfamic acid.

5.1 Three electrodes system

5.1.1 Voltametry

In order to understand what is happening on Nb electrode in ChCl – urea melts were made voltametry and polarization curves tests in the equal solutions but with different

working electrodes. First was glassy carbon electrode and after in the equal conditions were done tests on Nb electrode.

Voltametry is faster than polarization curves so it gives possibility to observe what is going on and in a which potential region. Polarization curves are slow but show what kinetic regime is defining the process what is the speed of process in all potential reinge. On Figure 5.5 is shown voltammogram which illustrates Sulfamic acid behaviour on glassy carbon electrode in ChCl-urea melt.
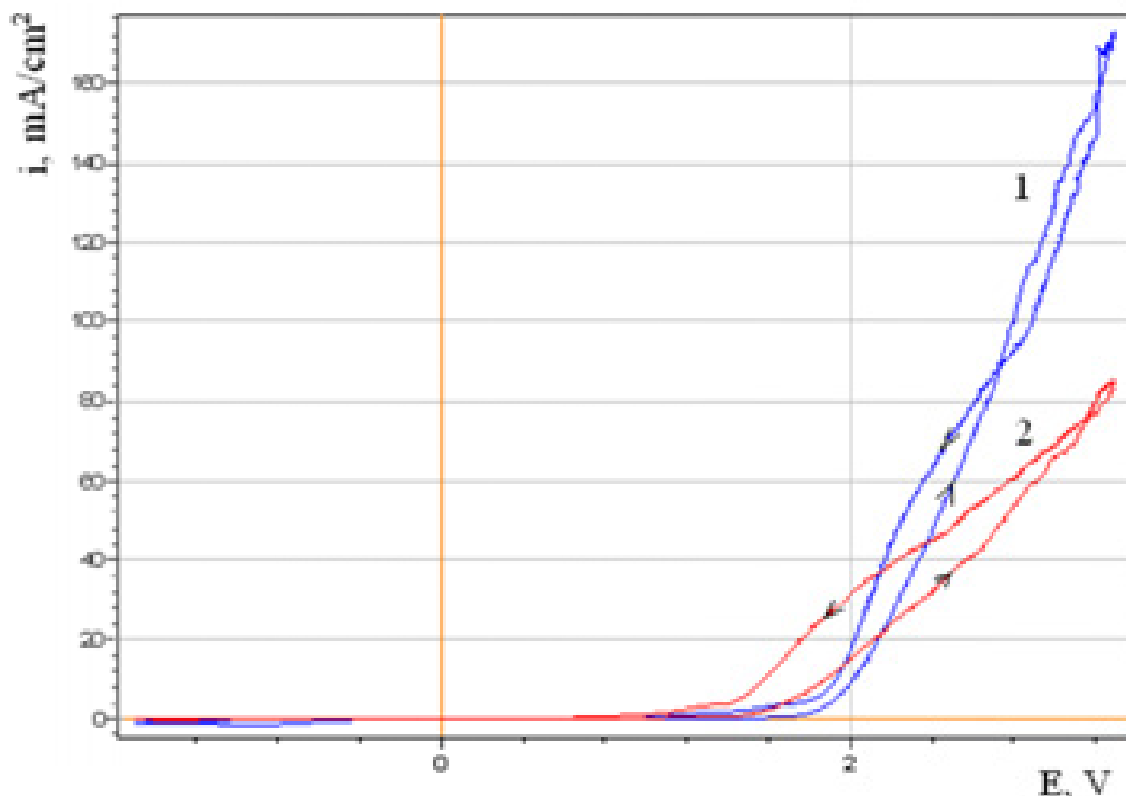
Figure 5.5: *Voltammogram taken on glassy carbon electrode vs. Nb wire, scan rate 100mV/sec.*
1 – ChCl-Urea as 1-4(mol); 2 - ChCl-Urea as 1-4(mol) in presence of 30g/l Sulfamic acid.

Sulfamic acid decreases anodic process current density. Versus Nb wire dropped into investigated solution anodic current on glassy carbon WE starts passing earlier. So, Sulfamic acid adding in to 1-4 ChCl-urea melt decreases electrochemical window in anodic direction and increases overvoltage.

Nb electrodes has a different form of the curve than glassy carbon in the 1-4 ChCl-urea melt (Figure 5.6). Main difference is in much bigger overvoltage, current starts to flow after 3 volts versus Nb wire in corresponding solution. In high voltage region with decreasing the potential current density increases during some time. There is much bigger positive hysteresis between straight and back sweep.
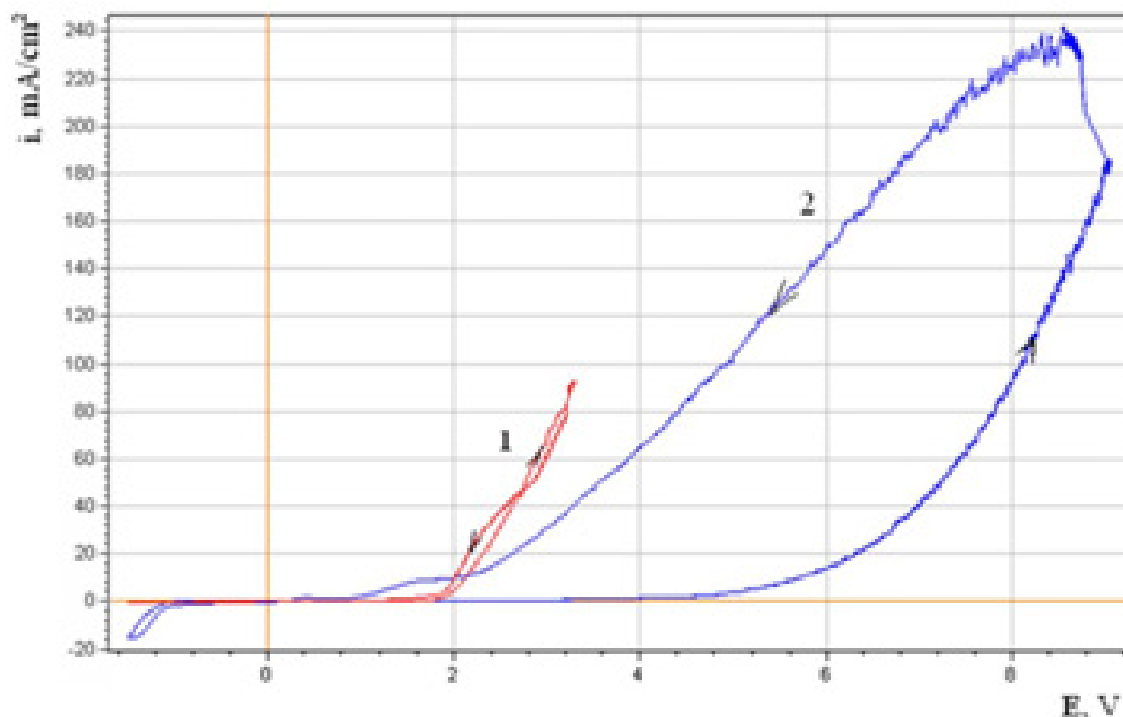
Figure 5.6: *Voltammogram taken in 1-4 (ChCl-Urea) melt vs. Nb wire, scan rate 100mV/sec.*
1 – on glassy carbon electrode; 2 - on Nb electrode.

Figure 5.7 illustrates influence of Sulfamic acid on Nb anodic dissolving in 1-4 ChCl-urea melt. Sulfamic acid decreases overvoltage and reverse slope. There is another key point, when current density is not enough high electrode starts to passivate and even next polarization to 14V will not break passive film(Figure 5.7 curve *3*) . In 2 electrodes system was possible to put bigger potential (65V) and were observed current flowing on passivated electrodes without using BCP.
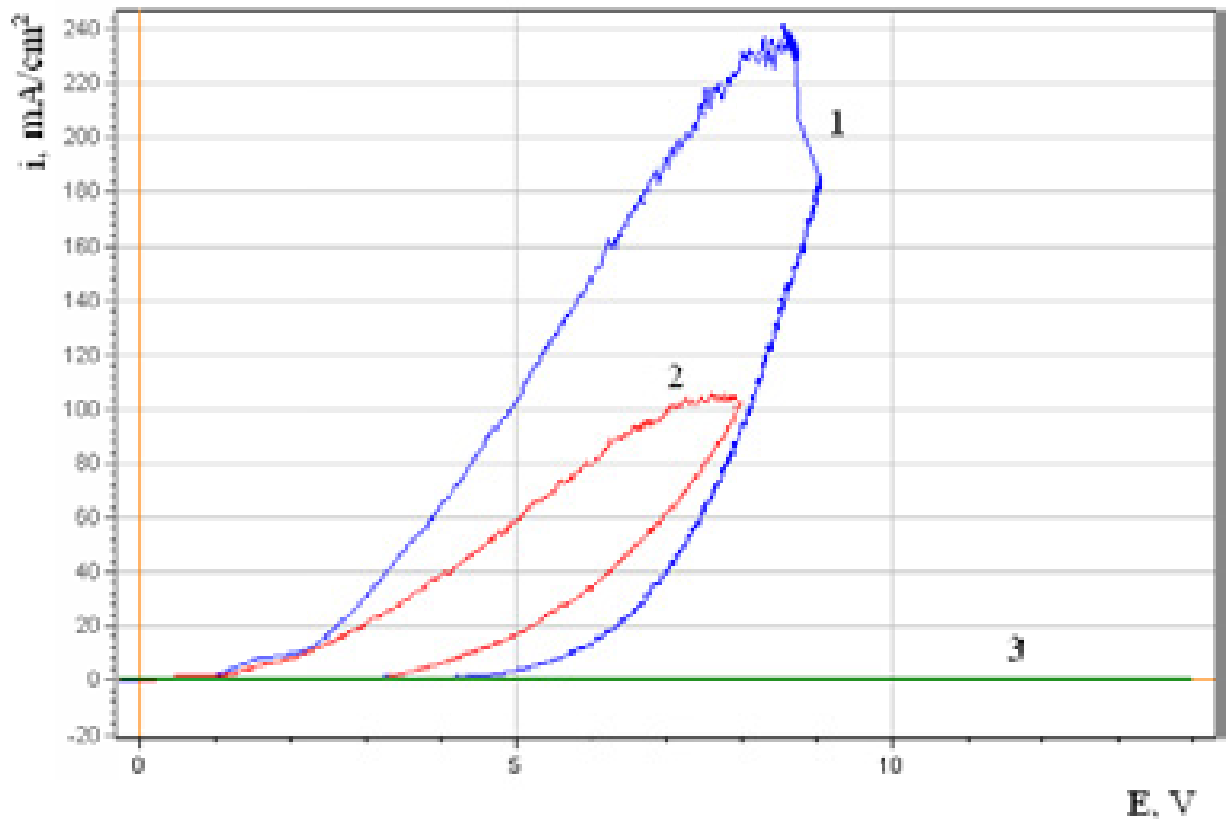
Figure 5.7: *Voltammogram taken on Nb electrode vs. Nb wire, scan rate 100mV/sec.*
1 – ChCl-Urea as 1-4(mol); 2 - ChCl-Urea as 1-4(mol) in presence of 30g/l Sulfamic acid

after BCP; 3 - ChCl-Urea as 1-4(mol) in presence of 30g/l Sulfamic acid after curve 2.

5.1.2   Polarization curves method

Interesting phenomena may be observed on Nb WE in different solutions. Using polarization curves was observed same order of current density of EP process in 49% HF (Figure 5.8 curve 1), 1-4 ChCl - urea melt with 30g/l SA (Figure 5.8 curve 2) and data obtained in sulfuric acid – methanol electrolyte(Figure 5.9 green line) during studding stability of electropolishing process [82]. 49% HF water solution was chosen like more aggressive relative Nb oxides film. Sulfuric acid – methanol electrolyte probably are very similar in mechanism to ChCl – urea solution because of their also use high electrical tension.
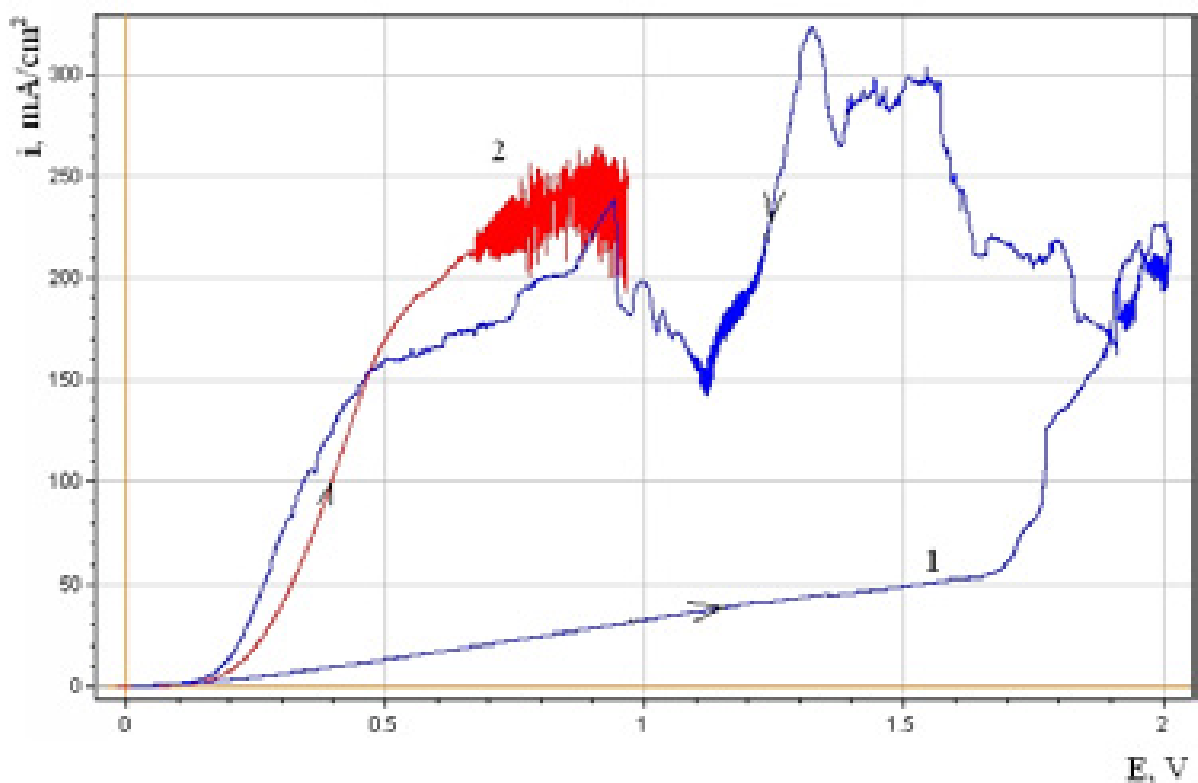
Figure 5.8: *Polarization curves taken on Nb electrode vs. Nb wire.*
1 – in 49% HF; 2 – in 1-4 ChCl – urea melt with 30g/l SA
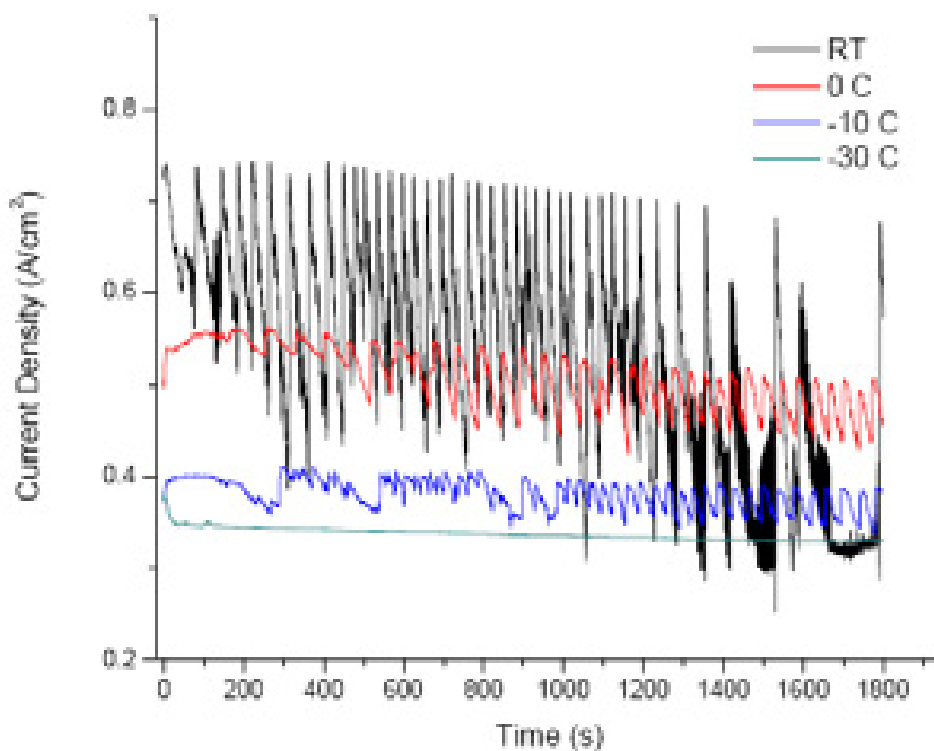
Figure 5.9:*Current density – time dependence observed in 0,1M Sulfuric acid solution in methanol at Nb electrode with tension 22V for different temperature.*

5.2 Two electrodes system

5.2.1 Influence of dissolved NbCl$_5$

In this chapter is observed dependence from quantity of Nb inside solution. In order to determine this dependence was prepared fresh 1-4 ChCl – urea solution and equal samples with working area 15cm^2. All samples were weighed before and after 5 min of electropolishing. Test was done in galvanostat mode with 0,6 A/cm^2 for a 10-20 seconds in overvoltage and 0,3 A/cm^2 during all process. Quality of surface was determined with profilometry measuring and results is presented like roughness – dissolved Nb concentration (Figure 5.10).

First sample roughness is not shown on a figure because it is more 7000nm. Roughness of samples electropolished with concentrations of dissolved Nb more than 4g/l are less than raw Nb and sometimes even close by average value to roughness of surface electropolished with classical EP. There is a huge difference between roughness of front and back sides.
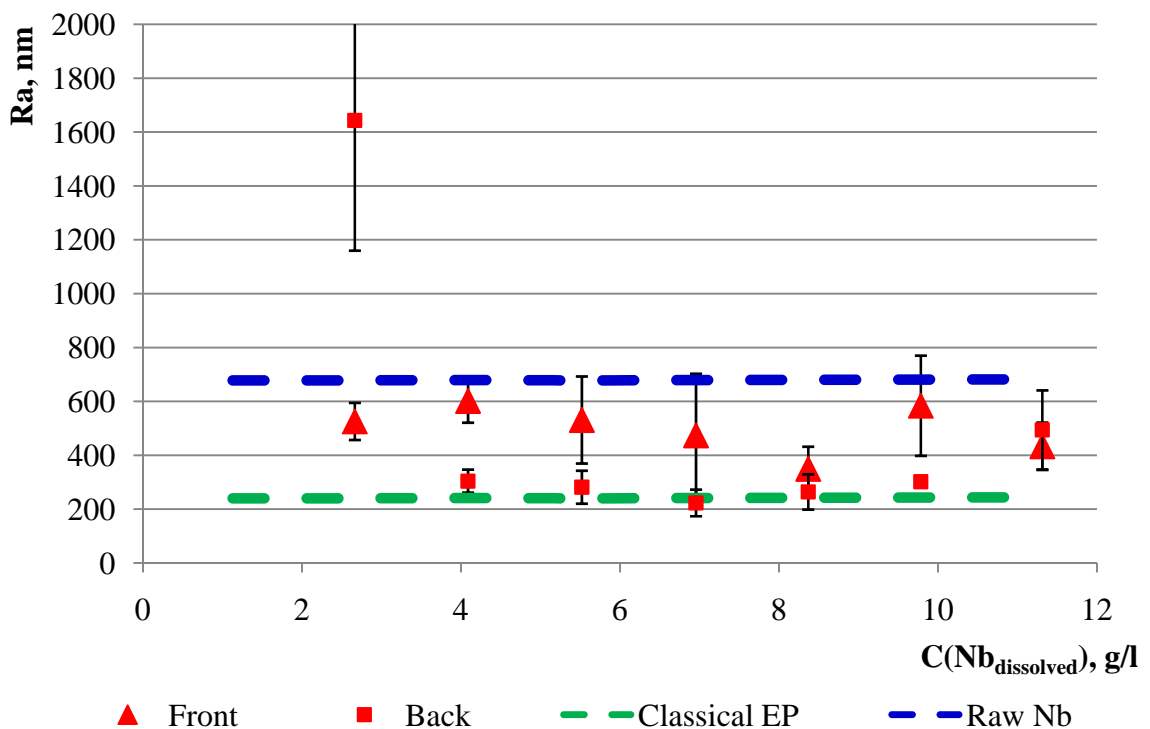
Figure 5.10: *Roughness dependence from dissolved Nb concentration*

In according to Figure 5.10 is obviously that electropolishing in ChCl – urea is comparable to Classical EP after dissolving of Nb in quantity 4 g/l. There is not uniform distribution of current between front and back side of samples.

5.2.2   Sulfamic acid – first success

Providing uniformity of current density was performed through searching surface active compounds which could be added to melt in a reasonable quantity without increasing melting/boiling point of melt. Were performed tests using alcohols (Butanol, ethanol) organic acids(tartaric, oxalic), butyl acetate but results were not satisfied. After was decided to make try on light oxidizer. Choice fall down to Sulfamic acid and result was enough good so was performed series of tests to determine its influence on Nb anodic dissolution in 1-4 ChCl – urea melt.

Was used galvanostat mode, overvoltage 65V for 10-20 seconds and time of process 5min as in previous experiments. Due to electropolishing process dependents from dissolved Nb concentration was performed preliminary dissolving of Nb.

First was determined optimal concentration of Sulfamic acid. Using same prepared before matrix melt were done electropolishing of samples with different concentration of Sulfamic acid. According to Figure 5.11 is understandable that with increasing of Sulfamic acid concentration roughness of front and back side of samples passes through the minimum which lies in region near SA concentration 30g/l. Front side roughness is comparable to roughness with Classical EP and back side roughness is even less.
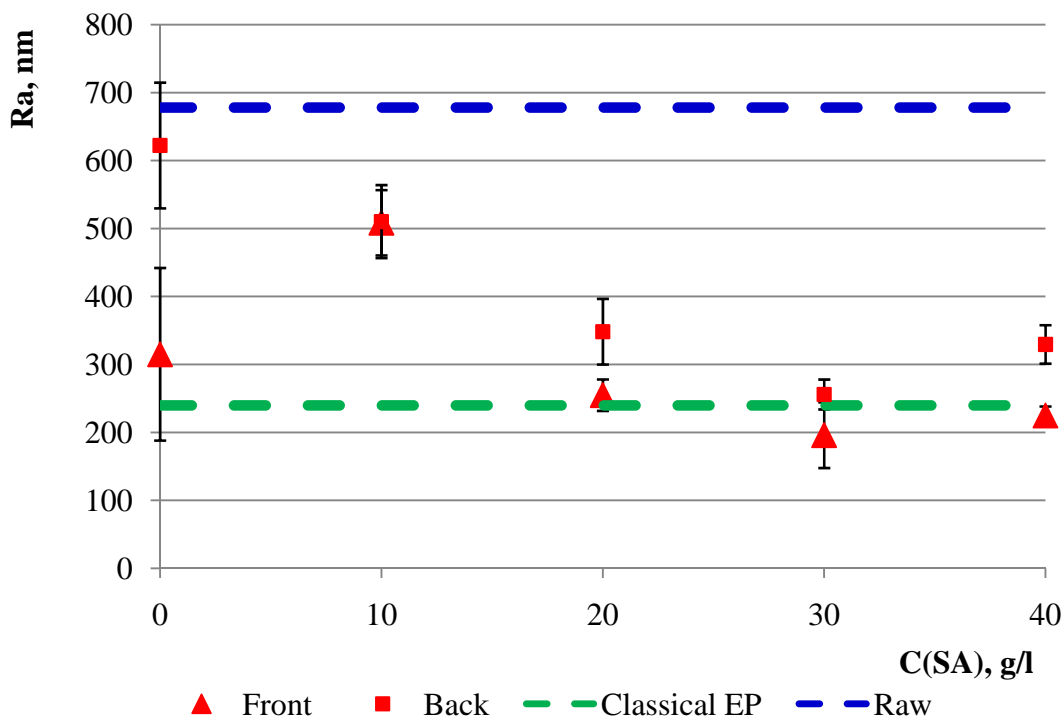
Figure 5.11: *Roughness dependence from Sulfamic acid concentration.*

Discovering Sulfamic acid influence was a great success for future development of Nb EP process.

Next step was determining best working current density or in another worlds smaller possible current density which will prove EP but with less heat generation.

For this test was used the equal to previous test matrix melt with Sulfamic acid concentration 30g/l. All samples were yielded to overvoltage 65V. Roughness of sample as function of current density is shown on a Figure 5.12.
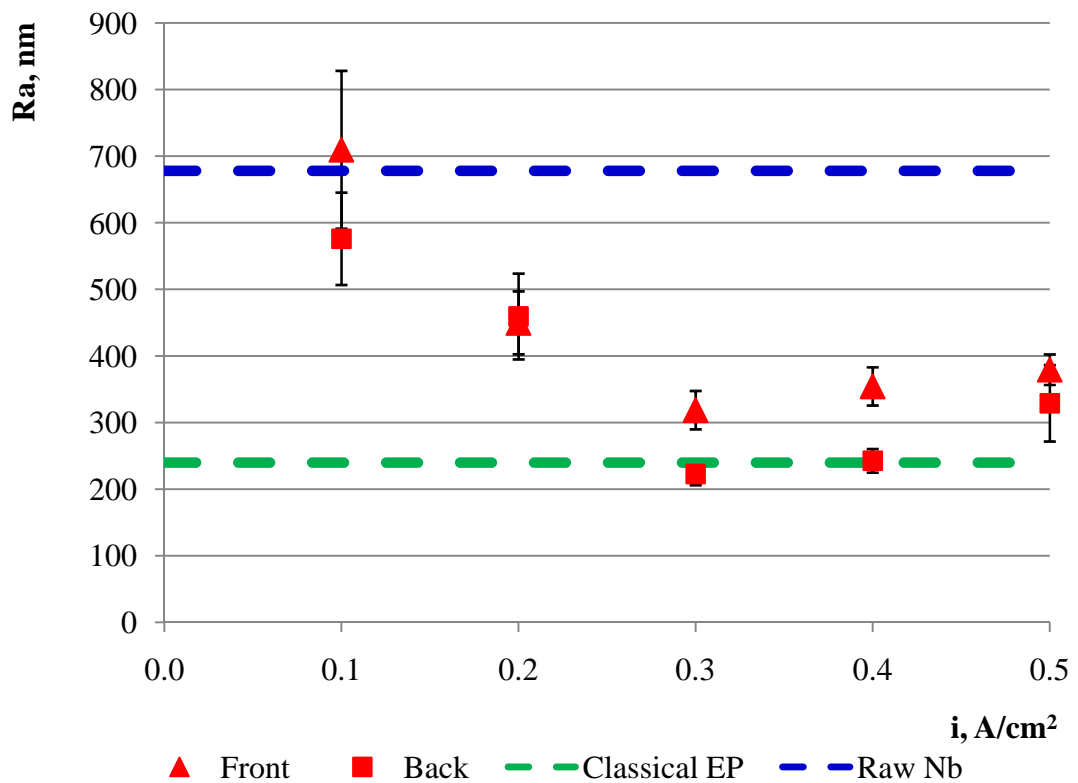
Figure 5.12: *Roughness dependence from current density.*

As against to concentration current density has more similar influence to front and back roughness and passes through the minimum near 0,3A/cm^2 as was .

When compounds composition of the solution and electrical parameters have become determined again was checked influence of dissolved Nb. For this task was used the same matrix solution with 30g/l Sulfamic acid and current density 0,3A/cm^2 and 65V overvoltage during 10-20 seconds. Results are presented on a Figure 5.13.
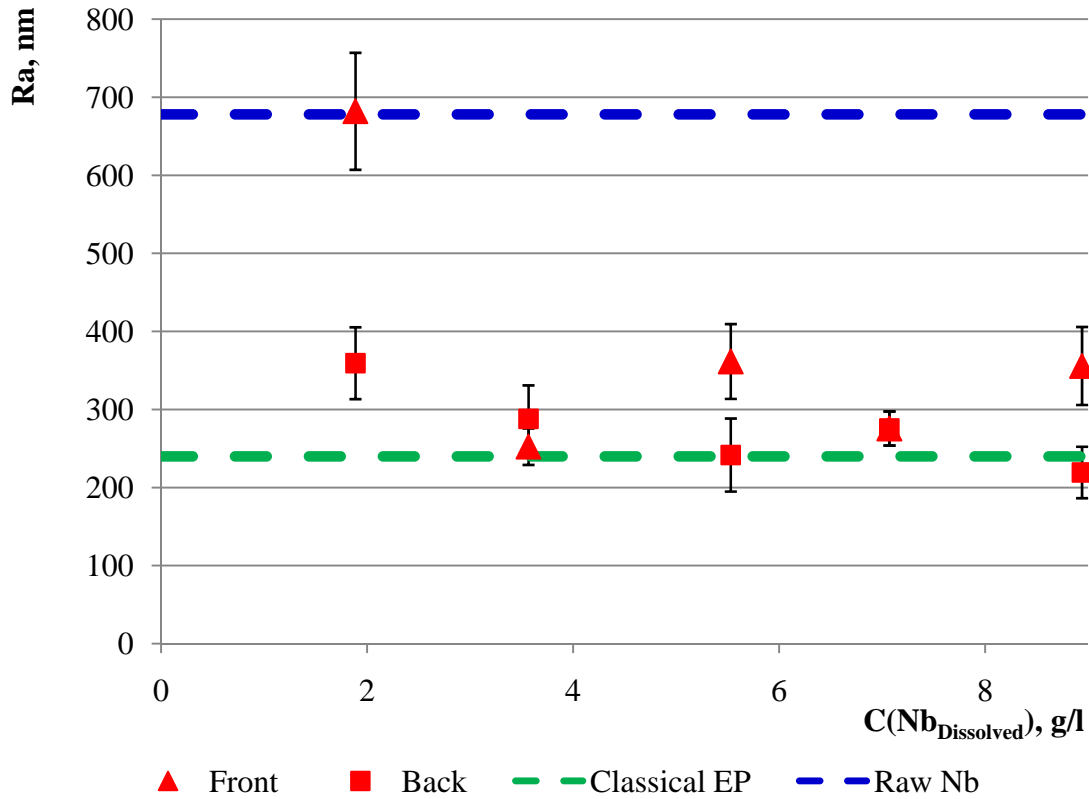
Figure 5.13: *Roughness dependence from dissolved Nb concentration.*

According to previous test of Nb concentration influence is understandable that there is necessity in preliminary Nb dissolving in quantity more than 2 - 4 g/l.

The proofing of previous testes was roughness determining with different time of EP process(Figure 5.14). Solution was prepared from the same matrix solution with previous Nb dissolving. After was put 30g/l Sulfamic acid. All samples were weighed before and after the EP process. Roughness of samples not strongly depended from time of the EP process but after 30 min of the EP process difference between front and back of samples is the least. Outward appearance of the samples is shown on a Figure 5.15. There is strong dissolving on the borders with shape changing on sample which was treated 60 min. It says about fast dissolving which can be determined from slope of line in coordinates time of treatment – removed thickness (Figure 5.16). Thickness was calculated from difference of samples weight.
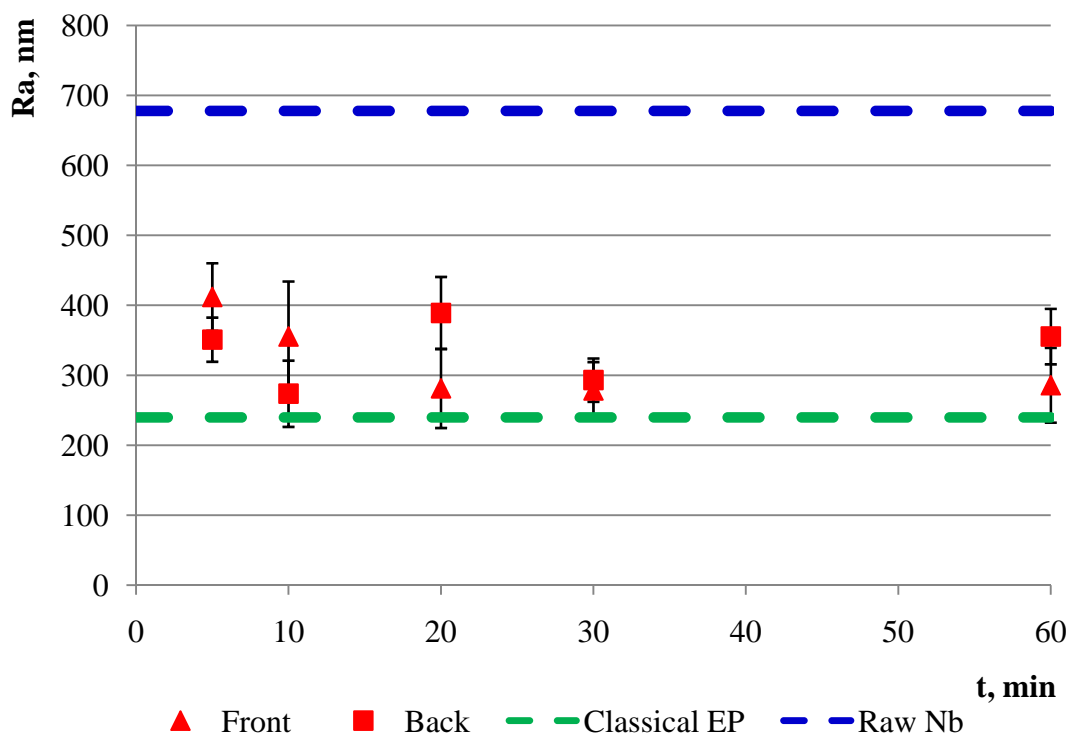
Figure 5.14: *Roughness dependence from process time.*

Figure 5.15: *Outward appearance of the samples electropolished with different time.*
a – front; b – back; 1 – 5min; 2 – 10 min; 3 – 20min; 4 – 30min; 5 – 60min.
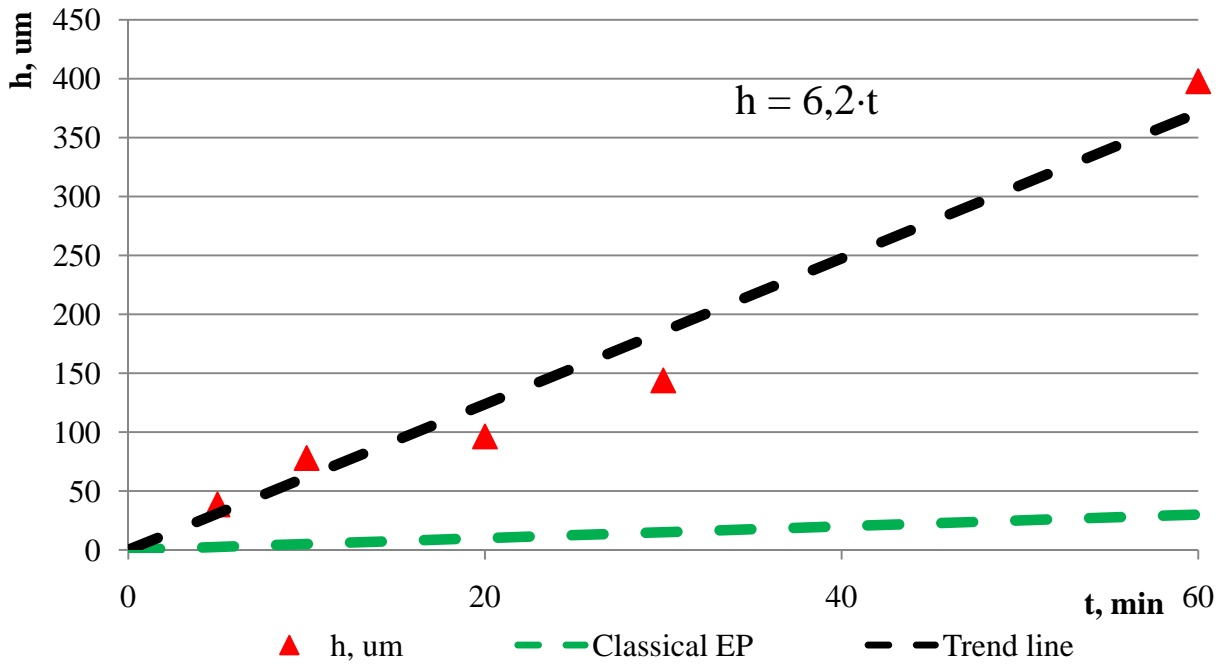
Figure 5.16: *Removed thickness dependence from time of process.*

Electropolishing in ChCl – urea is very fast, dissolving speed reaches 6,2 g/min. As is shown on the Figure 5.16 for removing 400μm is enough only one hour instead of 15 – 20 hours using Classical EP.

5.2.2.1 Summary

- ✓ Adding 30g/l Sulfamic acid in 1:4 choline chloride – urea melt gives possibility to obtain brightness surface, without spots and pitting on the both sides of the sample.
- ✓ The best result obtained with IL is comparable with the surface roughness obtained with classical EP (Figure 5.17)
- ✓ The back side roughness is the same to the front roughness: good current distribution around the sample.
- ✓ Main disadvantage is consisted from strong rising solution temperature which has critical influence on solution stability and marginally on quality of cavities surface quality. More about results obtained on 6GHz cavities electropolishing is written on chapter 5.3.
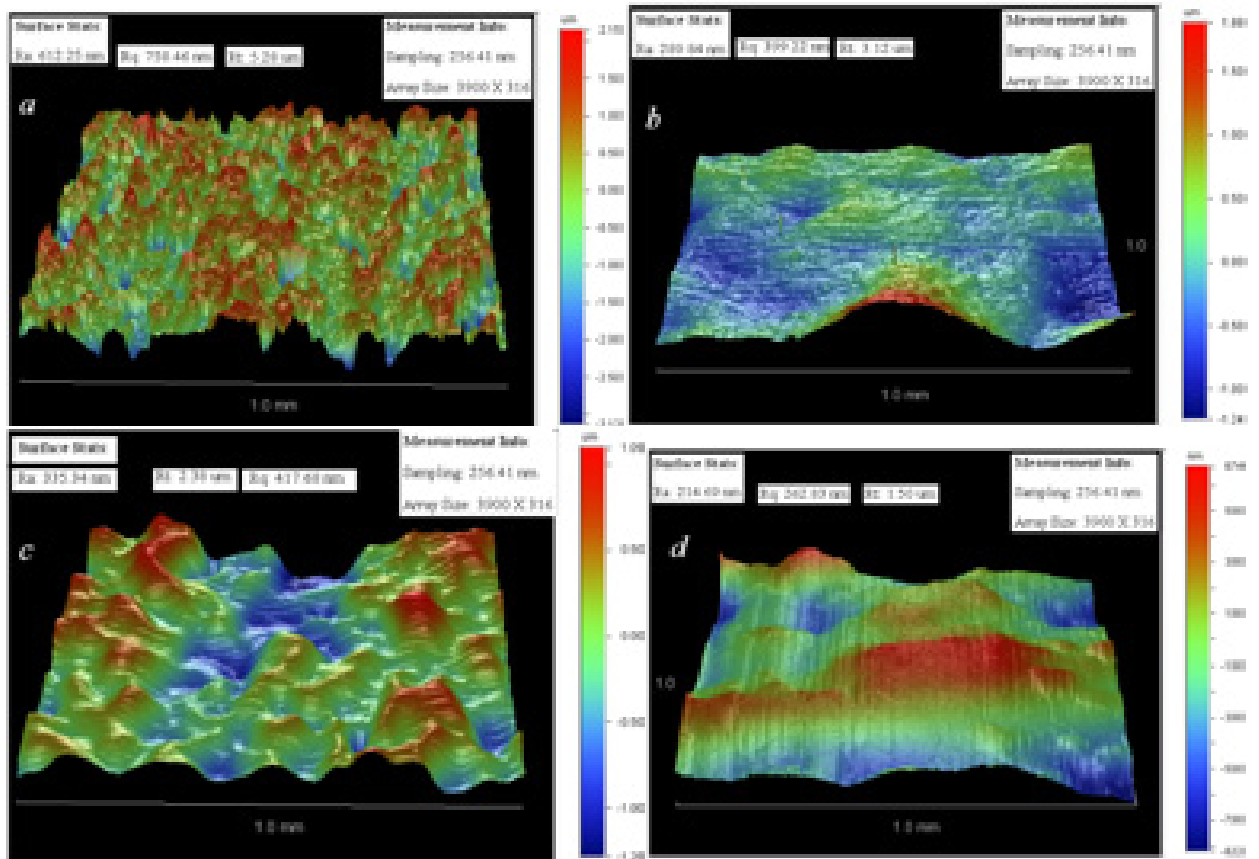
Figure 5.17: *Surface maps of different treatments .*

a – raw Nb; b – 10 min classical EP; c – 10 min IL; e – 60 min IL.

5.2.3   Influence of S and N containing compounds

When capacity for work with Sulfamic acid was determined was decided to look for another regulators similar in nature. Choice fall down to ammonium sulfate, ammonium sulfamate and ammonium persulfate.

5.2.3.1   Ammonium sulfate as alternative to Sulfamic acid

Galvanostate mode. i=0,3 A/cm^2 with overvoltage 65V. t = 5 min

	Sample 5	Sample 6	Sample 7
Electrolyte	1ChCl+4Urea, 10 min dissolving Nb. After adding 30g/L SA		
C($(NH_4)_2SO_4$), g/L	5,7	17	40
Ra(front), um	-	-	631±134
Ra(back), um	-	-	456±78

Table 5.1: *Ammonium sulfate experimental data.*

Using 40 g/l ammonium sulfate in 1-4 ChCl – urea melt is possible to treat Nb surface with good current distribution but samples could have play of colors.
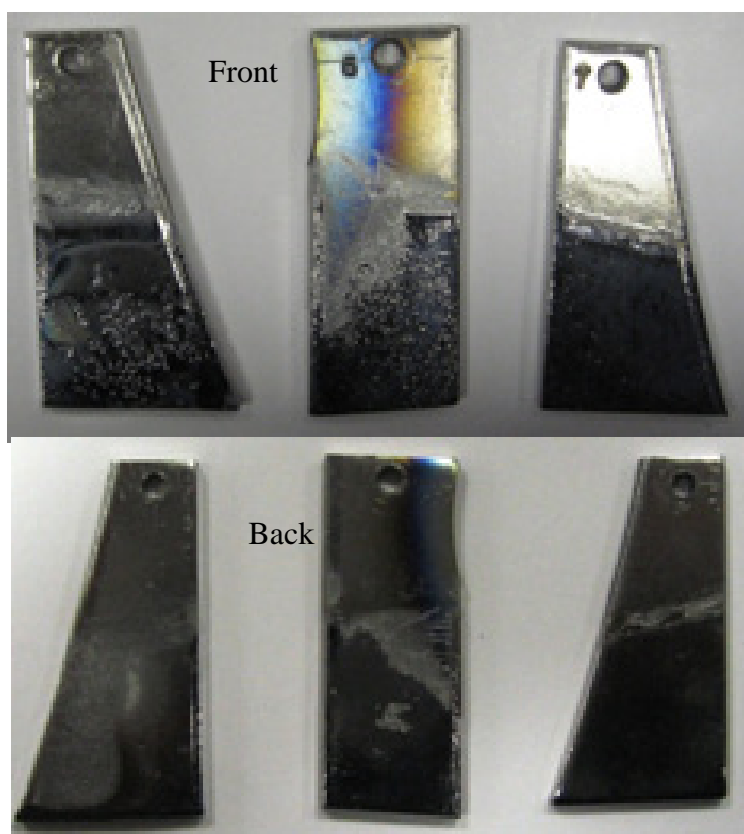
Figure 5.18: *Samples treated in ionic liquid with ammonium sulfate*

5.2.3.2 Ammonium sulfamate as alternative to Sulfamic acid

Galvanostate mode. i=0,3 A/cm^2 with overvoltage 65V. Galvanostate mode. t = 5 min

	Sample 61	Sample 62	Sample 63	Sample 64	Sample 64
C(NH$_4$OSO$_2$NH$_2$), g/L	10	20	40	50	50
Δm, g	0,482	0,439	0,397	0,412	0,526
Ra(front), um	-	-	262±62	447±86	685±209
Ra(back), um	-	-	259±73	300±75	166±26

Table 5.2: *Ammonium sulfamate experimental data*.

On Sample 64 is possible to work in automatic potentiodynamic mode using automatic software. This fact gives ground of presence stable plateau.
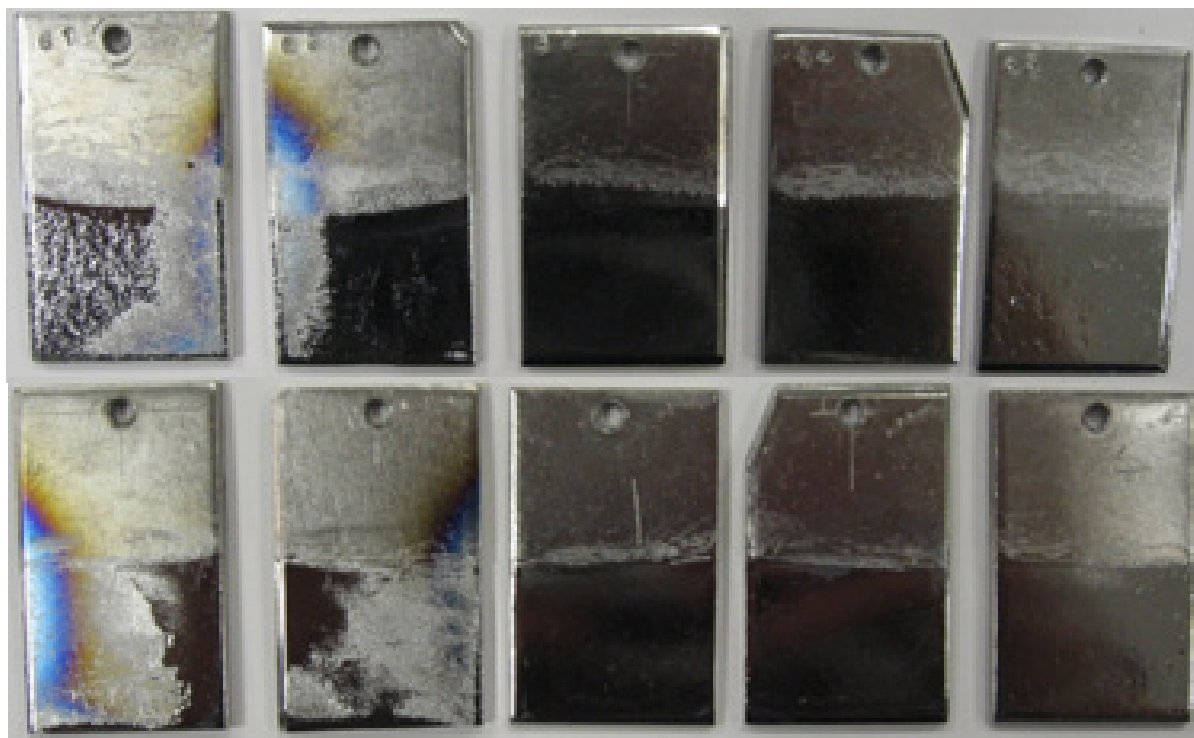
Figure 5.19: *Samples treated in ionic liquid with ammonium sulfamate*

Using 40 g/l ammonium sulfamate in 1-4 ChCl – urea melt is possible to treat Nb surface with good current distribution.

5.2.3.3 Ammonium persulfate

Automatic control potentiodynamic mode.

Solutin preparig:

1. Melting ChCl -Urea
2. Dissolving Nb
3. Adding Ammonium Persulphate.

	Sample 66	Sample 67	Sample 68	Sample 69	Sample 60
$C((NH_4)_2S_2O_8)$, g/L	2	5	10	10	15
Δm, g	0,482	0,439	0,397	0,412	0,526
Ra(front), um	-	1097±184	450±185	-	1485±385
Ra(back), um	-	734±334	1613±466	-	290±45

Table 5.3: *Ammonium sulfamate experimental data*.

This regulator is very reactive and during dissolving it oxides ChCl – Urea melt. Solution changes colour with increasing concentration of persulphate from light to dark brown and generates foam . So is necessary to put persulfate slow with ubundant agitation.
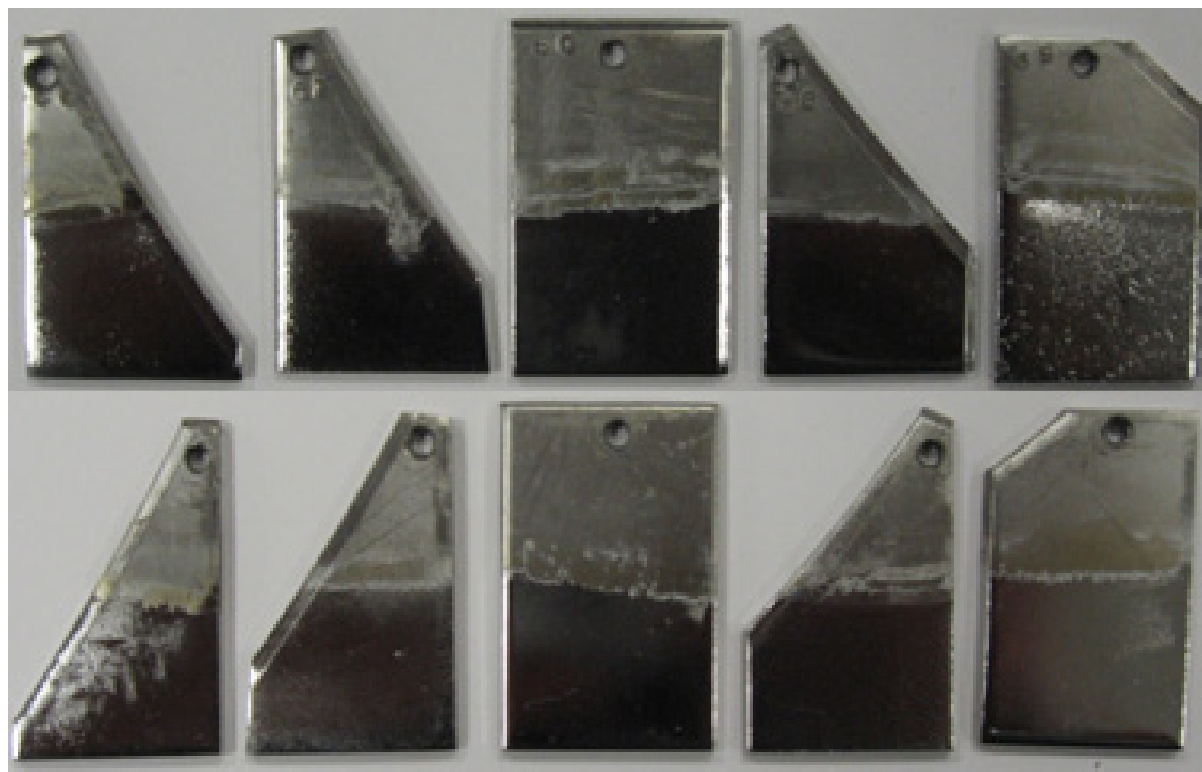
Figure 5.20: *Samples treated in ionic liquid with ammonium persulfate*

	Sample 71	Sample 72	Sample 73	Sample 74	Sample 75[5]
$C((NH_4)_2S_2O_8)$, g/L	10	11	12	20	20
Δm, g	0,482	0,439	0,397	0,412	0,526
Ra(front), um	-	752±138	-	-	1642±737
Ra(back), um	-	662±232	-	-	220±58

Table 5.4: *Ammonium persulfate experimental data.*

Adding PS is possible to work in automatic mode without overvoltage and with less working potential. There is stable plateau in potential range 20…30V which replies to current density 0,3 A/cm^2 range.

---

[5] Without stirring
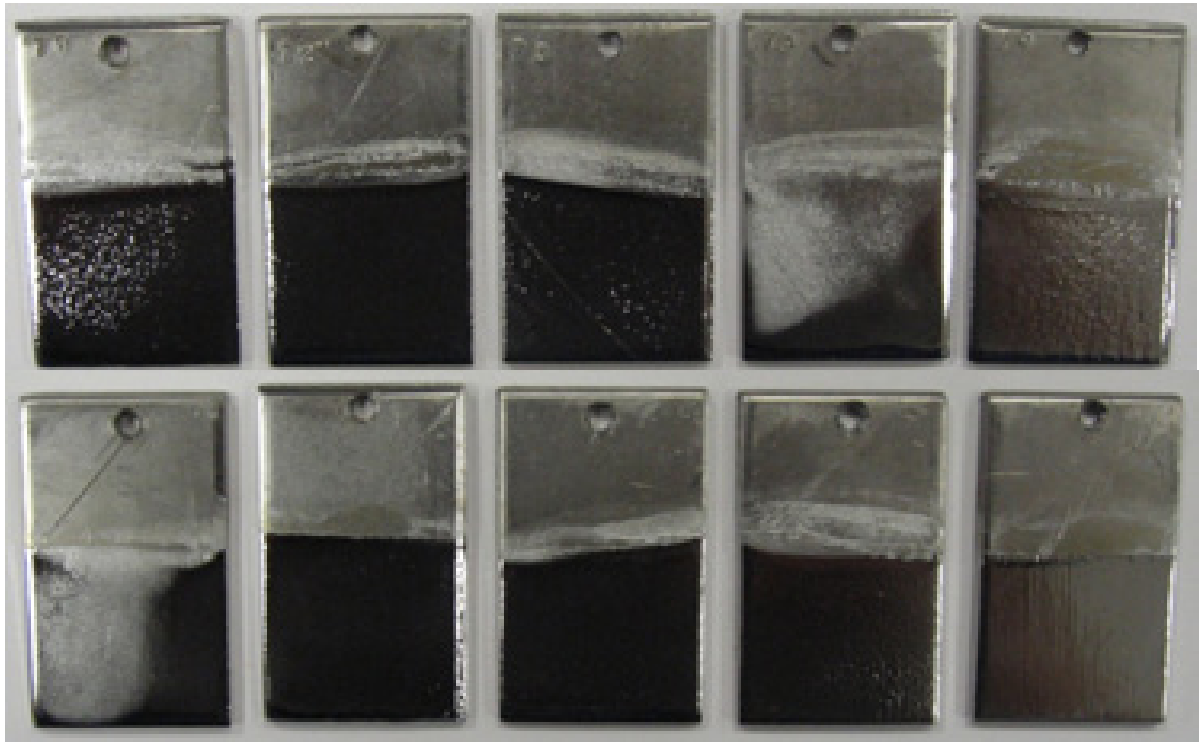
Figure 5.21: *Samples treated in ionic liquid with ammonium persulfate.*

5.2.3.4 Summary – Comparison between N and S-containing compounds as Nb EP-regulator.

From each of 3 last chapters was chosen best surface quality sample and their data were accommodated on a Table 5.5

Best results obteined on SA and Ammonium Sulphamate. Ammonium sulfate has own advantage like most stable, simple and less corrosive compound. Ammonium Persulphate gives a possibility to start electropolishing without overvoltages, but result on samples still not satisfied. Probably it will be possible to use Persulfate and SA or Ammonium Sulfamate togather.

Substance	Structural formula	C_{work}, g/L	Ra(front), um	Ra(back), um
Sulfamic acid		30	274±26	241±41
Ammonium sulfate [Sample 7]		40	631±134	456±78
Ammonium sulfamate [Sample 63]		40	262±62	259±73
Ammonium persulfate [Sample 72]		10	752±138	662±232
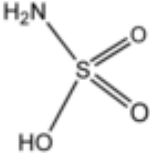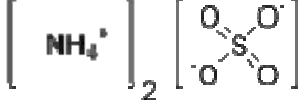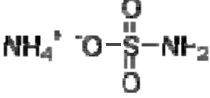
Table 5.5: *S and N containing regulators influence on surface quality comparison.*

Solution with Persulfate even without overvoltage has high working current and voltages (~0,3A/cm^2 and 20V) which brings to heating of solution. If potential is more termodynamical parameter which we not able to change than current is cinetic and it is possible to decres limit current density using solution with less quntity of NH$_2$- groups which means using solution 1ChCl-2urea, 1ChCl-1urea,..

5.2.4   Influence of ChCl and urea

5.2.4.1   Melt ChCl : Urea = 1 : 2

a) Sulfamic acid
Solution preparig:

1. Melting ChCl -Urea
2. Dissolving Nb
3. Adding sulfamic acid.

i~0,3 A/cm^2. Automatic mode. t = 5 min

	Sample 81	Sample 82	Sample 83	Sample 84	Sample 85
C(SA), g/L	10	20	30	40	45
Ra(front), um	-	-	-	1774±1749	2252±1982
Ra(back), um	-	-	-	346±160	1054±824

Table 5.6: *Experimental data of samples treated in1-2 ChCl –urea melt in presence of SA.*
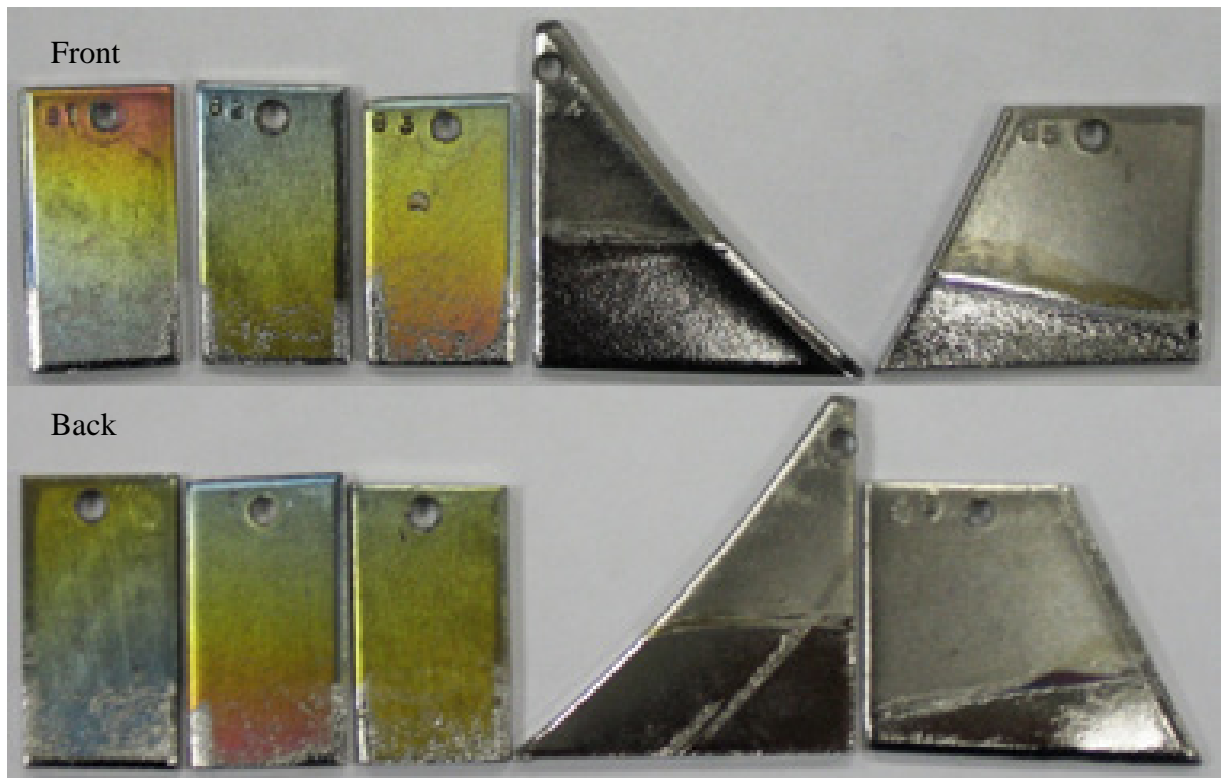
Figure 5.22: *Samples treated 1 -2 ChCl –urea melt in presence of SA.*

The best surface quality has been obtained in melt with 40 g/L SA.

b) Ammonium persulfate
Galvanostate mode, i~0,3 A/cm^2.

	Sample 86	Sample 87	Sample 88	Sample 89
C(PS), g/L	5	7,5	10	12,5
Ra(front), um	-	1640±479	1118±358	1929±659
Ra(back), um	-	435±202	5373±170	432±270

Table 5.7: *Experimental data of samples treated in1-2 ChCl –urea melt in presence of PS.*
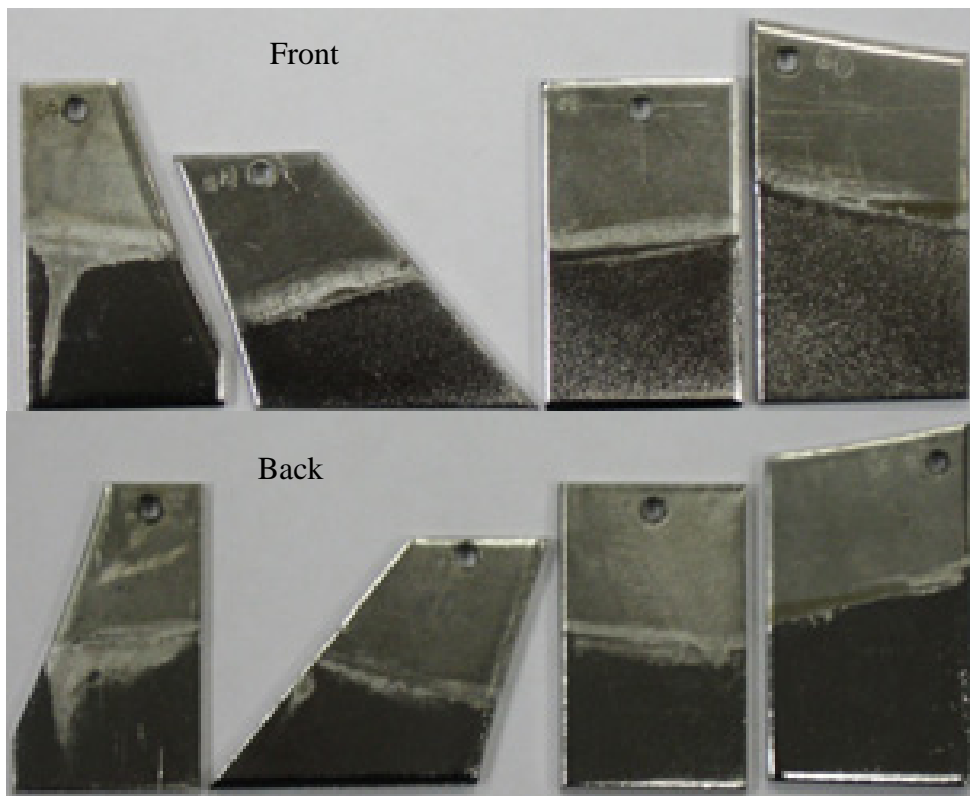
Figure 5.23: *Samples treated 1 -2 ChCl –urea melt in presence of SA.*

The best surface quality has been obtain in melt with 10 g/L PS.

5.2.4.2   Melt ChCl : Urea = 1 : 1

a)   *Sulfamic acid*

	Sample 91	Sample 92	Sample 93	Sample 94	Sample 95	Sample 96
C(SA), g/L	10	20	25	25	30	40
Ra(front), um	-	755±459	1895±468	1242±206	1343±288	-
Ra(back), um	-	1404±200	1655±679	779±296	380±94	-

Table 5.8: *Experimental data of samples treated in1-1 ChCl –urea melt in presence of SA.*
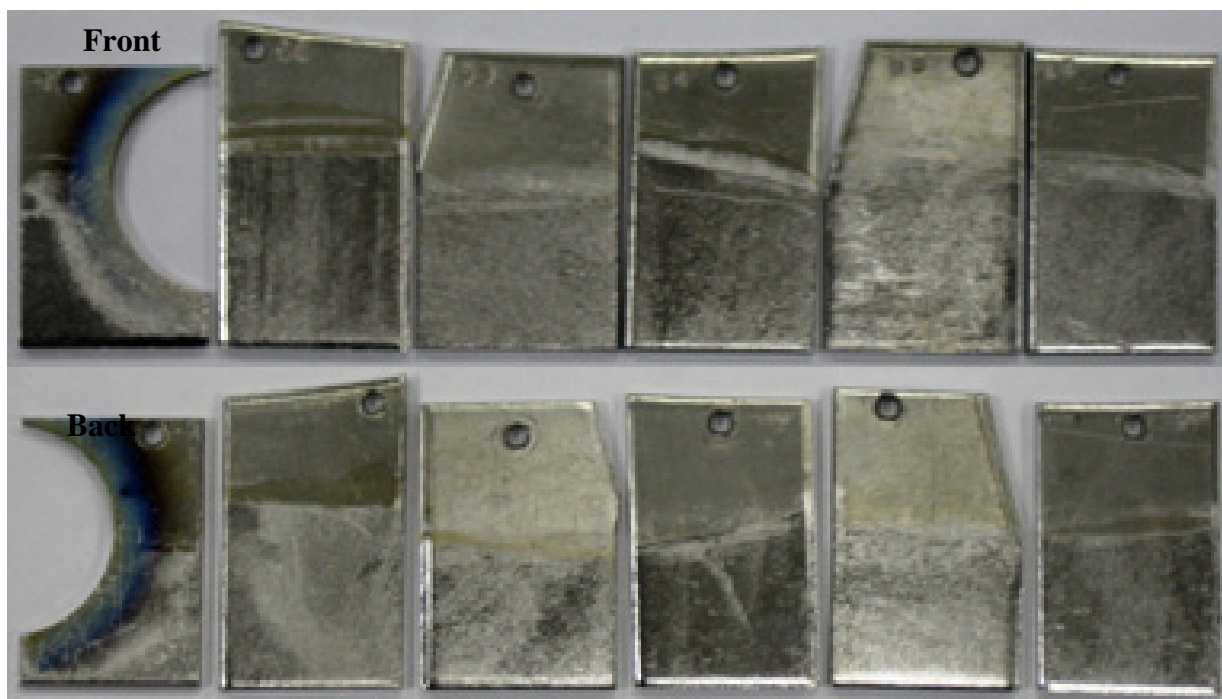
Figure 5.24: *Samples treated in 1 -1 ChCl –urea melt in presence of SA.*
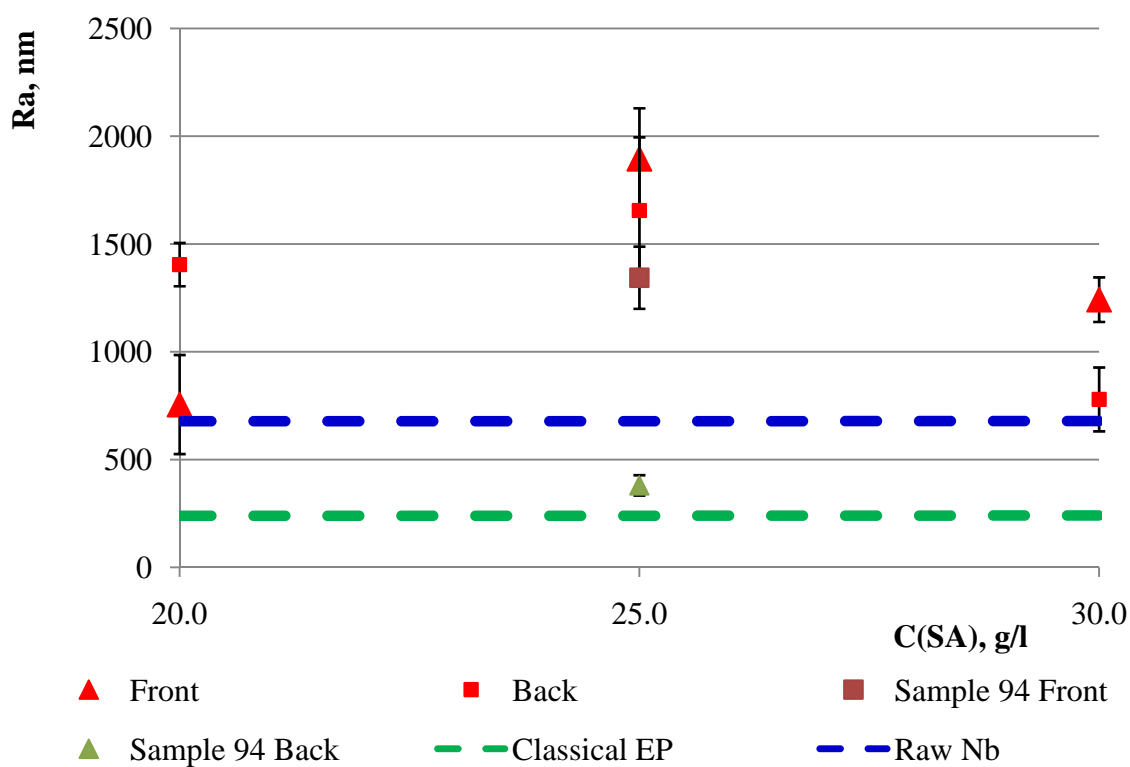
Figure 5.25: *Roughness of samples treated in 1 -2 ChCl –urea melt in presence of SA.*

b) *Ammonium persulfate*

Results are so bad that there was no reason to measure roughness on any of this samples.
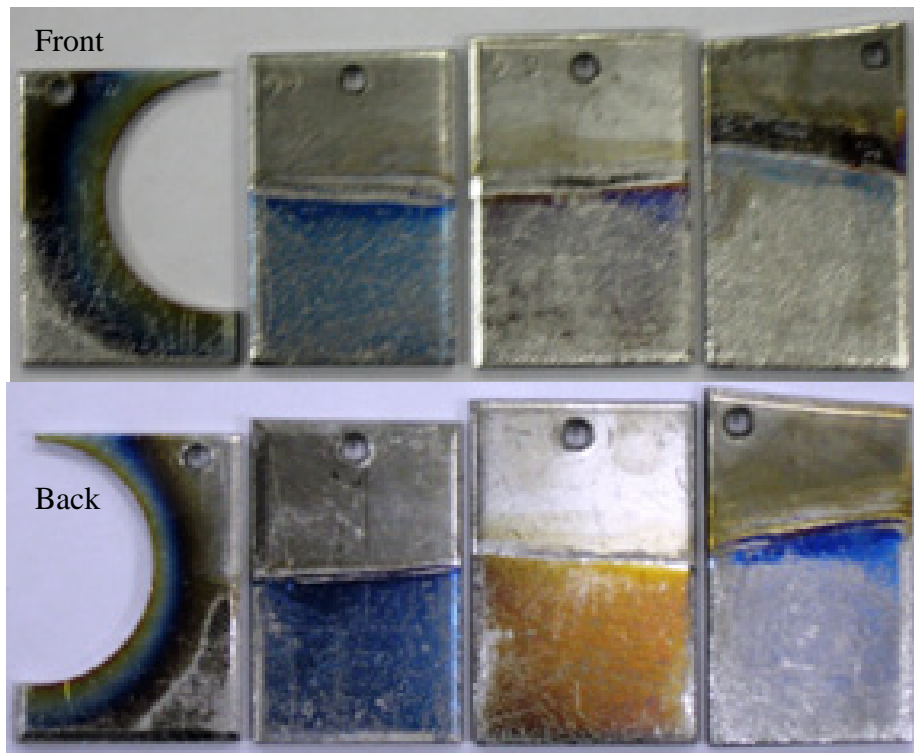
Figure 5.26: *Samples treated in 1 -1 ChCl –urea melt in presence of PS.*

5.2.4.3 Summary - Comparison between different composition of ChCl – Urea melts on samples surface quality.

This tests was done to check possibility to decrease contents of urea in the melt. In order to decreas current density by effect of breeding.

In first experiments on IL were observed that in 1-1, 1-2 and 1-3 melts (ChCl-Urea) is possible to dissolve some Nb but samples look like polished only in 1-4 melt. Increasing of samples surface quality has been observed In row 1-1, 1-2, 1-3, 1-4. This experiment shows fundamental role of urea instead of ChCl on Nb electrode process. Also Tumanova reported importance of urea in research of refractory metals electrochemical properties in Urea-NH_4Cl melt.

Collected dates for comparison are shown on a Table 5.9 and graphically Figure 5.27.

Substance	Composition ChCl : Urea	C_{work}, g/L	Ra(front), um	Ra(back), um
Sulfamic acid [Sample 41]	1-4	30	1 96±48	256±22
Sulfamic acid [Sample 84]	1-2	40	1774±87	346±80
Sulfamic acid [Sample 95]	1-1	30	1242±23	779±10
Ammonium persulfate [Sample 72]	1-4	10	752±14	662±23
Ammonium persulfate [Sample 88]	1-2	10	1118±36	537±85
Ammonium persulfate	1:1	-	-	-

Table 5.9: *Surface roughness comparison of samples treated in different ChCl –urea melts in presence of SA or PS.*
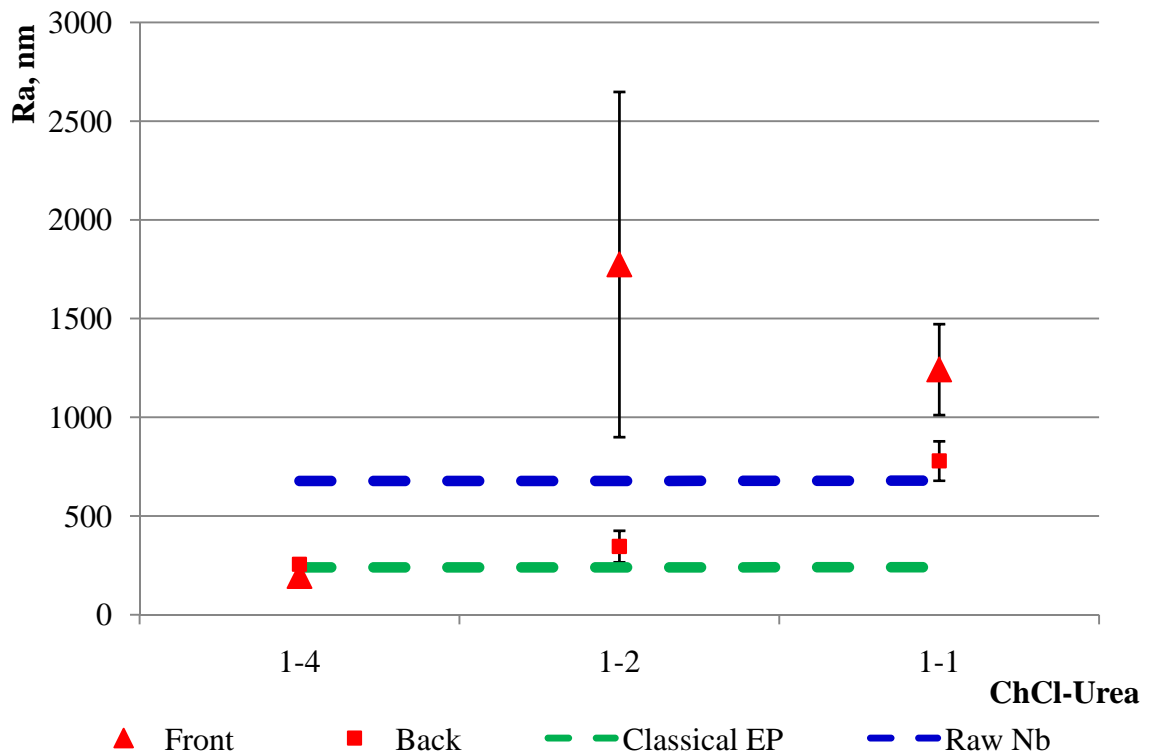
Figure 5.27: *Roughness dependence from ChCl – urea ratio in presence of Sulfamic acid.*

Urea pauperization in the melt brings to decreasing of Nb dissolution reaction efficiency. Instead of Nb dissolution on anode goes electrolyte decomposition.

If Nb dissolution depends of urea quantity, and concentration of regulators doesn't provide surface smoothing than becomes understandable that depassivation of Nb provides only overvoltage and regulators bring only uniform current distribution. Urea provides

dissolving and ChCl serves like melt creator, in another worlds component which generate matrix melt with urea. Also possible that – OH group of ChCl take part on cathode reaction but less than protons from urea because of their bigger mobility.

There is a reason to check how PS and SA can work together. SA can be used like usually as a current distribution regulator and particularly like regulator particularly like depassivating agent.

5.2.5   Influence of additional NbCl$_5$

Understanding what is necessary for preparing right solution needed for making technology more simple and cheaper. Was tried to put additional NbCl$_5$ in order to skip losing time for solution preparing.

i=0,3 A/cm^2 with overvoltage 65V. Galvanostate mode. t = 5 min

	Sample 1	Sample 2	Sample 3	Sample 8	Sample 9
Electrolyte	1ChCl+4Urea, 10 min dissolving Nb. After 30g/L SA added NbCl$_5$			1ChCl+4Urea+30g/L SA. Cool down to room temperature. 3 NbCl$_5$	
C(Nb$_{additional}^{5+}$), g/L	0	0,33	0,65	0,3	0,3
Δm, g	0,509	0,536	0,522	-	-
Ra(front), um	632±137	245±45	597±198	-	578±161
Ra(back), um	271±47	572±121	1206±410	-	322±218

Table 5.10: *Experimental data of samples treated in1-4 ChCl –urea melt in presence of additional NbCl$_5$.*

Adding NbCl$_5$ brought to pitting from both sides of samples. Appearance of samples looks more brightening and shining.

Temperature is increasing faster in the same range of potentials.

Samples 1, 2, 3 were electropolished on solution which was prepared from 1 part ChCl and 4 parts Urea. After melting in solution was dissolved NbCl$_5$ in temperature 120°C. Adding of Nb salt was accompanied by gazing and slogging. Full dissolving took more than 30min. After full dissolving of salt was added SA.

Samples 8, 9 were electropolished in solution prepared in order:

1.   Melting ChCl and Urea
2.   Cooling down to 40°C adding NbCl$_5$. Slow heating to 120°C.
3.   After full salt dissolving added SA.
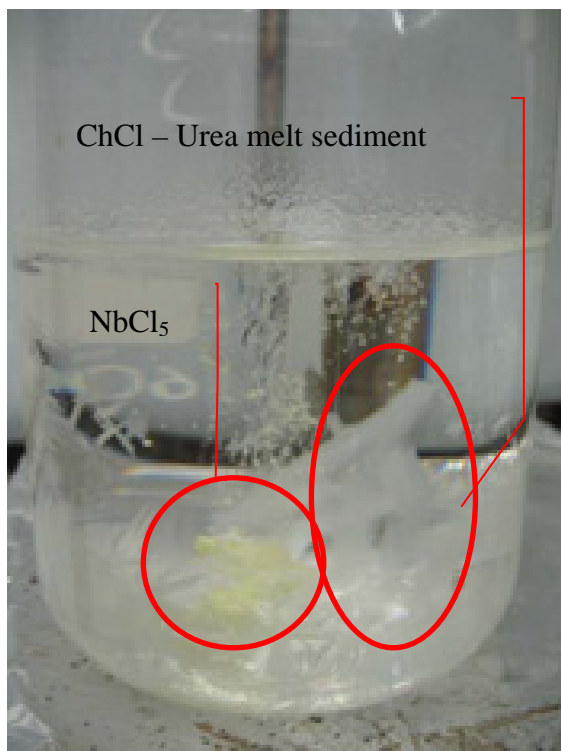
Figure 5.28: *dissolving of NbCl5 in 1-4 ChCl – urea melt.*

Summary: Adding of NbCl$_5$ in solution doesn't give a possibility to jump over preliminary electrochemical dissolving of Nb and brings to pitting and increasing of brightness. On a Figure 5.29 are shown roughness results obtained from samples which were electropolished with additional NbCl$_5$.
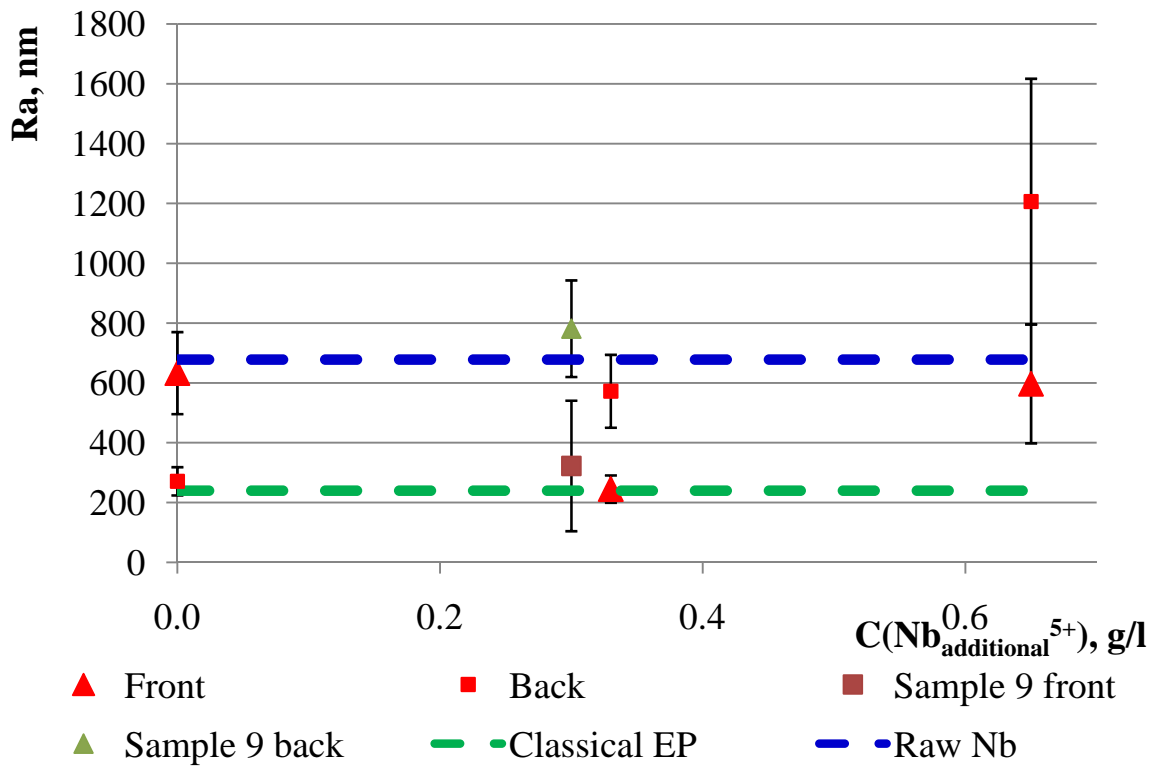
Figure 5.29: *Roughness of samples treated in presence of additional NbCl₅.*
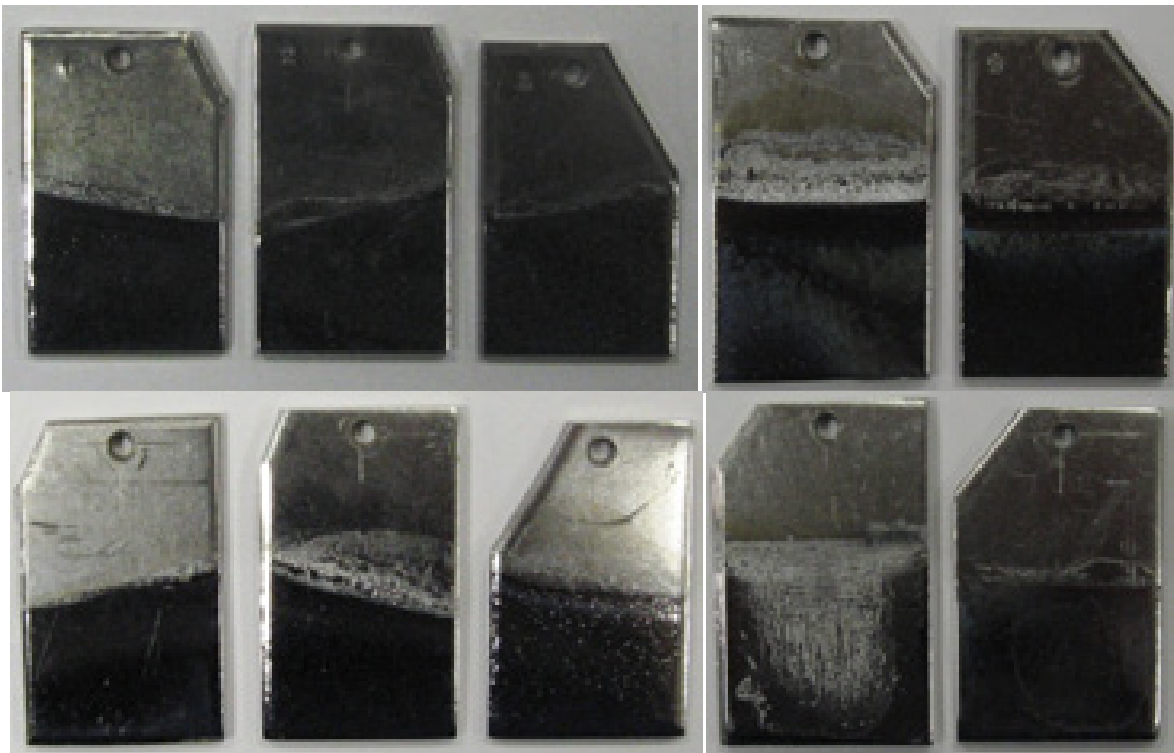
Figure 5.30: Samples treated in presence of additional NbCl₅.

5.2.6 Concurrently using PS and SA

Notwithstanding Sulfamic acid and ammonium persulfate have positive influence on Nb EP process using them separately is not enough. SA provides current distribution evenness which means uniform surface dissolving. PS allows to avoid overvoltage and to decrease working current density. This factors have strong influence on solution self heating during treatment.

Determining SA and PS best concentrations was done through the comparison of samples roughness changing SA concentration at PS concentration 0, 2.5 and 5g/l.

Solution preparing was done as usually, first was added PS and after color stabilizing was added SA. Was used automatic control potentiodynamic mode. Treatment time - 5 min.

5.2.6.1 C(PS) = 2,5g/L
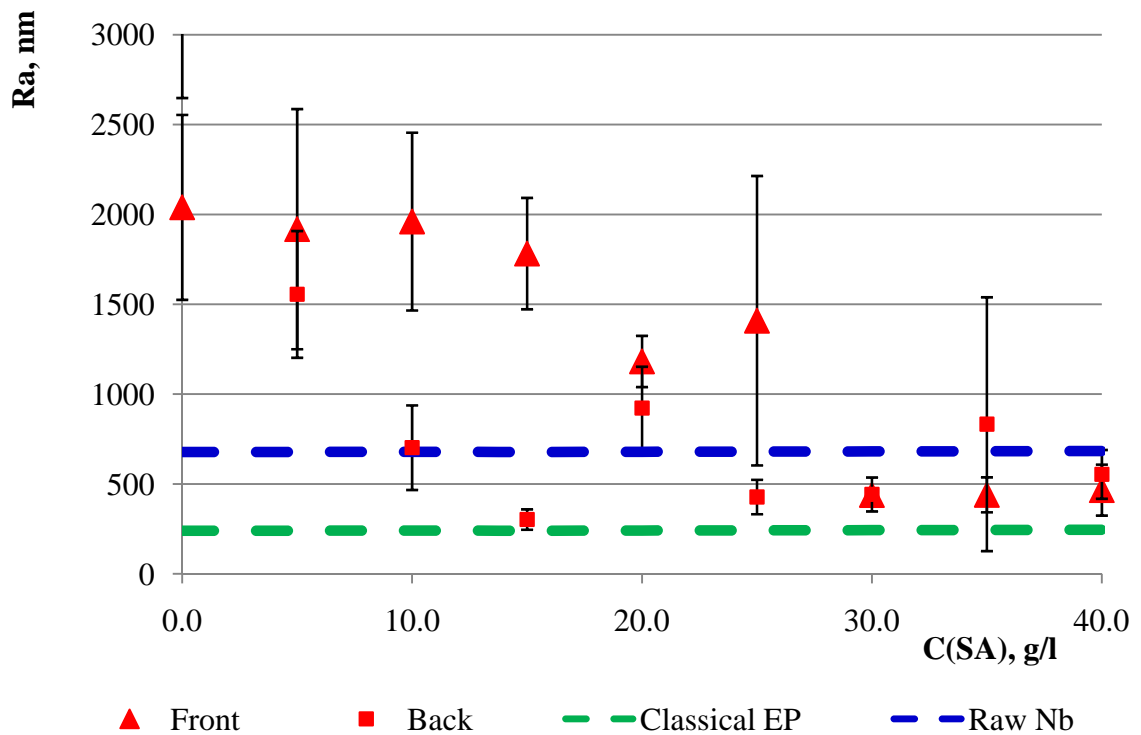
Figure 5.31: *Roughness of samples dependence from Sulfamic acid concentration in 1-4 ChCl – urea melt at 2,5g/l ammonium persulfate concentration.*

According to the Figure 5.31 with increasing SA concentration roughness of treated samples is falling down and has the best value near 30 g/l.

5.2.6.2 C(PS) = 5g/L
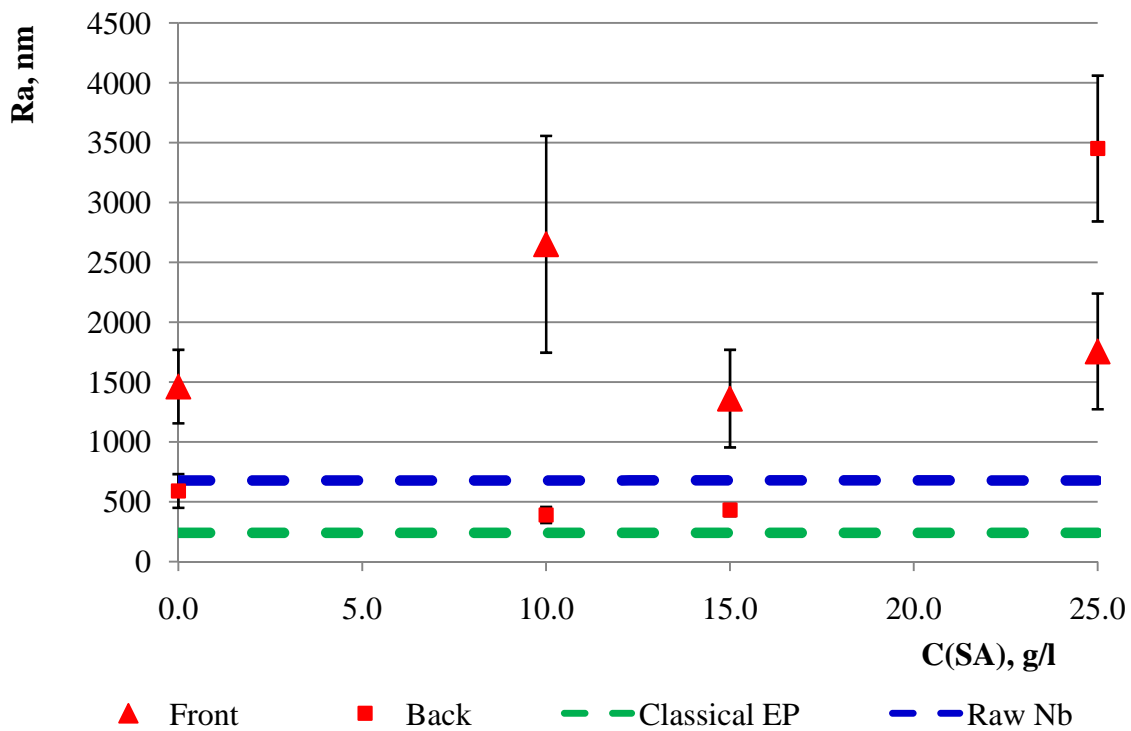
Figure 5.32: *Roughness of samples dependence from Sulfamic acid concentration in 1-4 ChCl – urea melt at 5g/l ammonium persulfate concentration.*

According to the Figure 5.32 with increasing SA concentration roughness of treated samples is falling down and has the best value near 30 g/l.

5.2.6.3 Summary - comparison between different composition of SA and PS used concurrently.
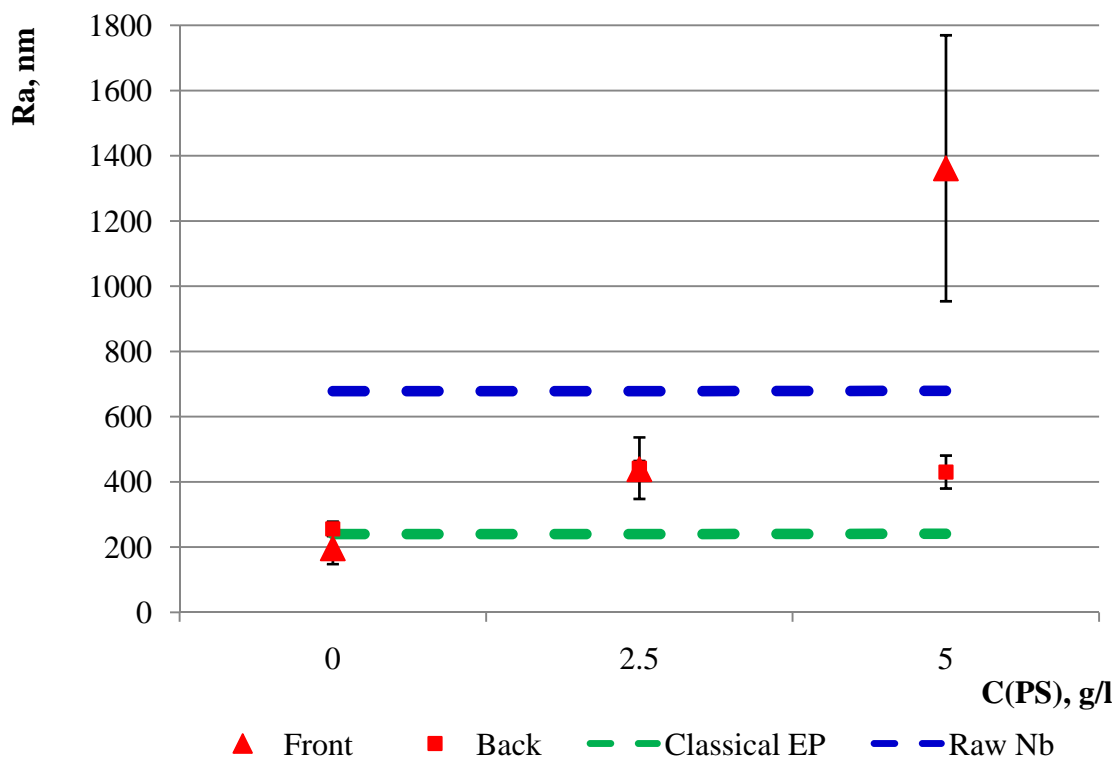
Figure 5.33: *Roughness of samples dependence from ammonium persulfate concentrations in 1-4 ChCl – urea melt in Sulfamic acid presence.*

According to Figure 5.33 is understandable that with increasing of PS concentration roughness is increasing and has reasonable value at PS concentration 2,5g/l.

In conclusion to tests which were done with two electrodes system is offered best solution with the next recipe:

Choline chloride - urea ratio	1-4
Sulfamic acid, g/l	30
Ammonium persulfate, g/l	2,5
t, °C	120
i range, A/cm^2	0,33
Potential range, V (Using automatic control software)	20-30

5.3   Application to 6GHz cavities

In this chapter will be reviewed system for electropolishing in ionic liquids developing and application of 1-4 ChCl – urea melt with 30g/l Sulfamic acid for EP 6GHz cavities.

In order to obtain a favorable current distribution, the cathode need to be far from anode. Unfortunately it is not possible inside the cavity. Cutoff part will be always in a few times nearer than cell part. To avoid this situation, a partially shielded cathode was used.

Was tried to work in two geometrical performances: horizontal and vertical. Horizontal EP didn't give content results because of very fast temperature rising, after 1 minute temperature inside the cavity was more 190°C which brought to degradation of electrolyte and to formation white viscous mass. In that places was done note a polishing but oxidizing.

With vertical EP were electropolished few cavities with relative success but there is also difficulties. High activity formation of cathode gas brings to saturation of electrolyte with H_2 (like the most probable cathode reaction in electrolyte which includes –OH and –NH_2 groups).

Molecules H_2 can oxidize on anode on viscous film surface. Time between bubbles adsorption and reduction there is no electrical field on anode surface which is passivating during this time.

Was designed EP system(Figure 5.35) where electrolyte comes from flanges and goes out from the cathode. For this reason cathode was made of tube 8mm in diameter with holes. During the pumping electrolyte goes through the holes inside the tube and takes with itself gas which evaluate from cathode reaction.

Figure 5.34: *6GHz cavity section.*
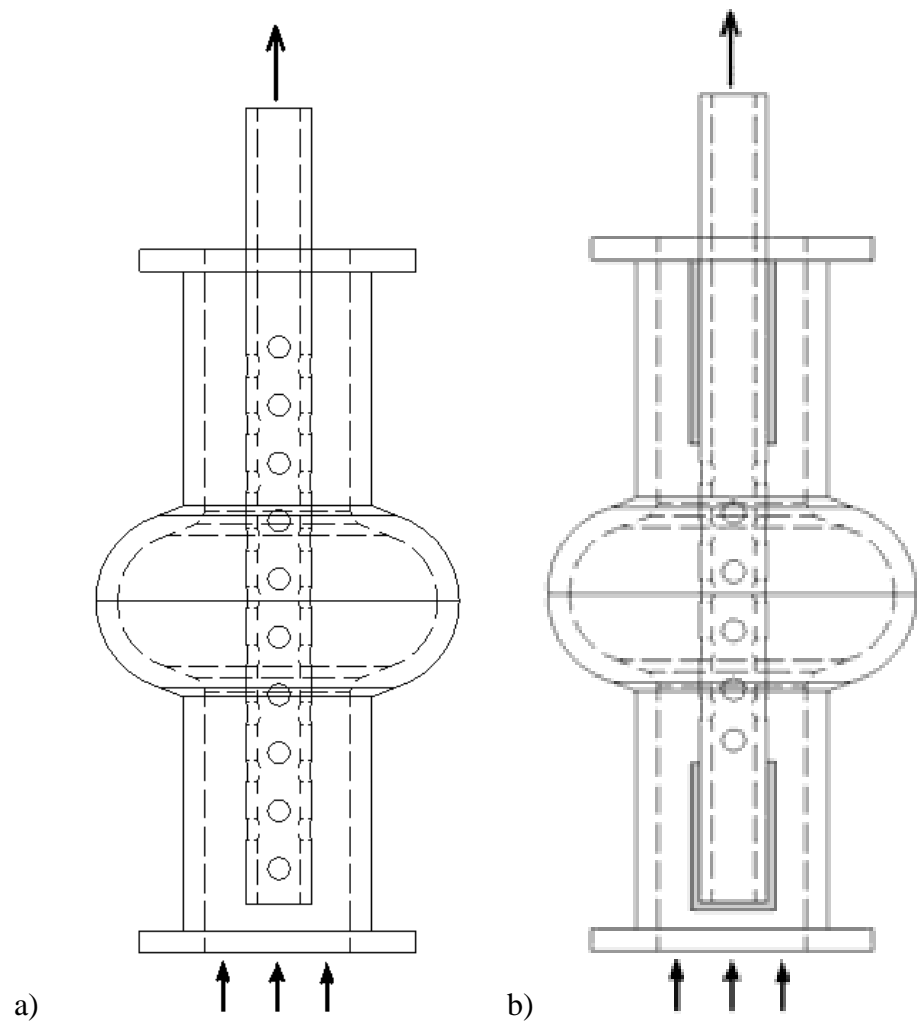
Figure 5.35: *Different cathode performance*
a – full holled cothode; b – center holled cathode.

In the beginning was used configuration *a* (Figure 5.35). Cutoff part of the cavities which were electropolished in this way had a good view(Figure 5.36), but from cell part removing of material is not enough(Figure 5.37). Was decided to cover with Teflon cathode across cutoff part of the cavity(Figure 5.35 configuration *b*). Cell part was electropolished good(Figure 5.39) but opposite effect appeared on a cutoff part(Figure 5.38).
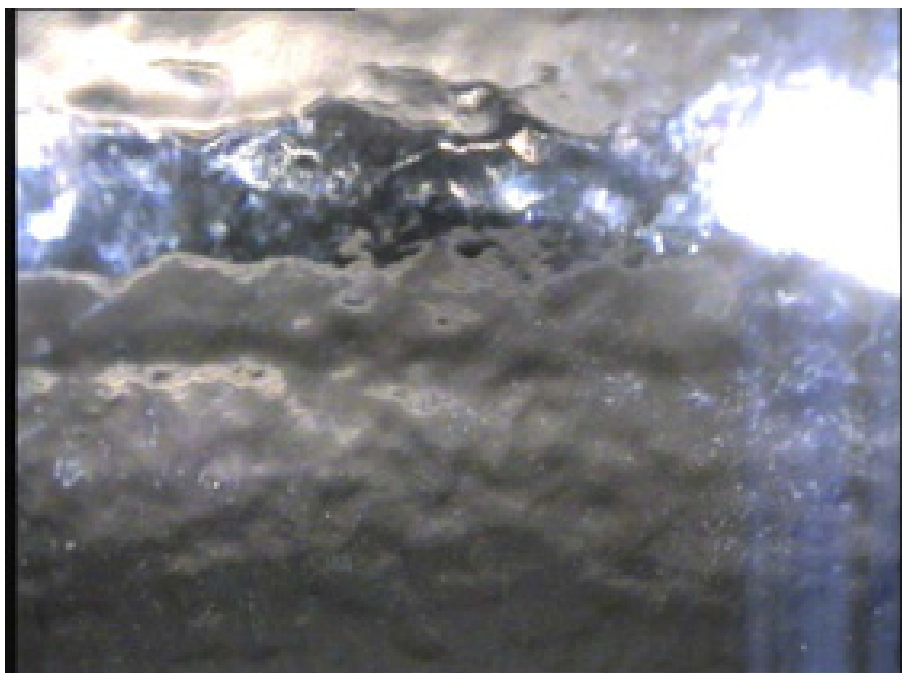
Figure 5.36: *Cutoff part of cavity electropolished in 1-4 ChCl – urea melt with 30 g/l SA with configuration a.*
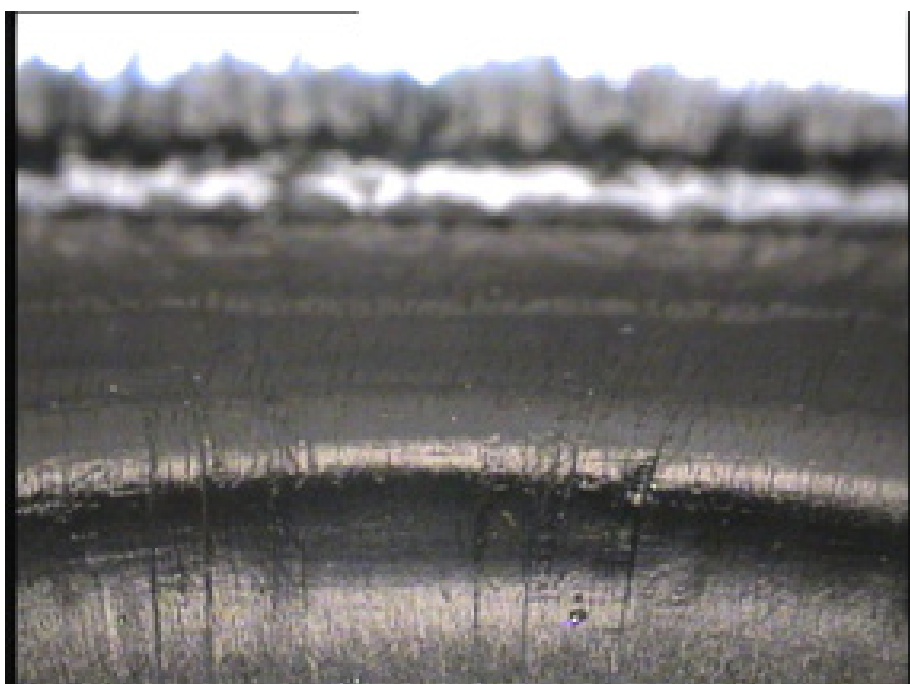
Figure 5.37: *Cell part of cavity electropolished in 1-4 ChCl – urea melt with 30 g/l SA with configuration a.*
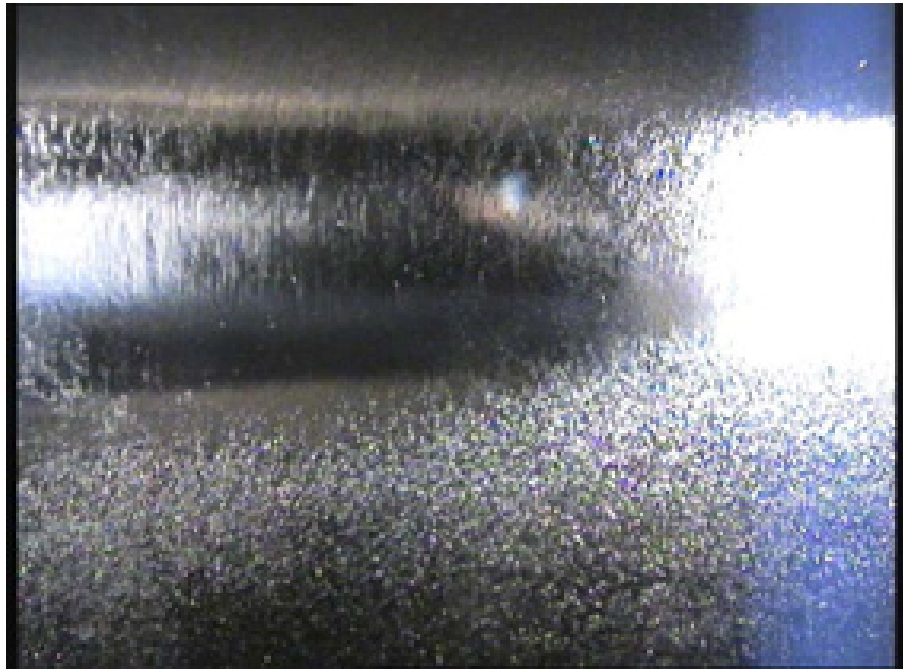
Figure 5.38: *Cutoff part of cavity electropolished in 1-4 ChCl – urea melt with 30 g/l SA with configuration b.*
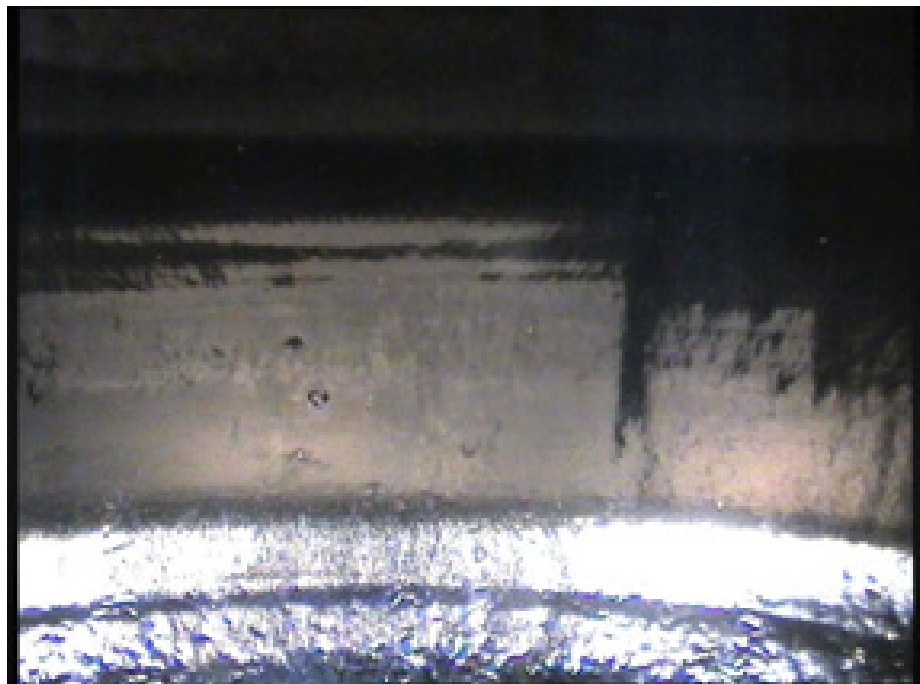
Figure 5.39: *Cell part of cavity electropolished in 1-4 ChCl – urea melt with 30 g/l SA with configuration b.*

6   Results

The classical electropolishing of Nb is a very well studied process. It is enough old and very dangerous but it does not have an alternative. In this work it has been shown that there are an the alternative methods which could be used instead of classical EP. This work is the continuation of previous works and publications which were done in Superconductivity Laboratory at LNL INFN.

First, were performed tests dedicated to matrix solution research, looking for limitations, Nb dissolving mechanism understanding. After was a search for a regulators which can provide equal current distribution on both sides of the sample using only one counter electrode. Success was not in delay, it was found that Sulfamic acid can provide uniform current distribution. Unfortunately there is the side of the medal. In order to break a strong oxide film on Nb was used high overvoltage which brings huge(for water solutions) current density. The behavior of current and potentials on the electrochemical cell provides enormous heating of solution. It is possible to avoid this problem using SA and PS concurrently. Then current density and working potential decrease. Also there is no necessity of overvoltage in the beginning of the process. All recipes which gave useful results for conclusion of work are reported in Table 6.1

ChCl-Urea ratio	Regulator	C, g/l	Mode	Electrical tension, V	Current density, A/cm^2	Roughness (front), nm	Roughness Back), nm	Note
1-1	Sulfamic acid	30	Manual	30…60	0,3	1242±23	779±10	No polishing
	Ammonium persulfate	10	Manual	20…40		-	-	No polishing
1-2	Sulfamic acid	40	Manual	30…60	0,3	1774±87	346±80	No polishing
	Ammonium persulfate	10	Autom.	20…40		1118±36	537±85	No polishing
1-4	Sulfamic acid	30	Autom.	30…60	0,3	274±26	241±41	Best
	Ammonium sulfate	40	Manual	30…60	0,3	631±134	456±78	Good
	Ammonium sulfamate	40	Manual	30…60	0,3	262±62	259±73	Good
	Ammonium persulfate	10	Autom.	20…40		752±138	662±232	Pitting
	Sulfamic acid + Ammonium persulfate	30 + 2,5	Autom.	20…40		438±25	441±94	Good

Table 6.1: *Principal recipes and their characteristics.*

Cavities were electropolished only with ChCl – urea 1-4 solution with 30 g/l SA. Electropolishing was done on current density $0,3A/cm^2$ in manual mode. Voltages were in range of 30…60V. 6GHz cavities that have been tested at 4,2 K, comparable by Q factor to the cavities electropolished with classical EP (Figure 6.1).. However it must be reported that this work is still preliminary. Found recipe is much less dangerous than classical EP and also it doesn't need preliminary treatment with BCP (Table 6.2).

	Classical EP	**Ionic liquids EP**
Composition	H_2SO_4 98% HF 49% - corrosive, dangerous and volatile	Choline Chloride, Urea and Sulfamic acid - No dangerous elements (salt form).
Process speed	$30-80mA/cm^2$ (30 μm/hour)	$300-500 mA/cm^2$ (350 μm/hour)
Pre-treatment	BCP	-
t, °C	room temperature	120-160

Table 6.2: *Comparison between conditions of Classical EP and EP in ChCl – urea melt.*

Electropolishing with ChCl – urea melt is competitive way to classical EP. It is much more secure because it doesn't need fluorine anions, most dangerous chemicals are Sulfamic acid and ammonium persulfate which have salt form in room temperature. Speed of process is more than 10 times faster and results on rf test are comparable with the best results obtained with classical EP. Only one dangerous factor is high temperature of working solution.
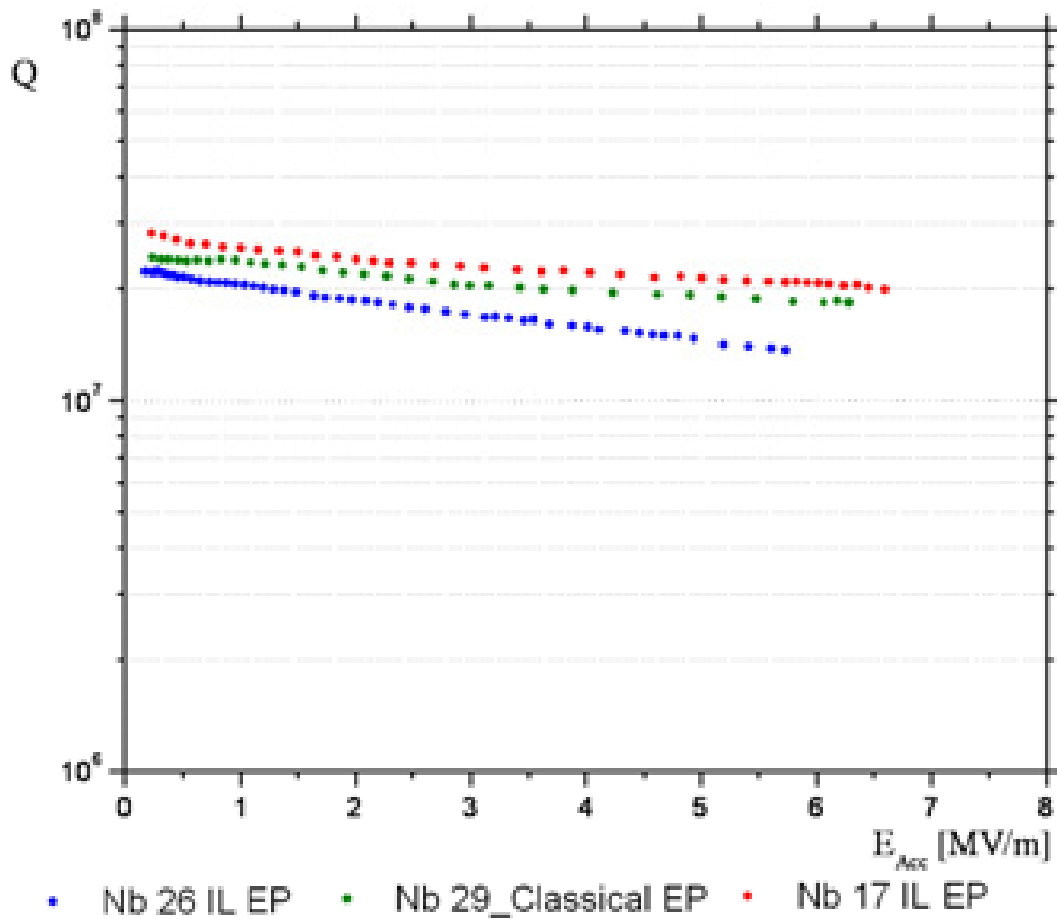
Figure 6.1: *Q-factor versus accelerating field at 4,2 K for a 6 GHz cavity electropolished by means of the standard HF recipe (intermediate curve signed by the green dots) and by the Choline Chloride base recipe containing Sulfamic acid (lower and higher curve signed respectively by the blue and red dots).*

7   Conclusions

In this work five main things were determined/proofed:

1. Choline Chloride - urea based Ionic liquids are a possible alternative to the hazardous standard electropolishing electrolyte based on hydrofluoric and sulphuric acid.

2. Choline Chloride – urea melt cannot be independently use for Nb electropolishing. A regulator role can be played by Sulfamic acid.

3. First 6GHz cavities electropolished in 1-4 ChCl – urea melt in presence of 30g/l SA have the same Q-factor as the best 6GHz cavities electropolished with Classical EP

4. Technological problems could also occur whenever one would think to apply the recipe to the fabrication of niobium cavities for particle accelerators. One for example is related to the high current density employed for the electropolishing. So high current density and overvoltage provide to great heating of solution inside the cavity with following degradation of solution.

5. Discovered way to decrease current density and to avoid overvoltage using SA and PS concurrently. Preliminary this recipe can be used for 6GHz cavities technologically and probably could be used for a real cavities.

8   Future development

The progress got on this work on 6GHz cavities electropolishing needs a lot of improving. It refers as finding a new additional/another adding and as EP system designing. Below are stated some ideas:

Design shaped cathode

Check possibility to use flow inside and outside the holed cathode.

Designing cooling system for solution.

Determine best concentration of SA and PS in concurrent use and electrical parameters(is offered to use multifactorial analyzing)

Discover new, better adding than SA and PS.

Determination solution life-time.

Put on application to accelerators cavities

List of figures

List of tables

Bibliography

[1]. *V. Palmieri, Advancements on Spinning of Seamless Multicell Reentrant Cavities., in: Proceedings of the 11th Workshop on RF Superconductivity, Lubeck, Germany, 2003, TuP26.*

[2]. *M. Peiniger, M.and Hein, N. Klein, G. Muller, Proceedings of the 3rd Workshop on rf superconductivity, 1987.*

[3]. *H. Padamsee, J. Knoblock, T. Hays, RF Superconductivity for Accelerators, Wileyand Sons, New York, 1998.*

[4]. *B. Dwersteg et al, operating Experience with Superconducting Cavities in HERA, Proc. 4th EPAC, London (1994) 2039.*

[5]. *. Cavallari et al, Acceptance Tests of Superconducting Cavities and Modules for LEP from Industry, Proc. 4th EPAC, London (1994) 2042 - 2044.*

[6]. *S. Noguchi et al, Recent Status of the TRISTAN Superconducting RF System (Proc. 4th EPAC, London (1994) 1891 - 1893 .*

[7]. *Shin-Ichi Kurokawa, B-Factory Commissioning and First Results, Proc. Pac 2001, Chicago (2001) .*

[8]. *S. Belomestnykh et al, Running CESR at High Luminosity and Beam Current with Superconducting RF System, Proc. 7th EPAC, Vienna (2000) 2025 – 2027 .*

[9]. *C. Reece et al, Performance Experience with the CEBAF SRF Cavities, Proc. IEEE PAC, Dallas (1995) 1512.*

[10]. *J. Andruszkow et al, first Observation of Self-Amplified Spontaneous Emission in a Free-Electron Laser at 109 nm Wavelength, DESY 00-066, ISSN 0418-9833 (2000).*

[11]. *T.E. Mason, The Spallation Neutron Source: A Powerful Tool for Materials Research, Proc. Pac 2001, Chicago (2001) .*

[12]. *D. Proch, Superconducting cavities for accelerators, Rep. Prog. Phys. 61 (1998) 431-482 .*

[13]. *TESLA – Technical Design Report, DESY 2001-011/ECFA 2001-209/TESLA Report 2001-23/TESLA FEL 2001-05 (2001) .*

[14]. *Belomestnykh S., Proceeding of the 1999 Particle Accelerator Conference ed. by A. Luccio et al (1999) p. 272.*

[15]. *Brown P. et al., Proceedings of the 9th Workshop on RF Superconductivity (1999) ed. By B. Rusnak, paper MOA001.*

[16]. *Reece C. et al., Proceedings of the 9th Workshop on RF Superconductivity (1999) ed. By B. Rusnak, paper MOA004.*

[17]. *Ciovati et al, Proceedings of the 10th Workshop on RF Superconductivity (2001) ed. By S. Noguchi, paper PT016.*

[18]. *Trines D., Proceedings of the 9th Workshop on RF Superconductivity (1999) ed. By B. Rusnak, paper FRA 003. .*

[19]. *Padamsee H, Proceedings of the 10th Workshop on RF Superconductivity (2001) ed. By S. Noguchi, paper FRA 003.*

[20]. *Proceedings de "14th International workshop on RF Superconductivity" (SRF 2009), p.155; web site:http://accelconf.web.cern.ch/AccelConf/srf2009/papers/tuobau07.pdf.*

[21]. *Proceedings de "14th International workshop on RF Superconductivity" (SRF 2009), p.149; web site: http://accelconf.web.cern.ch/AccelConf/srf2009/papers/tuobau06.pdf.*

[22]. *V. Palmieri, .Spinning of TESLA-Type Cavities: Status of Art., Proc. of the 9th Workshop on RF superconductivity, Santa Fe, USA, Nov. 1999, pp 532-537.*

[23]. *D. Landolt, Electrochim. Acta 32, 1 (1987).*

[24]. *A. Kutzelnigg, Metalloberflache 3, 867 (1951).*

[25]. *R. Weiner, Metalloberflache 27, 441 (1973).*

[26]. *H. Figour and P. A. Jacquet, French Patent No. 707526 (1930).*

[27]. *J. Edwards, J. Electrodeposition Techn. Sco. 28, 133 (1952).*

[28]. *R. Young, and E. Teague, Passivity of Metals, The Electrochemical Society,.*

[29]. *R. Grimn, and D. Landolt, Corros. Sci. 36, 1847 (1994).*

[30]. *M. Matlosz, Electrochim. Acta 40, 393 (1995).*

[31]. *R. Grimn, A. West, and D. Landolt, J. Electrochem. Soc. 139, 1622 (1992).*

[32]. *R. Grimn, and D. Landolt, Corros. Sci. 36, 1847 (1994).*

[33]. *P. Jacquet, Tans. Electrochem. Soc. 69, 639 (1936).*

[34]. *P. Jacquet, Metal Finishing 47, 48 and 83 (1949).*

[35]. *D. Landolt, R. Muller, and C. Tobias, J. Electrochem. Soc. 116, 384 (1969).*

[36]. *M. Datta, and D. Landolt, J. Electrochem. Soc. 122, 1446 (1975).*

[37]. *D. Landolt, R. Muller, and C. Tobias, J. Electrochem. Soc. 116, 1384 (1968).*

[38]. *T. Hoar, D. Mears, and G. Rothwell, Corros. Sci. 5, 279 (1965).*

[39]. *T. Hoar, Corros. Sci. 7, 341 (1967).*

[40]. *H. Tian, M. Kelley, C. Reece, and S. Corcoran, J. Electrchem. Soc. V155, D536 (2008).*

[41]. *J. McGeough, Principles of electrochemical machining, Chapman and Halls, Landon, (1974).*

[42]. *J. Wargner, J. Electrochem. Soc. 101, 225 (1954).*

[43]. *Godeke, A.(2006). Nb3Sn for Radio Frequency Cavities. Lawrence Berkeley National Laboratory: Lawrence Berkeley National Laboratory. Retrieved from: http://escholarship.org/uc/item/6d3753q7.*

[44]. *I. Nowak, M. Ziolek . "Niobium Compounds: Preparation, Characterization, and Application in Heterogeneous Catalysis",(1999), Chemical Reviews 99 (12): 3603–3624.*

[45]. *Holleman, Arnold F.; Wiberg, Egon; Wiberg, Nils; (1985). "Niob" (in German). Lehrbuch der Anorganischen Chemie (91–100 ed.). Walter de Gruyter. pp. 1075–1079.*

[46]. *Greenwood, Norman N.; Earnshaw, A. (1997), Chemistry of the Elements (2nd ed.), Oxford: Butterworth-Heinemann.*

[47]. *Cardarelli, Francois (2008). Materials Handbook. Springer London.*

[48]. *Volk, Tatyana; Wohlecke, Manfred (2008). Lithium Niobate: Defects, Photorefraction and Ferroelectric Switching. Springer. pp. 1–9.*

[49]. *Agulyansky, Anatoly (2004). The Chemistry of Tantalum and Niobium Fluoride Compounds. Elsevier. pp. 1–11.*

[50]. *Ram, R.S.; Rinskopf, N.; Liévin, J.; Bernatha, P.F. (2004). "Fourier transform emission spectroscopy and ab initio calculations on NbCl". Journal of Molecular Spectroscopy 228: 544–553.*

[51]. *Soisson, Donald J.; McLafferty, J. J.; Pierret, James A. (1961). "Staff-Industry Collaborative Report: Tantalum and Niobium". Industrial and Engineering Chemistry 53 (11): 861–868.*

[52]. *C. R. Lucas, J. A. Labinger, J. Schwartz (1990). Robert J. Angelici. ed. "Dichlorobis(η5-Cyclopentadienyl)Niobium(IV)". Inorganic Syntheses (New York: J. Wiley & Sons) 28: 267–270.*

[53]. *Lindenhovius, J.L.H. (2000). "Powder-in-tube (PIT) Nb/sub 3/Sn conductors for high-field magnets". IEEE Transactions on Applied Superconductivity 10: 975–978.*

[54]. *Nave, Carl R. "Superconducting Magnets". Georgia State University, Department of Physics and Astronomy. Retrieved 2008-11-25.*

[55]. *L.I.Antropov, "Teoreticheskaya Elektrokhimiya" (Theoretical Electrochemistry), Izd.Vysshaya Shkola, Moscow, 1969.*

[56]. *N. Kh. Tumanova, S.V. Volkov, E. A. Babenkov, N.I. Buryak and V.A. Bandur, Ukrainian Journal of Chemistry, 60 (1994) 518 (in Russian) .*

[57]. *S. Volkov, N. Tumanova, S. Kochetova, N. Buryak, Z. Naturforsh, 56a (2001) 70.*

[58]. *H. Padamsee, Supercond. Sci. Technol. 14, R28 (2001). .*

[59]. *9 R. Ballantimi, R. Parodi, Proceeding of the 9th workshop of RF superconductivity, Sante Fe, NM, p211 (1999).*

[60]. *H. Tian, C. Reece, M. Kelley, S. Wang, L. Plucinski, and K. Smith, Appl. Surf. Sci. 253, 1236 (2006). .*

[61]. *H. Tian, Surface study of niobium for superconducting radio frequency (SRF) accelerators, PhD thesis, College of William and Mary (2008).*

[62]. *H. Tian, G. Ribeil, M. Kelley, and C. Reece, Proceeding of 13th international workshop of RF superconductivity, Beijing, China (2007). .*

[63]. *K. Satio, Y. Kojina, T. Furuya, S. Mitsunobu, S. Noguchi, K. Hosoyama, T. Nalazato, T. Tajima, K. Asano, K. Inoue, Y. Lino, H. Nomura, and K. Takeuchi, Proceeding of 4th of RF superconductivity, KEK, Tsukuba, Japan, p635 (1989). .*

[64]. *E. Kato, S. Noguchi, M. Ono, K. Satio, T. Sjishido, H. Safa, J. Knobloch, and L. Lije, Proceeding of 9th of RF superconductivity, Santa Fe, NM, p328 (1999).*

[65]. *C. Boffo, P. Bauer, T. Reid, and R. Geng, Proceeding of 12th workshop of RF superconductivity, Ithaca, NY, p8 (2005).*

[66]. *Arsova, A. Prusi, T. Grcev, and L. Arsov, J. Serb. Chem, Soc. 71, 177 (2006). .*

[67]. *19 Q. Ma, and R. Rosenberg, Proceeding of the 2001 particle accelerator conference, Piscataway, NJ, 2, p1050 (2001).*

[68]. *A. Dacca, G. Gemme, L. Mattera, and R. Parodi, Appl. Surf. Sci. 126, 219 (1998).*

[69]. *J. Halbritter, Surf. Interf. Anal. 12, 354 (1998).*

[70]. *Q. Ma, and R. Rosenberg, J. Appl. Phys. 96, 7675 (2004). .*

[71]. *A. Dacca, G. Gemme, L. Mattera, and R. Parodi, Surf. Sci. Spec. 5, 332 (1998).*

[72]. *Y. Li, and L Young, Electrochem. Soc. 147, 1344 (2000).*

[73]. *D. Gabe, Metallography 5, 415 (1972).*

[74]. *L. Berlouis, and D. Schiffrin, Trans. Inst. Met. Finish 63, 52 (1985).*

[75]. *O. Piotrowski, C. Madore, and D. Landolt, Electrochim. Acta 44, 2289 (1999).*

[76]. *O. Piotrowski, C. Madore, and D. Landolt, J. Electrochem. Soc. 145, 2362 (1998).*

[77]. *http://www.gamry.com/App_Notes/Potentiostat_Primer.htm.*

[78]. *V. Palmieri, V. Rampazzo, F. Stivanello, Proceedings of the II workshop on "Pshing the limits of RF Supercondctivity: Thin films and new ideas, (2008) V .Palmieri ed.*

[79]. *M. Ceccato, "Elettropulitura del Niobio con Elettroliti a base di Liquidi Ionici", Master Thesis (2007) University of Padua.*

[80]. *G. Mondin, "Utilizzo di Liquidi Ionici per l'Elettropulitura di cavità superconduttive in Niobio", Degree Thesis (2008) University of Padua.*

[81]. *D. Rizzetto, "Applicabilita' dei Liquidi Ionici all'Elettropulitura del Niobio" Degree Thesis (2009) University of Padua.*

[82]. *Zhao X., Virginia Polytechnic Instytute, PhD Thesis (2009), p.42.*

[83]. *K. Halbach, R. Holsinger, Particle Accelerators 7 (1976) 213-222.*

[84]. *H. Padamsee, J. Knoblock, T. Hays, RF Superconductivity for Accelerators, Wiley and Sons, New York, 1998.*

[85]. *J. Jackson, Classical Electrodynamics, Wiley, New York, 2nd edition, 1975.*

[86]. *D. Jones, Principle and prevention of corrosion, 2nd Edition, Prentice Hall, Upper.*

[87]. *A. Bard, and L. Faulkner, Electrochemical methods: Fundamentals and Applications,.*